INFORMATION TO USERS

This manuscript has been reproduced from the microfilm master. UMI films the text directly from the original or copy submitted. Thus, some thesis and dissertation copies are in typewriter face, while others may be from any type of computer printer.

The quality of this reproduction is dependent upon the quality of the copy submitted. Broken or indistinct print, colored or poor quality illustrations and photographs, print bleedthrough, substandard margins, and improper alignment can adversely affect reproduction.

In the unlikely event that the author did not send UMI a complete manuscript and there are missing pages, these will be noted. Also, if unauthorized copyright material had to be removed, a note will indicate the deletion.

Oversize materials (e.g., maps, drawings, charts) are reproduced by sectioning the original, beginning at the upper left-hand corner and continuing from left to right in equal sections with small overlaps.

Photographs included in the original manuscript have been reproduced xerographically in this copy. Higher quality 6" x 9" black and white photographic prints are available for any photographs or illustrations appearing in this copy for an additional charge. Contact UMI directly to order.

ProQuest Information and Learning
300 North Zeeb Road, Ann Arbor, MI 48106-1346 USA
800-521-0600

The Effect of HIV Protease Inhibitors on Insulin Binding, Triglyceride Synthesis, Lipolysis, and Insulin Signaling in 3T3-L1 Adipocytes

Caterina Cammalleri

A Thesis

in

The Department

of

Biology

Presented in Partial Fulfillment of the Requirements
for the Degree of Masters of Science at
Concordia University
Montreal, Quebec, Canada

April 2002

Acknowledgements

I dedicate this thesis to my grandparents, Caterina and Giuseppe Argento, for their unconditional love and guidance. I would like to thank my husband, Danny, for his endless love and support and to my family for their love and understanding.

I would also like to acknowledge Dr.Ralph Germinario for giving me the opportunity to learn and practice science in his lab and to Sue-Colby Germinario for her knowledge and patience throughout the proceedings of my project. Last but not least, I am grateful to Catherine, Carolina, Julianna, and Hassan for all their help and friendship.

TABLE OF CONTENTS

RESULTS

LIST OF FIGURES

ABSTRACT

Retroviral protease inhibitors used as therapy for HIV-infection have been causally associated with serious metabolic side effects, including peripheral lipodystrophy, central adiposity, hyperlipidaemia, insulin resistance, and in some cases, type 2 diabetes. The etiology of this characteristic clinical syndrome remains unknown.

We demonstrate that the HIV protease inhibitors (PIs), saquinavir, indinavir, and ritonavir inhibit adipocyte differentiation of 3T3-L1 preadipocytes. Furthermore, they exert a dose-dependent increase in basal triacylglycerol synthesis followed by a concomitant decrease in insulin-stimulated triacylglycerol synthesis. However, PIs did not stimulate lipolysis under basal or norepinephrine-stimulated conditions in mature 3T3-L1 adipocytes. Also, this study reports an inhibition of specific ^{125}I-Insulin binding to insulin receptors in the presence of PIs throughout distinct stages of 3T3-L1 adipocyte differentiation. Additionally, this inhibition was found to be reversable upon removal of the PIs during the binding process. However, insulin binding affinities and processing were not affected by PIs.

To continue, we investigated whether the HIV protease inhibitor ritonavir altered insulin signaling. In cells not exposed to ritonavir, insulin led to a rapid increase of insulin-receptor substrate-1-phosphorylation. In ritonavir-treated cells, these insulin-stimulated increases were reduced by approximately 50%.

We conclude that HIV protease inhibitors are capable of selectively inhibiting the insulin response and contributing to the metabolic abnormalities seen in HIV-infected patients.

INTRODUCTION

1.1 The Human Immunodeficiency Virus Type-1

The human immunodeficiency virus (HIV-1), a retrovirus of the lentivirus subgroup, is responsible for the progressive immune system degeneration that leads to the development of AIDS, acquired immunodefiency syndrome. HIV infection commonly causes the progressive loss of CD4 T-lymphocytes and macrophages and thus, a loss of immune competence in infected individuals (1, 2, 3, 4). As a result, bacterial infections, viral infections or other opportunistic infections exploit the immunocompromised state of asymptomatic individuals. It is the presence of these opportunistic diseases that establishes in part the medical diagnosis of AIDS (6).

The first case of HIV infection was reported by the CDC (Centers for Disease Control) in 1981 (3). In 1983-84, the HIV virus was isolated and identified as the causative agent of AIDS. By 1985-86, the chief routes of HIV transmission (blood, sexual contact, mother-to-child), and the main targets cells for HIV infection (CD4 expressing cells) were established (6). Today, more than 36 million adults and children worldwide were estimated to be currently living with HIV infection or AIDS (AIDS Epidemic Update: UNAIDS, Geneva December 2000). Cumulatively to date, an estimated 20 million people have died from AIDS-associated disease. Extensive efforts in research continue to be made in order to eradicate this deadly virus. Emphasis is placed on treatments with Highly Active Anti-Retroviral Therapy (HAART) and prevention of HIV infection.

1.2 THE VIRION

The mature HIV virion (Fig 1) is an icosahedral shaped particle with 72 spikes formed by two major viral-envelope glycoproteins, gp120 and gp 41. They are derived from a 160 kDa precursor that is cleaved inside the cell into a gp120 external surface (SU) envelope protein and a gp41 transmembrane (TM) protein that transverses the lipid bilayer (7).

Under the lipid bilayer, is the myristylated p17 core protein that provides the matrix (MA) for the viral structure (8). The capsid protein (p24) forms the cone shaped core that encases the genomic RNA molecules and the nucleocapsid protein (NC, p7, p9). Inside the retroviral capsid are two identical positive sense single stranded RNA molecules dimerized at their 5' end. Associated with the nucleocapsid and RNA within the virion are the polymerase proteins, i.e. reverse transcriptase (RT), protease (PR), and integrase (IN). These are responsible for viral replication (9).

Figure 1 : The HIV-1 Virion

Schematic representation of the HIV-1 virion including: the external envelope glucoproteins, gp120 and gp41, the nucleocapsid protein (p7), the matrix protein (p17), the capsid protein (p24), reverse transcriptase (p51/p66), protease (p11), integrase (p32) and the viral genomic DNA.

B HIV-1 VIRION

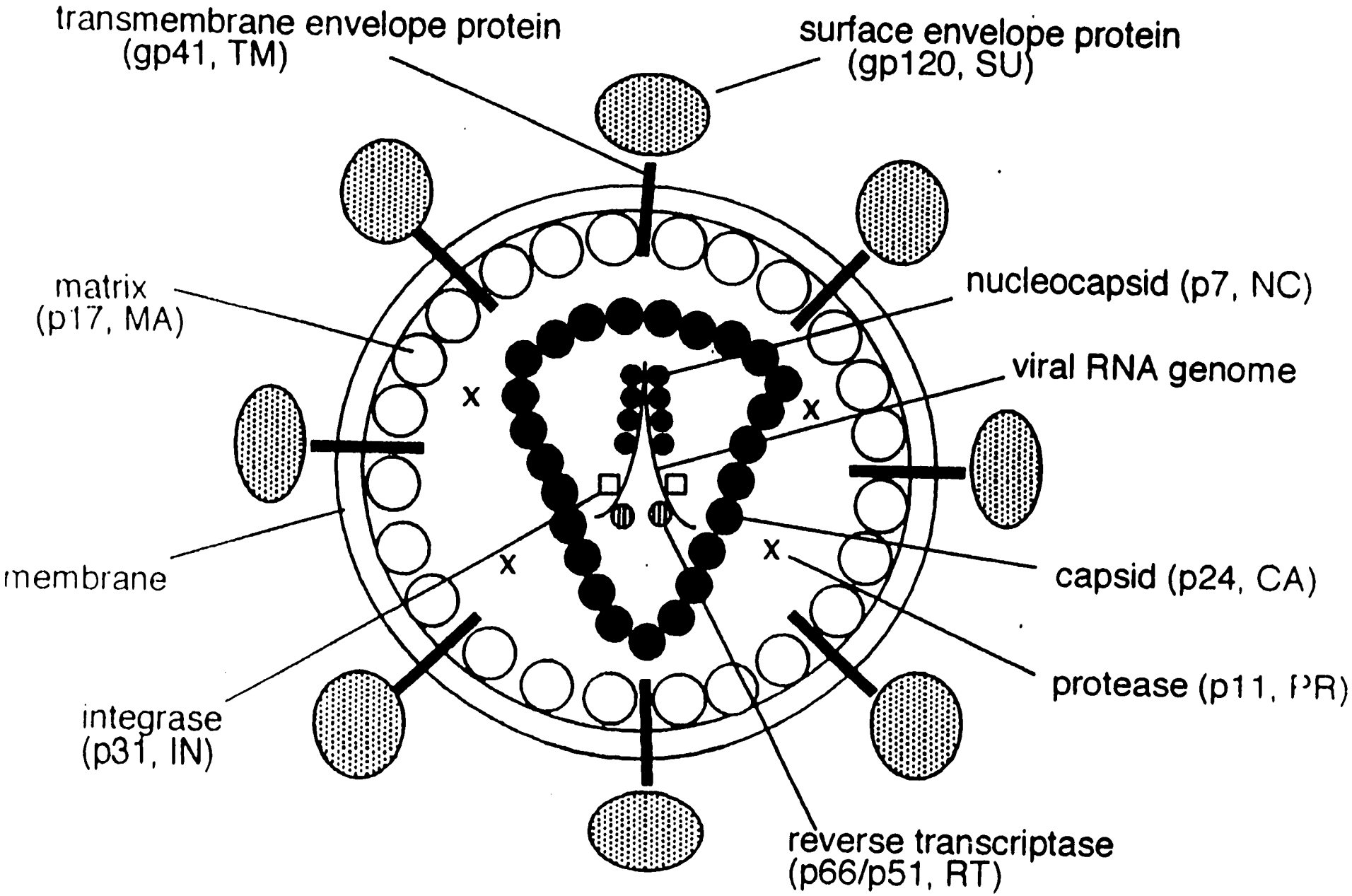

1.3 GENOMIC ORGANIZATION

There are three genes common to all retroviruses that define the essence of the retroviral life cycle. These are *gag*, *pol* and *env* genes. The *gag* gene encodes a polyprotein precursor that is subsequently cleaved by the viral protease during maturation into core proteins that package the viral genomic RNA (10). The *pol* gene encodes a precursor protein which is cleaved to yield the three enzymes: protease, which processes precursor proteins; reverse transcriptase, which copies the RNA into double stranded DNA provirus; and integrase, which integrates the provirus into the host cell genome (10). The *env* gene encodes a glycosylated polypeptide precursor (gp160) that is processed to form the exterior glycoprotein (gp120) and the transmembrane glycoprotein (gp41) (7). The envelope proteins are responsible for docking the virions onto the CD4 target cell and mediating entry of the virus by membrane fusion (Fig 2).

1.4 VIRAL LIFE CYCLE

HIV infection begins with the interaction of the HIV glycoprotein (gp) 120 with the CD4 molecule on the surface of the target cell. Following CD4 binding, a conformational change in the HIV gp120/gp41 complex is induced by interaction of gp120 with the chemokine receptors CCR5 of CXCR4. This change in conformation exposes gp41 allowing it to initiate fusion of the membranes. As the virus fuses with the cell, internalization of the viral core occurs, followed by the uncoating of the viral core and subsequent release of the viral RNA. Once in the cell cytoplasm, the viral reverse transcriptase becomes active and transcribes the viral RNA into a double-stranded cDNA

Figure 2: Genomic Structure of HIV-1

This is a schematic representation showing each of the nine genes of HIV-1 including the three classical retroviral genes gag, pol and env. The accessory proteins vif, vpu, vpr and nef and the regulatory proteins tat and rev.

A HIV-1 GENOME ORGANIZATION

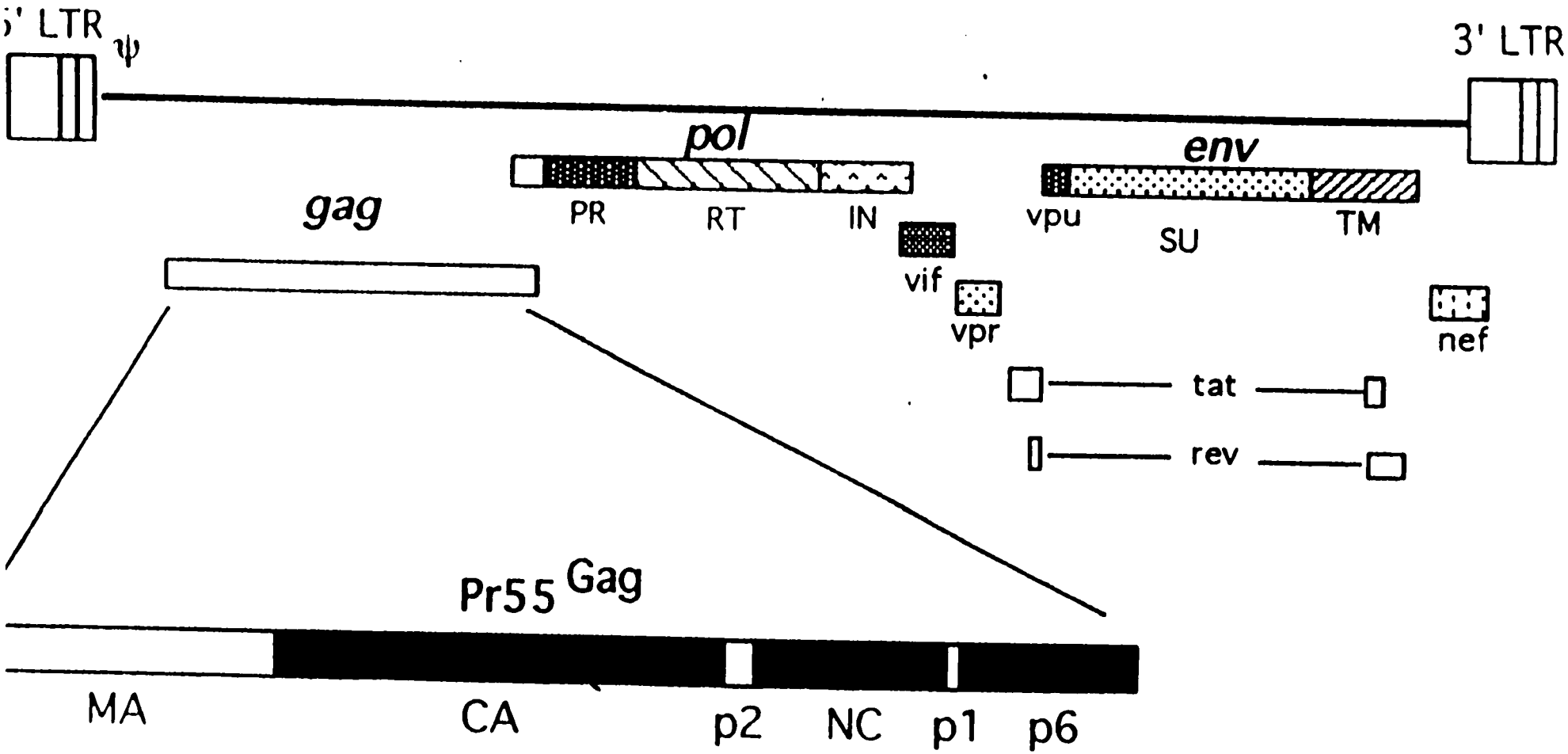

copy (11). A large nucleoprotein complex, the preintegration complex (PIC) carries out retroviral integration. PIC's contain several viral proteins including integrase, reverse transcriptase, matrix, nucleocapsid and Vpr. The provirus is targeted to the nucleus by nuclear localization signals of PIC proteins (12). Integrase recognizes specific sequences present at the ends of the viral DNA molecule and promotes their joining to host DNA. The provirus can then remain latent or be active (11). Resting cells are transcriptionally silent while replicating cells are transcriptionally active (13). Following synthesis of a full RNA trasncript by RNA polymerase II, a complex array of alternatively spliced viral mRNA's can be produced. The unspliced full length RNA transcript (9.2 Kb) corresponds to the viral genome and is used as the mRNA for translation of the *gag* and *pol* polyproteins. Singly spliced 4.5 Kb RNA transcripts encode the *Env, Vif, Vpr* and *Vpu* proteins. And finally, the multiply spliced 2 Kb RNA transcripts encode the regulatory proteins *tat, rev* and *nef* (9). The genomic RNA selected for encapsidation requires the presence of the psi sequence in the 5' untranslated region of HIV-1 RNA. Retrovirus assembly and maturation entail a series of highly regulated processes involving protein folding, transport of viral rpoteins to the site of virus budding, and limited proteolysis of polyproteins (14). The *env* (gp160) proteins pass through the E.R. and Golgi apparatus to be processed into gp120 and gp41 HIV envelope proteins. During movement through the Golgi apparatus, glycosylation of gp120 occurs (11). The *gag* and *gag-pol* polyproteins associate with the inner surface of the plasma membrane and interact with gp41 in the plasma membrane. During and after transport, the *gag* precursor recruits two copies of single stranded viral RNA genome and assembles into dense patches lining the inner face of the plasma membrane. The assembled *gag* protein complex induces membrane

curvature, leading to the formation of a bud (8). As the virus buds from the cell, it acquires a lipid coat, carrying the gp 120 and gp41 proteins. The virus is extruded into extra-cellular space in this immature state (11). During or immediately after budding, the viral protease cleaves the *gag* and *gag-pol* polyprotein precursors to the mature *gag* and *pol* proteins by what is believed to be an autocatalytic process. Protease cleavage leads to core condensation and the generation of a mature, infectious virion, which is now capable of initiating a new round of infection (8) (Fig 3).

Figure 3 : The HIV-1 Viral Life Cycle

This is a schematic representation of the various stages of the HIV-1 life cycle. The stages include: viral entry involving virus binding to CD4 and the respective co-receptor, uncoating of the viral RNA, reverse transcription of the RNA to DNA, nuclear translocation of the preintegration complex, integration of DNA into host DNA, production of viral RNA and proteins, viral assembly and release.

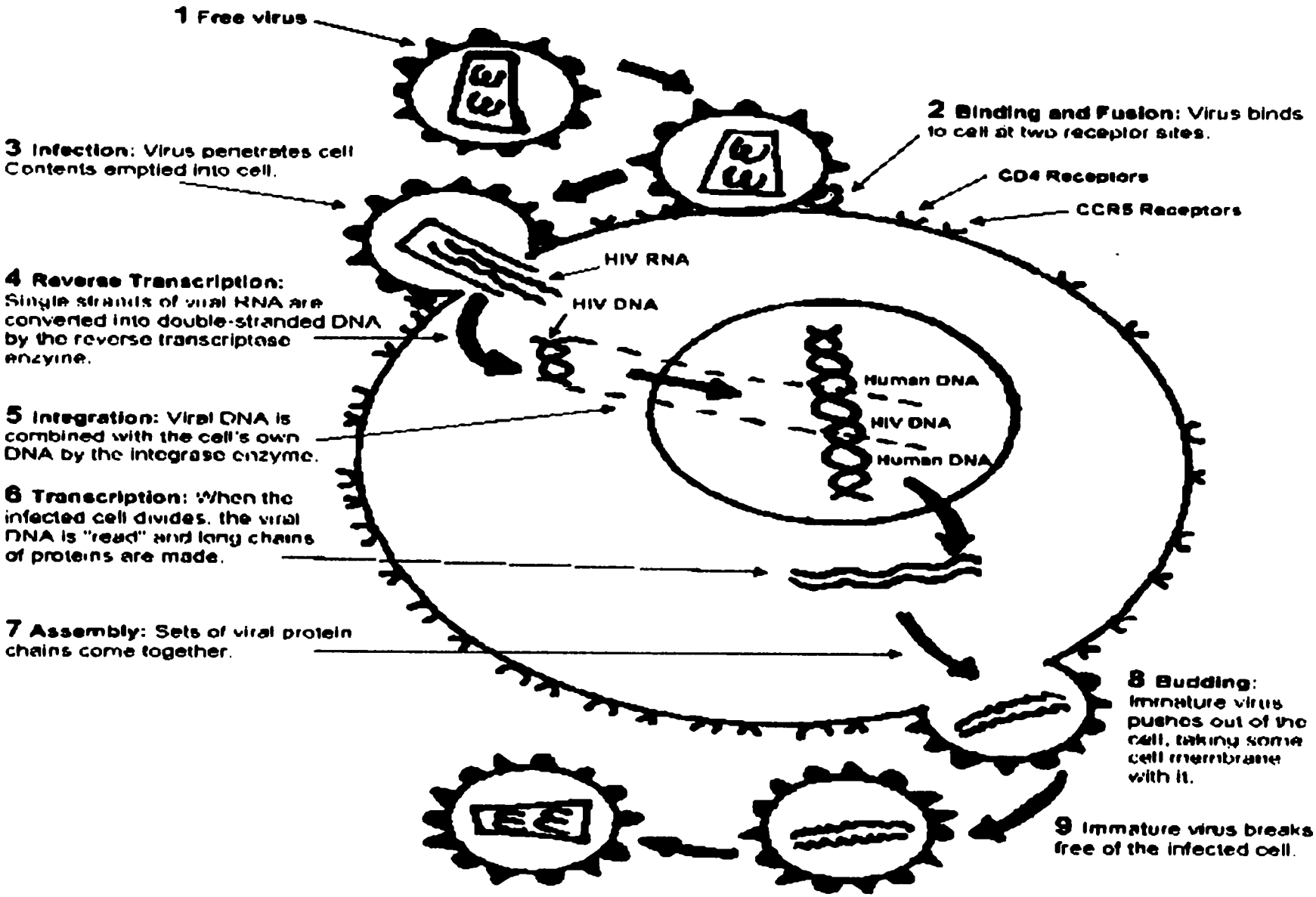
1 Free virus
2 Binding and Fusion: Virus binds to cell at two receptor sites.
CD4 Receptors
CCR5 Receptors
3 Infection: Virus penetrates cell Contents emptied into cell.
HIV RNA
4 Reverse Transcription: Single strands of viral RNA are converted into double-stranded DNA by the reverse transcriptase enzyme.
HIV DNA
Human DNA
HIV DNA
Human DNA
5 Integration: Viral DNA is combined with the cell's own DNA by the integrase enzyme.
6 Transcription: When the infected cell divides, the viral DNA is "read" and long chains of proteins are made.
7 Assembly: Sets of viral protein chains come together.
8 Budding: Immature virus pushes out of the cell, taking some cell membrane with it.
9 Immature virus breaks free of the infected cell.
10 Maturation: The protein chains in the new viral particle are cut by the protease enzyme into individual proteins that combine to make a working virus.

1.5 THE VIRAL PROTEASE: STRUCTURE AND FUNCTION

As with other retroviral proteases, HIV-1 protease (PR) is absolutely required for virion maturation and is therefore essential for viral infectivity (15, 16). Its inactivation, either by a single point mutation in the catalytic active site (Asp-25) or by mutational amino acid insertions within the protease, has drastic effects on the assembly, stability, and infectivity of the released virus particles (16, 17, 18, 19). HIV-1 protease (Fig 4) is a member of the aspartic family of proteases, containing the characteristic and conserved amino acid triplet Asp-Thr-Gly in its catalytic active site (20, 21, 22). The active protease is a dimeric enzyme, consisting of two identical monomers each with 99 amino acid residues which associate symmetrically to form the substrate binding cleft, each monomer contributing one catalytic aspartyl residue to the active site of the enzyme (20, 23, 24, 25, 26, 27, 28, 29). The two monomers are held together as a dimer by the amino- and carboxy-termini of the protease, which form a four-stranded antiparallel ß-sheet(30). Disruption of these interactions in the dimer interface, for example by truncation due to self-digestion (31) or by competition by peptides (32) leads to loss of enzymatic activity.

Figure 4 : Structure of the HIV-1 Aspartic Protease

This is a schematic representation of the HIV-1 protease structure. The active protease is a dimeric enzyme, consisting of two identical monomers each with 99 amino acid residues which associate symmetrically to form the substrate binding cleft, each monomer contributing one catalytic aspartyl residue to the active site of the enzyme. The two monomers are held together as a dimer by the amino- and carboxy-termini of the protease, which form a four-stranded antiparallel ß-sheet. The top panel shows the HIV-1 viral protease and the bottom panel shows the HIV-1 viral protease with a HIV protease inhibitor bound to the active site.

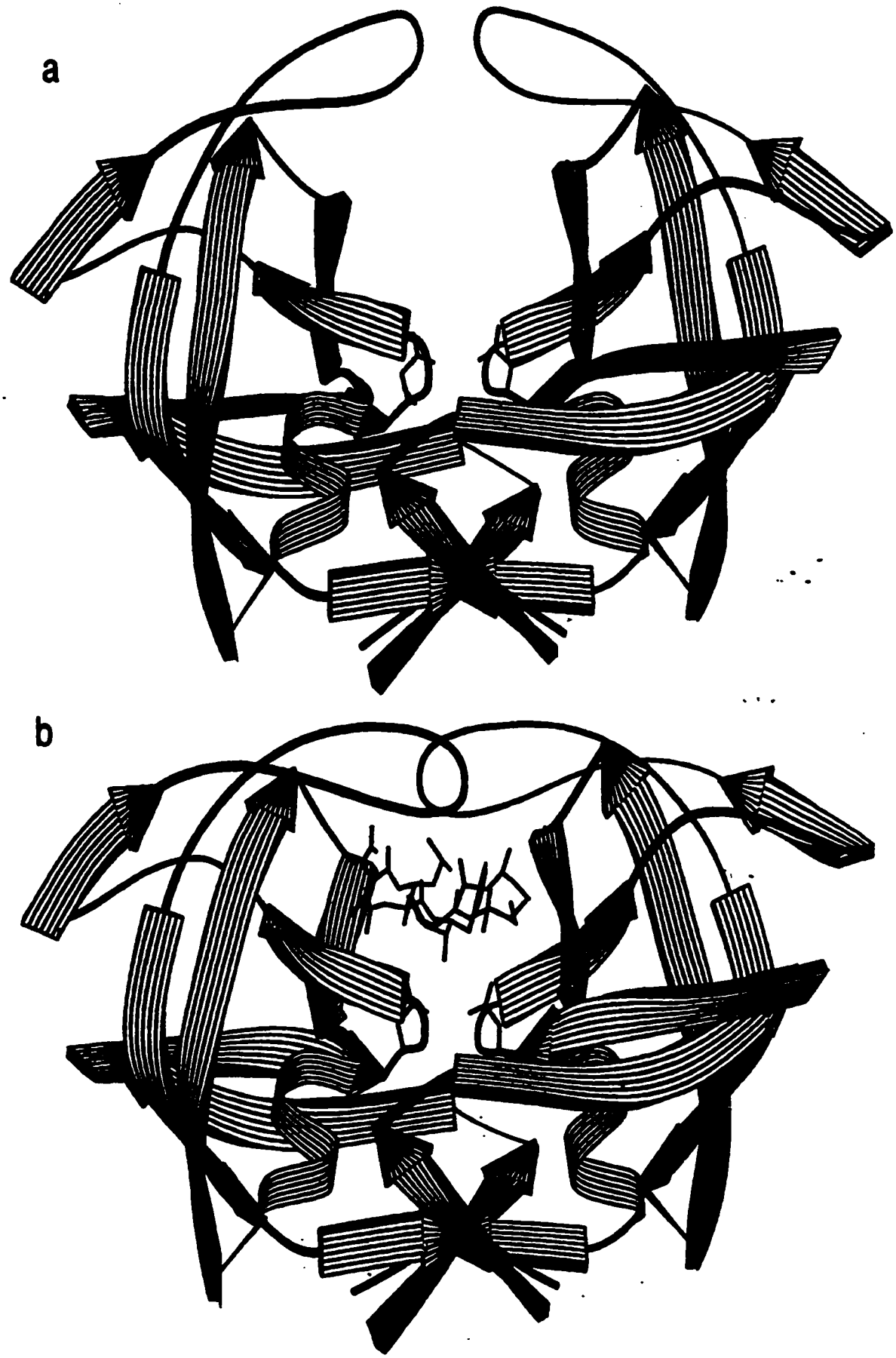
a
b

HIGHLY ACTIVE ANTI-RETROVIRAL THERAPY (HAART)

2.1 DRUG CLASSES

Antiviral therapy directed against human immunodeficiency virus type 1 (HIV 1) is now approaching its 15-year anniversary. All of these drugs inhibit HIV *in vitro*; all are associated with a decrease in viral RNA concentrations in serum, an increase in CD4 cell counts, and a reduced rate of progression to the acquired immunodeficiency syndrome (AIDS) and all prolong cell survival (33). The principle problems of these drugs are their limited antiviral activity, their toxicity, and their lack of a durable antiviral effect, which is partly explained by the development of resistance (33).

There are currently 3 major classes of antiretroviral drugs in general use: nucleoside analog reverse transcriptase inhibitors (NRTI), non-nucleoside reverse transcriptase inhibitors (NNRTI), and protease inhibitors (PI) (34). NRTIs function by inhibiting the synthesis of DNA by the viral reverse transcriptase. These molecules bear a structural resemblance to the natural building blocks of nucleic acids: the purine and pyrimidine nucleosides. Like natural nucleosides, the nucleoside analogs are phosphorylated within the cell. Reverse transcriptase fails to distinguish the phosphorylated nucleoside analogs from their natural counterparts, and attempts to use the drugs in the synthesis of viral DNA. When a nucleoside analog is incorporated into a strand of DNA being synthesized, the addition of further nucleosides is prevented. NNRTIs also inhibit the synthesis of viral DNA, but rather than acting as false nucleosides, the NNRTIs bind to reverse transcriptase in a way that inhibits the enzyme's activity (34). In 1988, the HIV-1 protease enzyme was crystallized and its 3-dimensional structure

determined. Computer modelling was then used to identify compounds that specifically fit into the substrate-binding pocket of the protease, thus potentially inhibiting its activity (35). PIs bind to the active site of the viral protease enzyme, preventing the processing of viral proteins into functional forms. The absence of this cleavage results in an immature virus that is incapable of infecting new cells (33).

2.2 HIV PROTEASE INHIBITORS

The Food and Drug Administration has approved of 5 HIV-1 protease inhibitors (Fig 5) for the treatment of HIV infection: saquinavir, indinavir, ritonavir, amprenavir, and nelfinavir. The PIs are highly protein bound. It is unbound drug that is active, so the higher the protein binding the less drug is available to inhibit virus production. This creates a bioavailabilty problem. Protein binding, bioavailabilty, and metabolism in the liver (which can cause drug interactions with other drug metabolites) all can lower the concentration of protease inhibitors in blood serum (34). Saquinavir and ritonavir are effective in delaying disease progression and prolonging life. Saquinavir is the best tolerated of the compounds but has limited oral bioavailability and the smallest effect on HIV RNA and CD4+ cells levels. Ritonavir is potent with sufficient bioavailability, but has the greatest intolerance and is associated with a formidable list of drug interactions. Indinavir has a profound and sustained effect on HIV RNA levels; however, its ability to limit disease progression is not yet established (35).

Figure 5: Structures of HIV-1 Protease Inhibitors

The following shows the structures of the three HIV protease inhibitors used in this study; saquinavir, indinavir, and ritonavir. They are peptide-mimicking coumpounds that resemble the transition state of the natural substrate.

Structures of HIV Protease Inhibitors

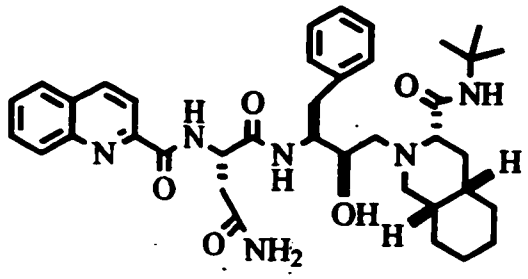

Ro 31-8959 Saquinavir

(D

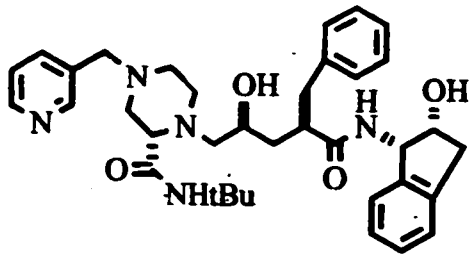

MK-639 (L-735,524) Indinavir

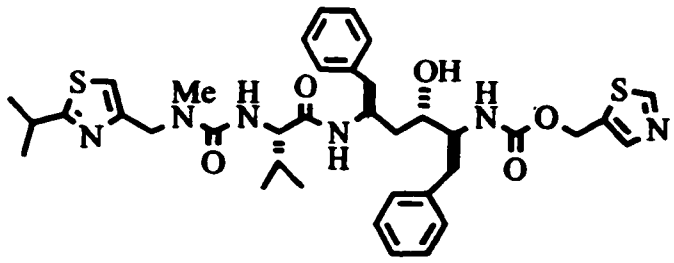

A-84538 (ABT-538) Ritonavir

2.3 METABOLIC PERTUBATIONS OF HIV PROTEASE INHIBITORS

It has long been known that during progression of HIV infection patients may undergo a progressive weight loss and changes in body composition, particularly in fat and muscle masses, and in metabolic pathways, particularly in lipid metabolism (36). This is known as the wasting syndrome. With the introduction of potent antiretroviral combination treatment, including protease inhibitors (PIs) and the subsequent prolonged survival of HIV-infected patients, the incidence of these changes has been dramatically reduced (36). Since 1996, the year in which HAART was introduced, the number of patients dying of AIDS and related opportunistic infections in industrialized countries has decreased by two-thirds (36). However, new disorders involving lipid, glucose metabolism and body fat have acquired more clinical importance (36). A significant portion, ranging from 5% to 75%, of HIV-infected patients receiving PIs notice changes in lipid metabolism and body fat distribution after an average of 10 months taking ritonavir-saquinavir and more than 1 year for indinavir (36). Protease-inhibitors therapy is associated with a syndrome of peripheral fat wasting, central adiposity, hyperlipidaemia, and insulin resistance, referred to as lipodystrophy syndrome (37) (Fig 6). Fat depositions in the breasts of women and over the dorsocervical spine ("buffalo hump") have also been reported (37). Recognized laboratory features of the lipodystrophy syndrome include increased triglycerides, total cholesterol, and low-density lipids, and a decrease in high-density lipids. Also a normal to increased serum glucose, an increase in insulin and C peptide, and a decrease in glucose tolerance (38). Three large and well-known studies from which estimates of the prevalence of lipodystrophy in HIV-infected individuals have been reported are based on Australian, Swiss, and US patient cohorts (39). Taken together,

these studies show a prevalence rate of approximately 50 percent in these populations (39). The US cohort involving 1077 HIV-infected patients reported 22%-28% of its patients with body shape changes, 10%-13% with fat accumulation, and 17%-33% with fat loss (39). Regarding lipid changes, Carr reports elevated triglycerides and elevated total cholesterol in 50% and 58% of PI-therapy recipients versus 22% and 11% in-patients not receiving PIs (39). These findings raise the concern that the lipodystrophy syndrome may be associated with increased atherosclerotic complications and heart disease. Studies of flow-mediated vasolidation, a standardizeable measure of endothelial function, which is considered to be a reflection of cardiac risk, showed abnormalities in subjects on PI therapy (40).

The cause of lipodystrophy in HIV-infected individuals is not known. A number of hypotheses have been put forth as to the mechanism causing lipodystrophy. One hypothesis is the structure homology theory presented by Carr and colleagues in 1998. They searched human protein and genomic databases and observed homologies between the catalytic site of HIV protease and two human proteins: a region incorporating a lipid-binding domain in the low density lipoprotein-receptor related protein (LRP) and with a C-terminal region of the cytoplasmic retinoic-acid binding protein type 1 (CRABP-1) (41). They reasoned that this structural homology allowed protease inhibitors to bind to these proteins and inadvertently disrupt regular fat metabolism, leading to hyperlipideamia, loss of subcutaneous adipocytes, and fat accumulation (41). The next hypothesis is the mitochondrial toxicity theory involving NRTI-therapy. NRTIs inhibit DNA polymerase gamma to a certain extent, in a manner that parallels their effect on reverse transcriptase. The system breaks down when damaged mitochondrial DNA reaches a threshold

proportion above 70 percent. Cells begin to suffer from energy deficiencies and turn to anaerobic processes outside the mitochondria. Anaerobic respiration is much less efficient than mitochondria's oxidative process and produces lactic acid, an acidifying substance that severely perturbs blood chemistry (42). This proposed mechanism links the development of lactic acidosis with disrupted fat metabolism (42).

It is likely that fat redistribution and the metabolic abnormalities seen in HIV-infected patients are the result of several etiologies. In other words, observations may not necessarily reflect a single syndrome, but rather, a number of unique complications occurring simultaneously. Beyond the direct effect of protease inhibitor therapy or mitochondrial toxicity, other potential etiologies that may prove to play a role include HIV infection itself, underlying genetic predisposition, cytokine activation, immune reconstitution, and hormonal influences (40).

Figure 6 : Photograph of a Patient with HIV-1 Related Lipodystrophy

What you see is someone whose lipid (fat) levels in the arms and legs has dropped precipitously, while he has developed fatty deposits around her/his trunk and abdominal organs. This is not the usual subcutaneous fat that lies below the skin and above the muscles, but rather visceral fat that lies directly around the vital organs. Some people have a small fat pad on the back of their neck, but the man below has a much more pronounced accumulation. Normal activities like sleeping on one's back or holding the head erect are significantly impaired by such a protrusion. Sometimes surgery is used to remedy the situation. The following pictures were taken from the October 29, 1998 issue of the *New England Journal of Medicine*'s section *Images in Medicine*.

3T3-L1 MOUSE FIBROBLASTS (PRE-ADIPOCYTES)

3.1 GROWTH AND DIFFERENTIATION

White adipose tissue (WAT) is mainly composed of adipocytes, cells that store energy in the form of triglycerides in times of nutritional affluence and release free fatty acids during nutritional deprivation. WAT mass is determined by the balance between energy intake and expenditure and is controlled by genetic neuroendocrine and environmental factors (43, 44). Perturbations of this steady state can lead to increased or decreased amounts of WAT, such as seen, respectively, in obesity or in the lipodystrophic syndromes (44). Obesity affects between 25% and 30% of the population in industrialized countries and its frequency is still rising (45). It is an independent risk factor for insulin resistance, non-insulin-dependent diabetes mellitus and coronary artery disease (45). Cell culture models, like the 3T3-L1 immortalized mouse preadipocyte cell lines, have been instrumental in the understanding of adipocyte differentiation. These cells are morphologically similar to fibroblastic preadipose cells found in the stroma of adipose tissue, and once differentiated, they exhibit virtually all the characteristics associated with adipocytes present within adipose tissue (46).

The first step of adipocyte differentiation involves arrest of cell proliferation and at least one round of DNA replication and cell doubling (47) (Fig 7). Recent work suggested that the cell-cycle status of preadipocytes during and after clonal expansion correlate with their Rb phosphorylation status; Rb is first hyperphosphorylated during the clonal expansion and later becomes hypophosphorylated in the terminal differentiation phase (43). Activation of the adipogenic program in these cells is typically accomplished over a

period of 7-11 days by pulsed treatment with a hormonal cocktail. Differentiation regimens involve the treatment of post-confluent cells (cultured in the presence of fetal calf serum), with insulin, isobutylmethylxanthine (a phosphodiesterase inhibitor), and dexamethasone (a corticosteroid) for 4 days, followed by an additional 3 days of insulin only (48). Typically, by day 7 of treatment, greater than 90% of the cells will have differentiated into adipocytes. Preadipocytes differentiate into adipocytes in a process orchestrated by a set of interdependently acting transcription factors, including peroxisome-proliferator-activated receptors (PPARs), the CCAAT-enhancer-binding proteins, and the adipocyte differentiation and determination factor (ADD)-1, also known as the sterol regulatory element binding protein (SREBP)-1 (43). Together these transcription factors stimulate the expression of adipocyte-specific genes such as those for lipoprotein lipase (LPL), leptin and the fatty acid binding protein, aP2.

PPARs are members of the nuclear hormone receptor superfamily. After dimerization with the retinoic X receptor (RXR) and ligand activation, they control the expression of LPL, acyl coenzyme A synthase, fatty acid synthase (FAS) and phospho-enol pyruvate carboxykinase which are all involved in coordinating fatty acid uptake and storage (49, 50, 51). One of the PPARs, PPARγ2 was elegantly shown by Tontonoz *et al.* to be a key player in adipocyte differentiation (52, 53). The transcriptional activity of the PPARγ protein can be modulated by the binding of ligands, by post-translational modifications and by interaction with other nuclear receptors and various cofactors (43). Thiazolidinedione antidiabetic agents and prostaglandins J2 derivatives, which are synthetic and natural ligands of PPARγ respectively, all facilitate adipogenesis (43).

Figure 7: Summary of *in vitro* Adipocyte Differentiation

Individual discrete stages of *in vitro* adipocyte differentiation are depicted at the top along with a schematic illustration of the emerging phenotypes. Day of Differentiation refers to the time frame generally used in the laboratory when differentiating 3T3-L1 cells. Note that there is no time assigned to preconfluent or proliferating cells and also that on day 0 when cells are hormonally stimulated to differentiate they are confluent. Cells can be maintained for some time and continue to accumulate lipid beyond day 4, however, by that time there are significant intracytoplasmic lipid droplets detectable in most cells. The lower half of the figure depicts the temporal expression pattern of many genes regulated during 3T3-L1 adipocyte differentiation. Solid bars represent the approximate time period during the differentiation program when individual genes are expressed (they are not indicative of relative levels of expression).

Summary of in vitro Adipocyte Differentiation of 3T3-L1 Preadipocytes

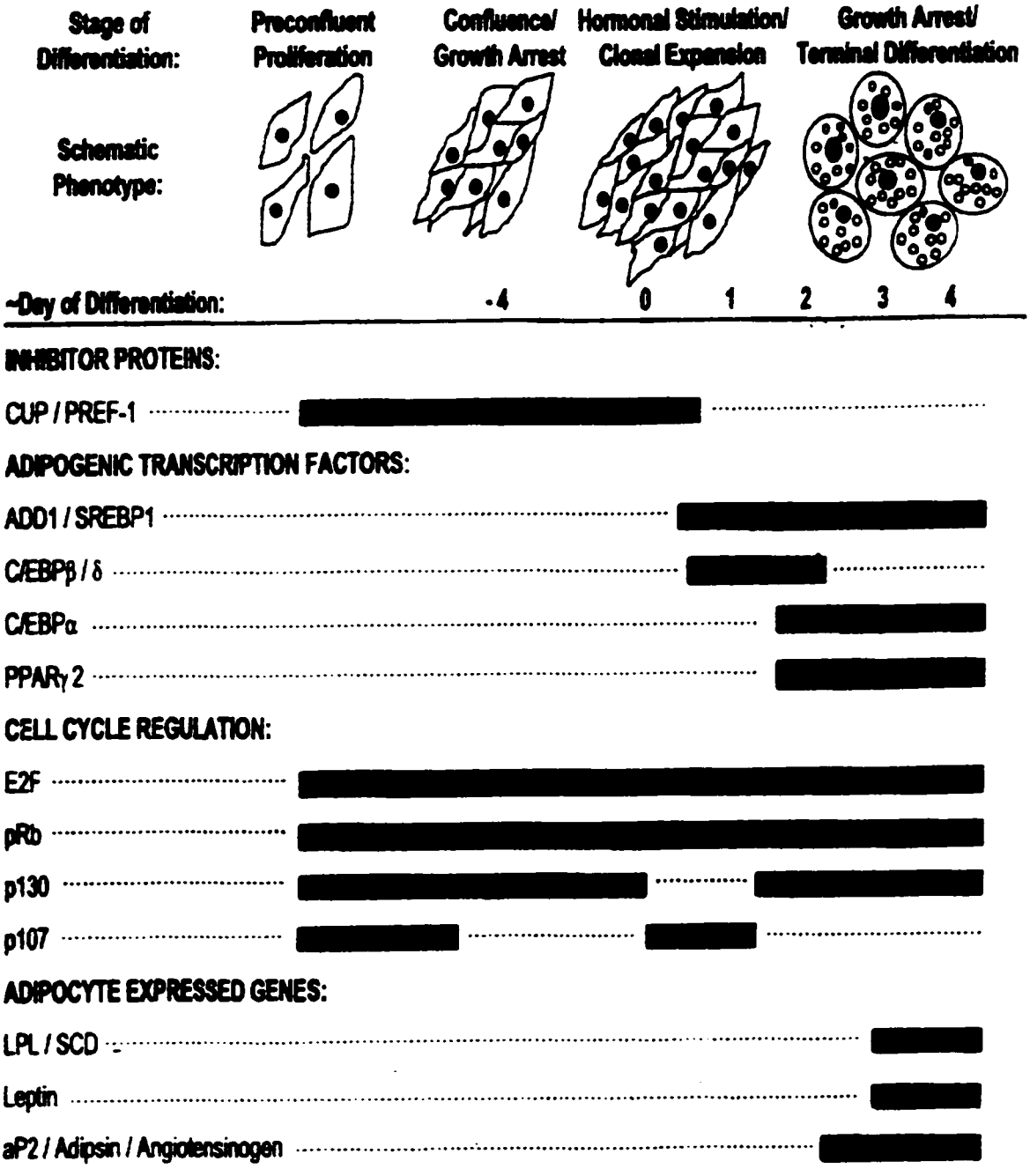

Three members of the C/EBP family of transcription factors- C/EBP α, β and γ, are expressed at defined times during adipogenesis (54). Adipogenic hormones such as glucocorticoids, cyclic AMP and insulin induce a transient increase in the expression of C/EBPβ and γ early in adipocyte differentiation (55). C/EBPβ, in synergy with C/EBPγ, then induces PPARγ expression in the preadipocyte, subsequently triggering full-blown adipocyte differentiation. C/EBPα plays an important role in the later stages of differentiation by sustaining high levels of PPARγ expression and by maintaining the differentiated adipocyte phenotype (43). Wang *et al.* showed one line of evidence to support this role for C/EBPα whereby adipocytes from mice in which the C/EBPα gene was disrupted by homologous recombination failed to accumulate lipids in adipose tissue (56).

ADD-1 and SREBP-1, which are rodent and human homologs, were independetly cloned and characterized as transcription factors implicated, respectively, in the control of adipocyte differentiation (57) and in cholesterol-regulated transcription (58). The expression of ADD-1/SREBP-1 is induced during differentiation of adipocytes, where it activates transcription of target genes involved in both cholesterol metabolism and fatty acid metabolism (59). Direct evidence of the adipogenic effect of ADD-1/SREBP-1 was provided by its capacity to induce fat accumulation and adipocyte differentiation when over expressed in fibroblasts with a retroviral vector (59).

There are factors that are involved either in the reversal and/or inhibition of the adipogenesis process. Exposure of 3T3-L1adipocytes to TNF-α results in lipid depletion and a complete reversal of adipocyte differentiation. TNF-α exerts its anti-adipogenic action by downregulating the expression of C/EBPα and PPARγ (43). Another inhibitory

molecule is retinoic acid (RA). RA blocks adipogenesis by interfering with C/EBPbeta-mediated transcription, which is only essential in the early stages of adipogenesis (60). In addition, RA can inhibit PPARγ action by displacement of the active PPARγ-RXR heterodimer from its response element. RA favors the formation of the inactive RAR-RXR heterodimer over the PPAR-RXR dimer (43). Another factor with anti-adipogenic activity is Pref-1. Pref-1 is expressed in preadipocytes but is absent in adipocytes and its constitutive expression inhibits expression of PPARγ and C/EBPα suggesting that it acts as negative regulator of adipocyte differentiation (61).

3.2 REGULATION OF ADIPOSE CELL NUMBER IN MAN

Adipocyte size and number appear to be regulated in a coordinated manner. In weight gain, adipocyte volume and number increase. Similarly, when adipose loss occurs, adipocyte volume and number decrease. This suggests that local (paracrine) systems may be in part responsible for the regulation of adipose mass (62). Lipogenesis and lipolysis are well-characterized processes affecting adipose cells (63). Insulin and acylating stimulating protein are the major lipogenic influences and catecholamines, thyroid hormones and growth hormone are the major lipolytic influences (64).

The identification of adipocyte stem cells (preadipocytes) and the recognition of the adipocyte replication/differentiation program provided a mechanism by which adipose cells could be acquired at any stage of life. Inversely, two distinct mechanisms of adipocyte loss have been described – dedifferentiation and apoptosis. Adipocyte dedifferentiation is the in vitro process in which terminally differentiated cells revert

morphologically and biochemically to preadipocytes (62). These reverted cells have lost cytoplasmic lipid and display the gene expression patterns of preadipocytes. Further studies by Petruschke and Hauner (65) have demonstrated that tumour necrosis factor induces dedifferentiation in human adipocytes. Prins *et al.* demonstrated that human adipocyte apoptosis may be induced *in vitro* and that it occurs *in vivo*, at least in a proportion of patients with malignancy (62).

In adipose tissue, known molecular regulators of adipose cell number include insulin, ligands for the peroxisome proliferator activated receptor-γ, retinoids, corticosteroids and tumour necrosis factor-α. The net effect of these is the concerted alteration in adipocytes volume and number (62). Insulin is the classical anabolic hormone and when in excess, appears to promote adipose tissue gain (66). This appears to occur disproportionately in the visceral depot, and is seen in patients with the syndrome of hyperinsulinaemia, hypertension, hyperlipidaemia (Syndrome X) (67), and patients with non-insulin dependent diabetes (68). That the adipose deposition is visceral in all these groups indicates that the distribution pattern cannot be explained by portal-systemic differences in insulin concentrations, and therefore is likely to reflect site-related differences in the (pre) adipocyte response to insulin (62).

Overall regulation of adipose mass involves endocrine, paracrine, and possibly autocrine systems. Hypothalamic centers appear to control appetite, metabolic rate and activity levels in a co-ordinated manner. Within the hypothalamus, known weight regulatory molecules include glucagon-like peptide-1, neuropeptide Y and leptin. Leptin is a peptide hormone that has the effect of reducing food intake, increasing metabolic rate

and causes significant adipose tissue loss when administered parenterally to *ob/ob* mice (which lack intact leptin) and normal rodents (62).

4.INSULIN SIGNALING SYSTEM

4.1 INSULIN AND ITS RECEPTOR

Human insulin has a molecular weight of 6,000 daltons and consists of two chains held together by two sulfhydryl bonds (Fig 8). The A-chain consists of 21 amino acids and possesses an intra-sulfhydryl bridge between amino acids 6 and 11 and the B-chain is comprised of 30 amino acids. Studies have shown that amino acids 24 to 26 of the B-chain and the amino terminal of the A-chain are extremely important in maintaining the molecule's structural integrity and hence, binding capabilities. Insulin mediates a wide spectrum of biological responses including stimulation of glucose uptake (in muscle and adipose tissue), glycogen, lipid and protein synthesis, antilipolysis, activation of transcription of specific genes, and modulation of cellular growth and differentiation (69). The insulin receptor is an alpha2/beta2 tetramer (Fig 9). The alpha-subunit is located entirely at the extracellular face of the plasma membrane and contains the insulin-binding site whereas the beta-subunit is a transmembrane peptide (69). This dimer of two alpha- and two beta-subunits is held together by an inter alpha-alpha and two inter-alpha-beta disulfide bonds (70). The intracellular portion of the beta-subunit contains the insulin-regulated tyrosine protein kinase (71). Insulin binding activates the tyrosine kinase leading to autophosphorylation of tyrosine residues in several regions of the intracellular beta-subunit and various cellular proteins (72).

Figure 8: The Insulin Molecule

The structure represents the three-dimensional structure of the porcine insulin molecule as determined by X-ray crystallography and molecular model computer generation. Numbers on the backbone molecule correspond to the amino acids numbered from the amino-terminal end of the protein chains. –S-S- denotes disulfide bridges between amino acids. The inserted legend lists the amino acid sequence for both the A chain and the B chain and shows inter- and intra-disulfide bridges for porcine insulin.

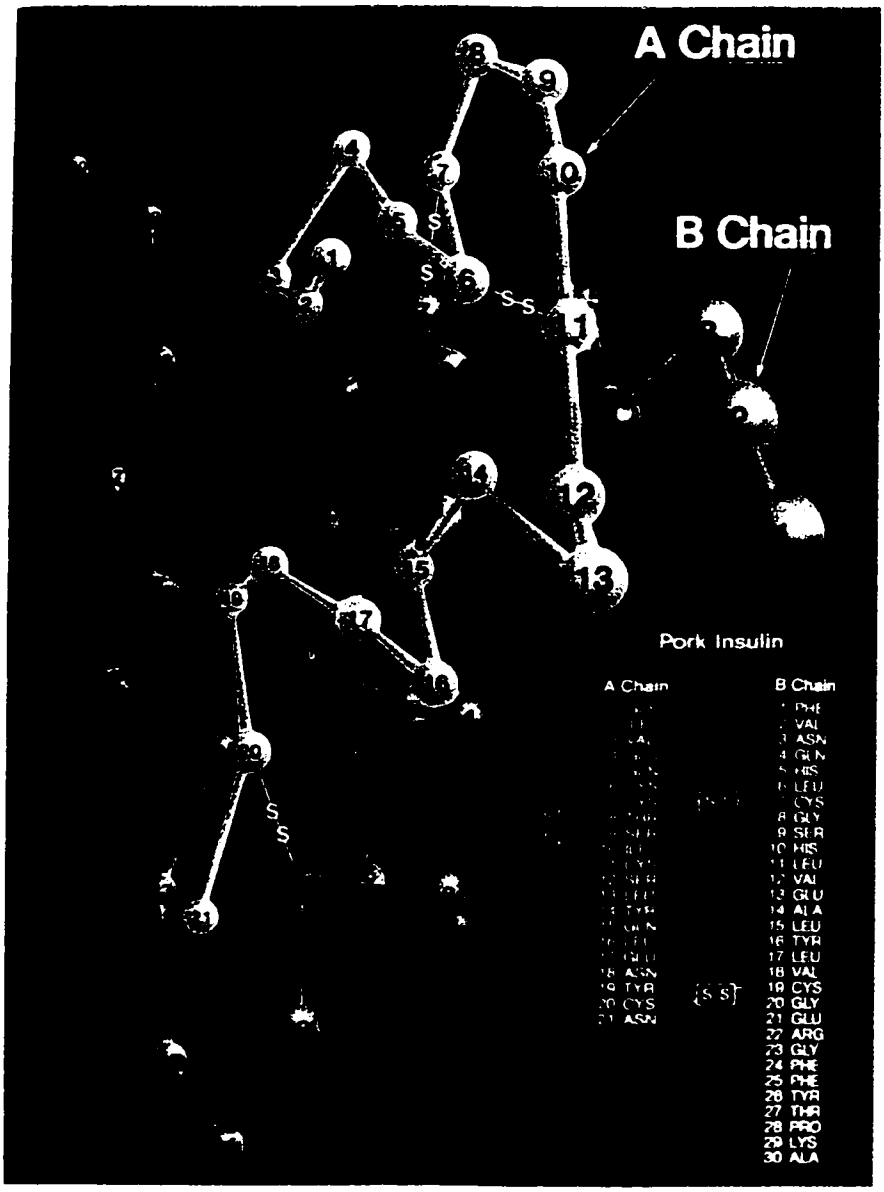
A Chain
B Chain
Pork Insulin
A Chain
B Chain
1 PHE
2 VAL
3 ASN
4 GLN
5 HIS
6 LEU
7 CYS
8 GLY
9 SER
10 HIS
11 LEU
12 VAL
13 GLU
14 ALA
15 LEU
16 TYR
17 LEU
18 VAL
19 CYS
20 GLY
21 GLU
22 ARG
23 GLY
24 PHE
25 PHE
26 TYR
27 THR
28 PRO
29 LYS
30 ALA

Figure 9: Structure of the Insulin Receptor

The insulin receptor is depicted. The α-subunit is composed of 723 amino acids and has the insulin-binding domain. • cysteine residues: broken lines, disulfide bridges. The β-subunit has 620 amino acids and 3 compartmental domains: extracellular, transmembrane, and cytosolic. Cytosolic domain has 3 clusters of tyrosine residues that can be phosphorylated on insulin binding (represented as Pi in a circle) and exogenous tyrosine kinase activity. Both β-subunits are phosphorylated; phosphotyrosines are only depicted on one-half for convenience.

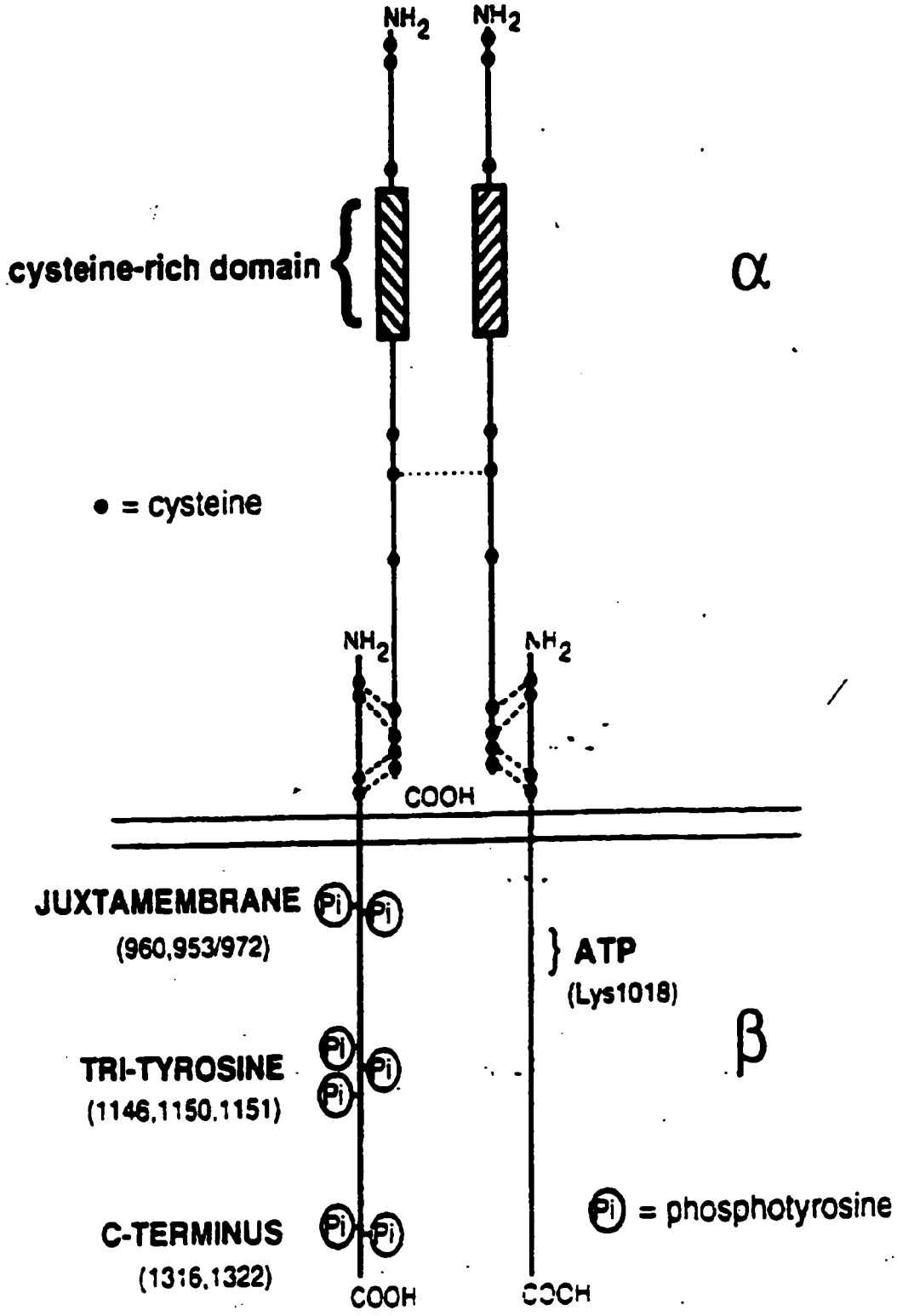
NH2
NH2
cysteine-rich domain
α
• = cysteine
NH2
NH2
COOH
JUXTAMEMBRANE
(960,953/972)
Pi
Pi
} ATP
(Lys1018)
β
TRI-TYROSINE
(1146,1150,1151)
Pi
Pi
Pi
C-TERMINUS
(1316,1322)
Pi = phosphotyrosine
COOH
COOH

4.2 INSULIN INTERNALIZATION AND DEGRADATION

The initial cellular processing of insulin and the insulin receptor includes binding of the ligand to the receptor and endocytosis of the ligand-receptor complex (73, 74, 75). Shortly after internalization, dissociation occurs within an acidic endosomal vesicle (14). Following dissociation, morphological (76) as well as subcellular fractionation techniques (77) have demonstrated that receptor and ligand physically segregate and move into separate vesicular structures. Most of the internalized insulin is targeted into a pathway where the ligand is degraded to low molecular weight products, which are then released from the cell (78, 79). A smaller fraction of internalized insulin traverses a non-degradative, retroendocytotic pathway and is released intact. In contrast, only a small fraction of internalized receptors are degraded and most are recycled back to the plasma membrane to be reutilized (80, 81).

4.3 INSULIN SIGNALING CASCADE

Many of the molecular actions of insulin involve protein phosphorylation and dephosphorylation. Although the insulin receptor is a tyrosine kinase that undergoes ligand-dependent activation, many of the resulting downstream changes in phosphorylation/dephosphorylation occur on serine and threonine (69). The following will review the signaling cascade responsible for translating the binding of insulin to its receptor into endpoint biological responses, with specific focus on the molecular mechanisms mediating stimulation of glucose uptake (Fig 10).

Figure 10: Insulin Signalng Pathways that Regulate Glucose Metabolism in Adipocytes

Glut 4 is stored in intracellular vesicles. Insulin binds to its receptor in the plasma membrane, resulting in phosphorylation of the receptor and insulin-receptor substrates such as IRS molecules. These substrates form complexes with docking proteins such as phosphoinositide-3-kinase at its 85-kd subunit (p85) by means of SH2 (Scr homology region 2) domains. Then p85 is constitutively bound to the catalytic subunit (p110). Activation of phosphoinositide-3-kinase is a major pathway in the mediation of insulin-stimulated glucose transport and metabolism. It activates phosphoinositide-dependent kinases that participate in the activation of protein kinase B/Akt and atypical forms of protein kinase C (PKC).

Insulin Signaling Pathways That Regulate Glucose Metabolism in Adipocytes

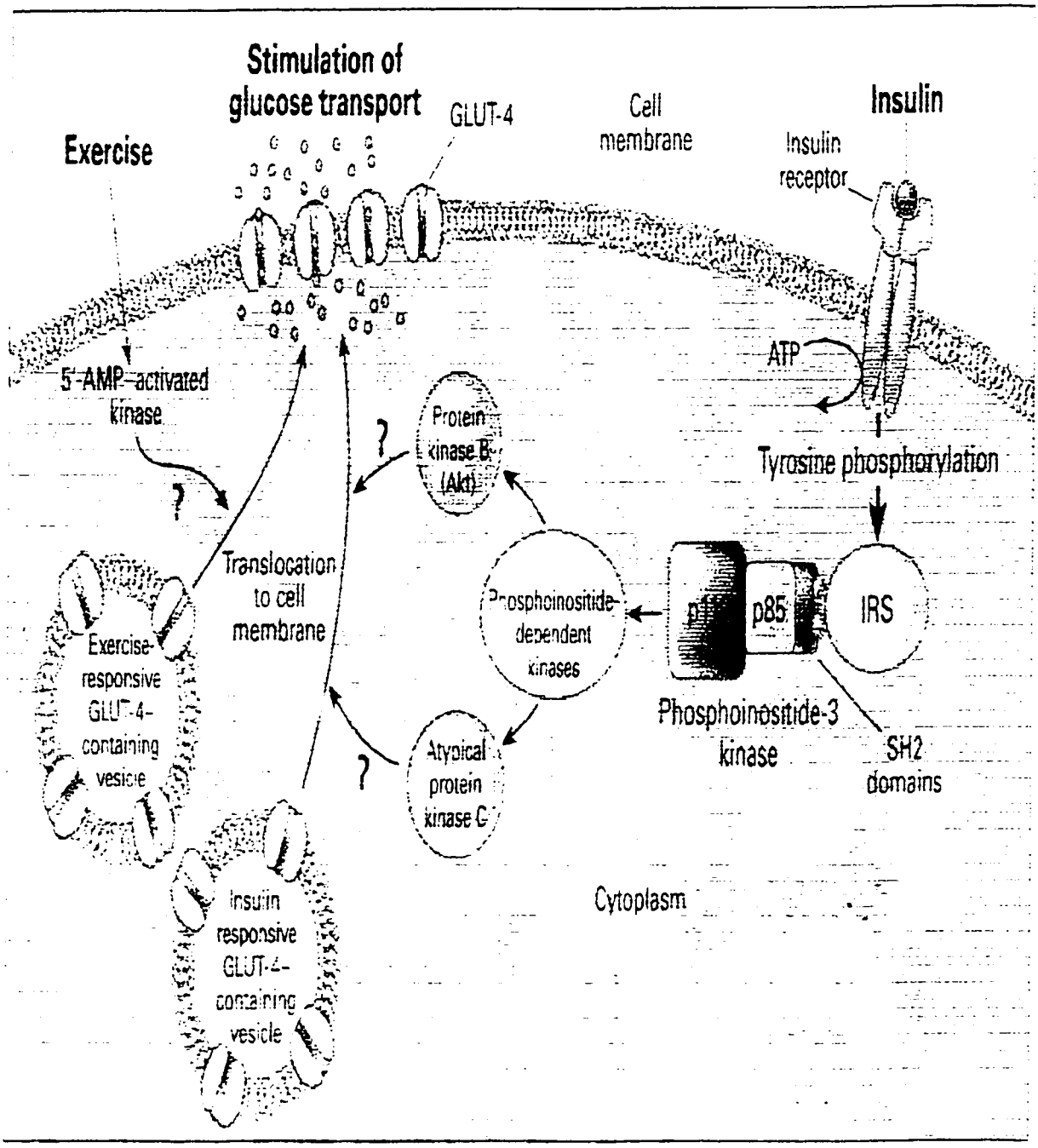

Insulin binding activates the tyrosine kinase leading to the autophosphorylation of tyrosine residues and the tyrosine phosphorylation of the IRS-1 proteins. The insulin receptor substrate-1, IRS-1, was the first docking protein identified and serves as the prototype for this class of molecules. Three related proteins have recently expanded this family, including IRS-2, IRS-3 and IRS-4 (69). All the IRS-proteins have the same overall architecture: an NH_2 –terminal pleckstrin homology (PH) and/or phosphotyrosine-binding (PTB) domains; multiple tyrosine residues that create SH2-binding sites; proline-rich regions to engage SH3 or WW domains; and serine/threonine-rich regions (82). The PTB domain provides IRS-1 coupling to the insulin receptor. This domain binds specifically to the phosphorylated NPXY motif in the juxtamembrane region of the insulin receptor (83). Inoue *et al.* (84) showed that tyrosine phosphorylation of IRS-1 occurs mainly in the intracellular membrane (IM) compartment with relatively low levels in the cytosol, implying a localization of signaling by this substrate of the insulin receptor.

Tyrosine-phosphorylated IRS-proteins generate downstream signals by the direct binding to the SH2 domains of various enzymes and adaptor proteins like phosphatidylinositol-3-kinase (PI3-kinase), phosphotyrosine phosphotase, SHP2, Grb2, and Nck (82). PI3-kinase plays a major role in many insulin-regulated responses including stimulation of glucose transport. PI3-kinase exists as a heterodimer, which consists of an adaptor 85-kDa subunit tightly, associated with a catalytic 110-kDa subunit (85, 86). PI3-kinase catalyzes the phosphorylation of phosphoinositides at the D3 position of the inositol ring (87). PI (3,4,5)P_3 is the major lipid product formed by PI3-kinase when activated by insulin (69). In 1990, experiments by Endeman and Ruderman *et al.* (69) demonstrated that insulin treatment increases PI3-kinase activity in phosphotyrosine immunoprecipitates.

Insulin, at concentrations as low as 0.3 nmol/L, stimulates the accumulation of PI (3,4,5)P_3 by about 10 times basal levels within 5 minutes. PI3-kinase association to IRS-1 is greater in the IM than in the cytosol (84). Inoue *et al.* observed an insulin-stimulated recruitment of PI3-kinase from the cytosol to the IM suggesting that the activated insulin receptors continue to phosphorylate IRS-1 in the IM, leading to a continuous recruitment of PI3-kinase to the IM (84).

Several enzymes appear to carry the signal initiated by PI3-kinase activation to its final destination. PKB is thought to be downstream of PI3-kinase and has been implicated in regulating GLUT 4 translocation and glucose uptake. Protein kinase B, PKB, is the cellular homologue of the transforming oncogene v-akt (88). PKB is a PH domain-containing serine/threonine kinase (89). Three isoforms of PKB have been identified. PKB-α is the major isoform activated by insulin in muscle, hepatocytes, and adipocytes. PKB-β is activated in adipocytes only. PKBγ is activated by insulin in cell culture models (90). It is now accepted that the primary mechanism for the activation of PKB by insulin is phosphorylation of two sites, Thr 308 and Ser 473 in PKB-α. Phosphorylation at Thr 308 (PKB-α), Thr 309 (PKB-β), Thr 305 (PKB-γ) is achieved by the recently cloned PDK1 (phosphoinositide-dependent protein kinase). The kinase responsible for Ser 473 phosphorylation has not been cloned yet, but has been named PDK2 (91). Taken together, the accepted mechanism for PKB activation involves interaction with PI (3,4,5)P_3 through its PH domain. This interaction with phosphoinositol lipids recruits PKB to the plasma membrane and results in conformational changes in PKB so that Thr and Ser become accessible to phosphorylation by PDK1 and PDK2, respectively (92, 93). Overexpression of wild-type or constitutively active PKB-α results in upregulation of glucose transport and

redistribution of GLUT 4 to the plasma membrane in muscle and fat cells and insulin increases the association of PKB-β with GLUT 4-containing vesicles (69).

Insulin-stimulated glucose transport can be accounted for primarily by translocation of glucose transporters, mainly GLUT 4, from intracellular pools to the plasma membrane. Martin *et al.* found, using cryosections of 3T3-L1 adipocytes, that GLUT 4 is largely distributed between the TGN (trans-golgi network), endosomes and tubulo-vesicular elements in basal cells, but the major effect of insulin is on the tubulo-vesicular elements located in the peripheral cytoplasm (94). Observations by Martin *et al.* are consistent with a model in which GLUT 4 is selectively targeted to a compartment under basal conditions that is specifically affected by insulin. This is through the generation of specific exocytotic GLUT 4 vesicles, similar to synaptic vesicles, or through concentration and retention in sub-domains of the endosomal system. The v-snare, vamp2, has been implicated in the insulin dependent trafficking of GLUT 4 and VAMP2 is highly co-localised with GLUT 4 in adipocytes (94, 95). Martin *et al.* concluded that insulin-responsive vesicles are competent to dock and fuse directly with the plasma membrane in an analogous manner to synaptic vesicles (95).

4.4 REGULATION OF THE INSULIN SIGNALING SYSTEM

Insulin can simultaneously stimulate the phosphorylation of some proteins and the dephosphorylation of others. One tyrosine phosphatase, PTPase 1B, has emerged as a possible candidate for a negative regulator of insulin action because of its ability to dephosphorylate the insulin receptor in vitro (69).

INSULIN SIGNALING AND ACTION IN ADIPOCYTES

5.1 INSULIN STIMULATED GLUCOSE UPTAKE

Glucose is an important source of energy for most living organisms. Tissues such as the brain need glucose constantly, and low blood concentrations of glucose can cause seizures, loss of consciousness, and death. However, prolonged elevation of blood glucose concentrations, as in poorly controlled diabetes, can result in blindness, renal failure, cardiac and peripheral vascular disease, and neuropathy. During fasting, most of the glucose in the blood is supplied by the liver, independently of insulin. After a meal, the rise in blood glucose levels rapidly stimulates insulin secretion, which results in increased glucose transport, metabolism, and storage by muscle and adipocytes. In addition, insulin inhibits glucagon secretion and lowers serum free-fatty-acid concentrations, contributing to the sharp decline in hepatic glucose production (96). The adipocyte contains two isoforms of a family of proteins that facilitate transport of glucose across the plasma membrane: GLUT 1, the constitutive glucose transport and GLUT 4, the insulin-sensitive glucose transporter. Both of these are proteins are integral membrane proteins (97). In regard to diffentiating 3T3-L1 preadipocytes, GLUT 1 is present in both phenotypes, fibroblast and adipocyte, while GLUT 4 is expressed only in the latter phenotype (98). GLUT 1 is distributed between the plasma membrane and an intracellular vesicular storage site (99). GLUT 4 under basal conditions resides almost exclusively intracellularly but translocates to the plasma membrane when cells are acutely stimulated with insulin (100).

5.2 INSULIN RESISTANCE AND TYPE 2 DIABETES

Insulin resistance, defined as an impaired ability of cells or tissues to elicit a normal response to a given insulin concentration, is commonly seen in individuals at an increased risk for cardiovascular disease and type 2 diabetes (101, 102). Furthermore, insulin resistance precedes the development of type 2 diabetes and also identifies individuals at an increased risk for this disease (103, 104). Conditions known to be associated with insulin resistance, such as obesity, smoking, and treatment with certain drugs (i.e. HIV protease inhibitors), also carry an increased risk for the development of type-2 diabetes (105). Substantial efforts have been made to identify proteins that impair critical steps in insulin signal transduction in individuals with insulin resistance.

In 1999, Carvalho *et al.*, investigated the development of insulin resistance in healthy, nondiabetic subjects and found that low IRS-1 expression, defined as <50% of normal, identified individuals with insulin resistance. Furthermore, this expression was associated with a larger waist/hip circumference ratio, a well-established marker for insulin resistance and propensity for type-2 diabetes (106). Recently, Carvalho *et al.*, found that low IRS-1 expression is associated with a marked impairment in donwstream insulin signaling, including PI3-kinase activation and serine phosphorylation of PKB/Akt; maximally insulin-stimulated glucose transport is impaired; and GLUT 4 protein expression is also markedly reduced. In fact, all these perturbations are similar, in terms of extent and proteins involved, to what is seen in fat cells from subjects with manifest type-2 diabetes. In addition, they observed a low mRNA expression for both IRS-1 and GLUT 4

in diabetic cells compared to the control group, suggesting that this expression occurs at the level of gene transcription (105).

Impairment of insulin stimulated glucose uptake may also result from the up-regulation of proteins that inhibit the signaling pathways. The increased expression and activity of several protein-tyrosine phosphatases (PTPs) has been observed in skeletal muscle and adipose tissue in insulin-resistant, obese states in rodents and humans. Venable *et al.* showed that high level overexpression of PTP1B (non-transmembrane tyrosine phosphatase) in 3T3-L1 adipocytes leads to a substantial impairment of tyrosyl phosphorylation of the insulin receptor and IRS-1, and a comparable decrease in insulin-stimulated PI3-kinase activity (107). However, these biochemical consequences were not sufficient to affect insulin-stimulated glucose transport over a wide range of insulin concentrations. Thus, their results suggest that PTP1B overexpression alone is unlikely to have significant effects on glucose disposal in fat cells.

5.3 TRIACYLGYLCEROL SYNTHESIS

Fatty acids are stored for future use as triacylglycerols in all cells, but primarily in adipocytes. Triacylglycerols constitute molecules of glycerol to which three fatty acids have been esterified. The major building block for the synthesis of triacylglycerols, in tissues other than adipose tissue, is glycerol. Adipocytes lack glycerol kinase, therefore,

Figure 11 : Triacylglycerol Synthesis

The following depicts the pathway for triacylglycerol synthesis in adipocytes, via the production of dihydroxyacetone phosphate from glucose during glycolysis. Reduction of dihydroxyacetone phosphate is catalyzed in adipocytes by glycerol phosphate dehydrogenase. Glycerol-3-phosphate is joined to two fatty acyl groups to form diacylglycerol-3-phosphate, also known as phosphatidic acid, which is a precursor to phospholipids and triacylglycerols . Conversion to triacylglycerols involves hydrolysis of the phosphate group to form diacylglycerol followed by addition of a third acyl group from a fatty acyl-CoA.

Phosphatidic Acid Synthesis

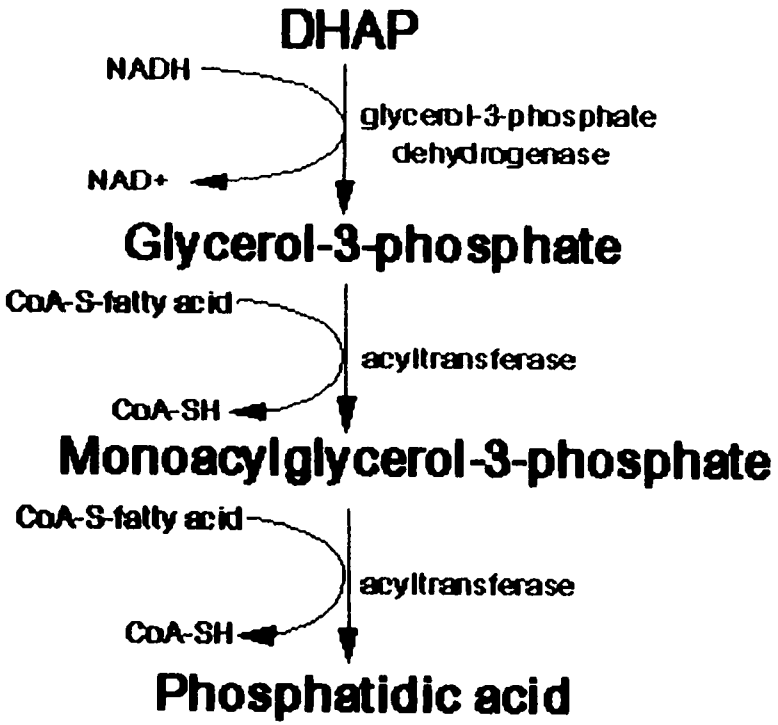

Triacylglycerol Synthesis

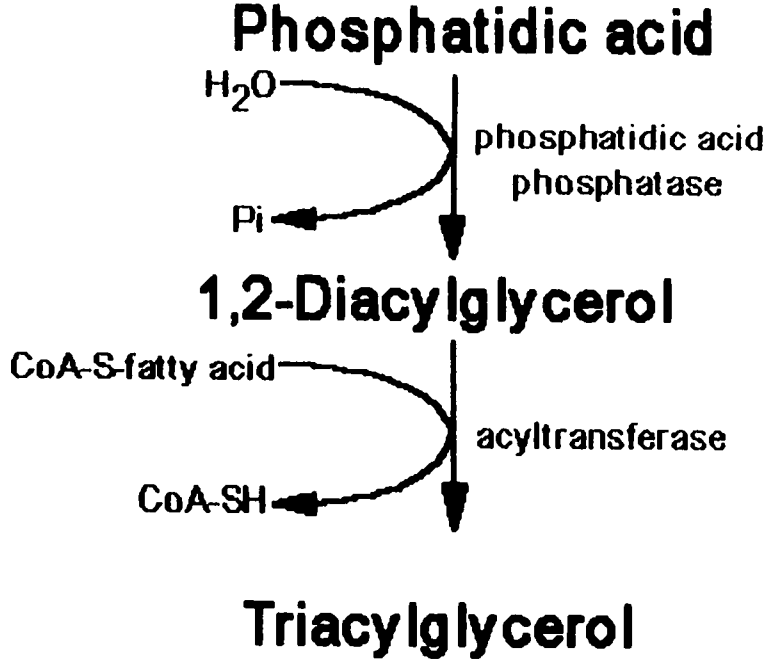

dihydroxyacetone phosphate (DHAP), produced during glycolysis, is the precursor for triacylglycerol synthesis in adipose tissue. This means that adipocytes must have glucose to oxidize in order to store fatty acids in the form of triacylglycerols. The glycerol backbone of triacylglycerols is activated by phosphorylation at the C-3 position by glycerol kinase. The utilization of DHAP for the backbone is carried out through the action of glycerol-3-phosphate dehydrogenase, a reaction that requires NADH. The fatty acids incorporated into triacylglycerols are activated to acyl-CoAs through the action of acyl-CoA synthethases. Two molecules of acyl-CoA are esterified to glycerol-3-phosphate to yield 1,2-diacylglycerol phosphate (phosphatidic acid). The phosphate is then removed, by phosphatidic acid phosphatase, to yield 1,2-diacylglycerol, the substrate for addition of the third fatty acid (Fig 11 & 12). Intestinal monoacylglycerols, derived from the hydrolysis of dietary fats, can also serve as substrates for the synthesis of 1,2-diacylglycerols. Glucose acts as a sensor in adipose tissue metabolism. When glucose levels are adequate, continuing production of glycerol-3-phosphate for synthesis of triacylglycerols. When intracellular glucose levels fall, the concentration of glycerol-3-phosphate falls also, and fatty acids are released from adipocytes for export as the albumin complex to other tissues (108).

Figure 12 : Triacylglycerol Synthesis in Adipocytes

Insulin stimulates glucose uptake into adipose cells, at least partly by translocating the glucose transporter (a membrane protein that carries out facilitated diffusion of glucose) from the cytosol (where it resides in the absence of insulin) to the cell surface, in response to insulin. The glucose is converted to dihydroxyacetone phosphate (DHAP) via the glycolytic pathway and is oxidized to glycerol-3-phosphate, which then becomes the glycerol backbone for triacylglycerol synthesis. The fatty acids incorporated into triacylglycerols are activated to acyl-CoAs through the action of acyl-CoA synthethases.

Triacylglycerol Synthesis in Adipose Tissue

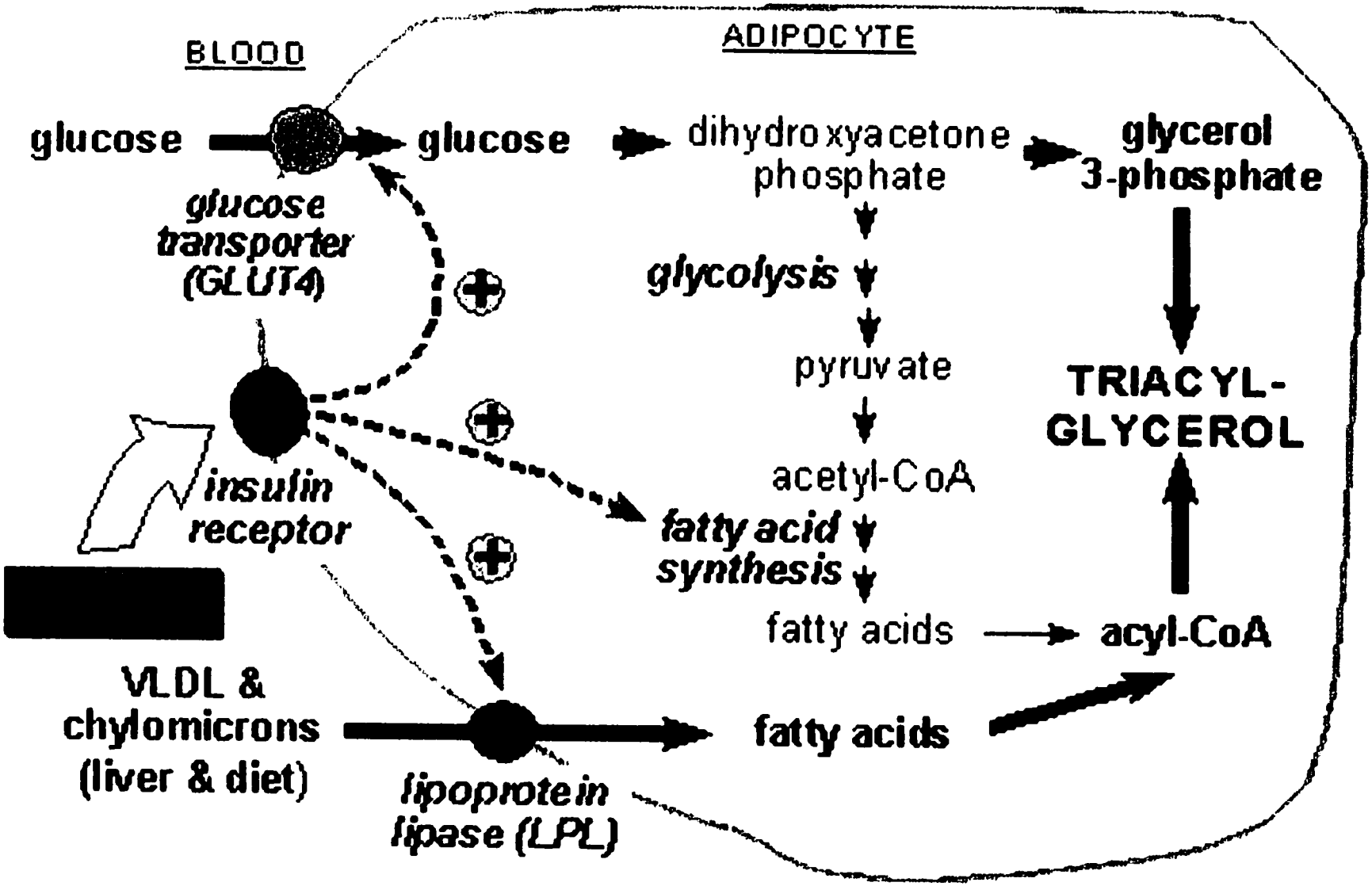

5.4 Regulatiom of Fatty Acid Metabolism

Insulin resistance is characterized by impaired responsiveness to endogenous or exogenous insulin. Loss of responsiveness is associated with a "clustering" of cardiovascular risk factors that includes abdominal obesity, hypertension, dyslipidemia, glucose intolerance, hyperinsulinemia, and non-insulin dependent diabetes mellitus (NIDDM); this association is referred to as the insulin resistance syndrome (IRS). Insulin's glucoregulatory effects are predominantly exerted in three tissues: liver, muscle, and fat. In the liver, insulin inhibits the production of glucose by inhibiting gluconeogenesis and glycogenolysis and also promotes glycogen storage (108). In muscle and adipose tissue, insulin stimulates the uptake, storage, and metabolism of glucose.

A complete understanding of the mechanism responsible for insulin resistance is currently not available. Defects leading to insulin resistance may occur at several levels: prereceptor (abnormal insulin), receptor (decreased receptor number or affinity), glucose transporter (decreased GLUT 4 molecules), or postreceptor (abnormal signal transduction and phosphorylation) (109). NIDDM is associated with resistance to the ability of insulin to inhibit hepatic glucose output and stimulate the uptake and use of glucose by fat and muscle (108). The number of insulin receptors is somewhat decreased in several tissues of non-diabetic obese patients and lean or obese patients with NIDDM, possibly as a result of receptor down-regulation due to basal hyperinsulinemia (108). The ability of insulin to stimulate autophosphorylation and tyrosine kinase activity is impaired in insulin receptors derived from fat, skeletal muscle, liver, of patients with NIDDM.

There is now mounting evidence that elevated insulin levels can contribute to the development of plasma lipid abnormalities and atherosclerosis. The characteristic lipid

profile in an individual with NIDDM includes decreased serum HDL-cholesterol (HDL-C), increased serum very low density lipoprotein (VLDL), elevated small, dense low density lipoprotein (LDL) and an increase in triglyceride levels (110). Insulin resistance impairs the normal suppression of free fatty acid (FFA) release from adipose tissue in the postprandial state (109). Increased FFA released from abdominal adipose tissue and delivered to the liver by the portal circulation, offers a substrate for increased synthesis of triglycerides (a rate-limiting step in the production of VLDL), lowers glucose uptake, and stimulates hepatic glucose production. Hyperinsulinemia also downregulates the activity of lipoprotein lipase, an enzyme important for VLDL metabolism (109). Thus, hyperinsulinemia increases production and decreases metabolism of VLDL resulting in high plasma triglyceride concentrations. HDL particles are synthesized by the liver but are also derived from liver metabolism of VLDL remnants and dietary lipids. Therefore, reduced VLDL metabolism contributes to a decrease in plasma HDL. Individuals with insulin resistance syndrome have a 43% decrease in LPL enzymatic activity, so that less VLDL triglyceride is taken by fat tissue (110) (Fig 13).

Figure 13 : Overview of the alterations in plasma lipid transport and lipoprotein metabolism observed in visceral obesity. Altered sex steroid and glucocorticoid levels have been associated with the insulin resistant-hyperinsulinaemic state,which characterizes visceral obesity. The specific enlargement of visceral adipocytes is associated with increased free fatty acids (FFA) levels in the portal and systemic circulations. This leads to an increased triglyceride synthesis and VLDL secretion, which by itself may exacerbate the insulin-resistant state. The slower catabolism of triglyceride-rich lipoproteins due to a reduced lipoprotein lipase (LPL) activity in the skeletal muscle and a blunted response of adipose tissue LPL during meals may explain the reduced plasma HDL-cholesterol levels in visceral obesity. Hepatic triglyceride lipase activity is also increased which leads to a further reduction in plasma HDL-cholesterol levels. The elevated triglyceride levels also favour the transfer of lipids among lipoproteins, leading to the triglyceride enrichment of HDL and LDL, whereas VLDL are enriched cholesterol esters, a process that is believed to be atherogenic. The small triglyceride-rich LDL and HDL particles are good substrates for the enzyme hepatic-triglyceride lipase, leading to the formation of dense LDL particles which show elevated concentrations in coronary heart disease patients.

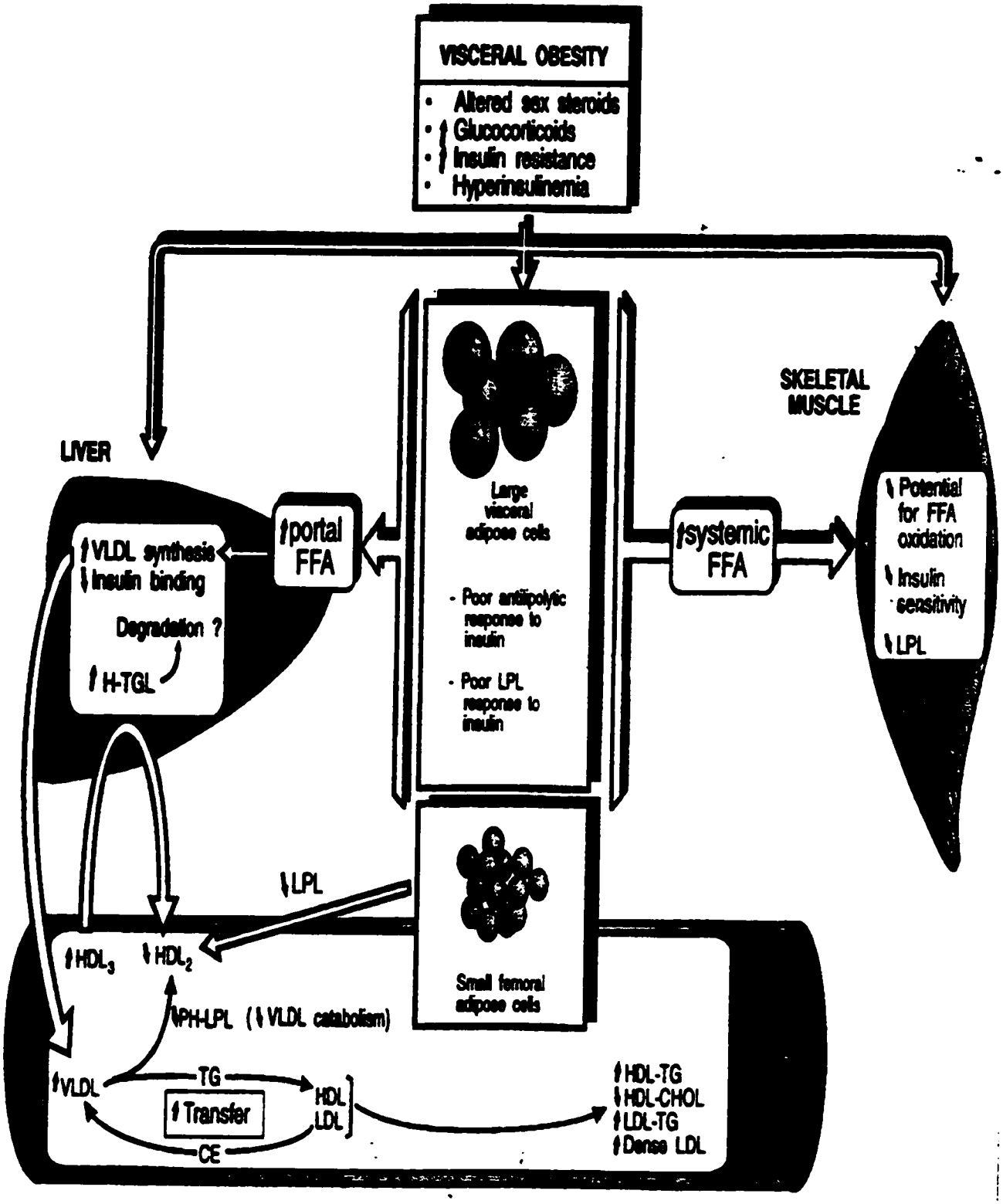
VISCERAL OBESITY
• Altered sex steroids
• ↑ Glucocorticoids
• ↑ Insulin resistance
• Hyperinsulinemia
LIVER
SKELETAL MUSCLE
Large visceral adipose cells
- Poor antilipolytic response to insulin
- Poor LPL response to insulin
↑portal FFA
↑systemic FFA
↑VLDL synthesis
↓Insulin binding
Degradation ?
↑H-TGL
↓Potential for FFA oxidation
↓Insulin sensitivity
↓LPL
↓LPL
Small femoral adipose cells
↑HDL3
↓HDL2
↑PH-LPL (↓VLDL catabolism)
↑VLDL
TG
↑Transfer
CE
HDL
LDL
↑HDL-TG
↓HDL-CHOL
↑LDL-TG
↑Dense LDL

6.0 LIPOLYSIS

6.1 MECHANISMS REGULATING ADIPOCYTE LIPOLYSIS

The primary sources of fatty acids for oxidation are dietary and mobilization from cellular stores. Fatty acids from the diet are delivered from the gut to cells via transport in the blood. Fatty acids are stored in the form of triacylglycerols primarily within adipocytes. In response to energy demands, the fatty acids of stored triacylglycerols can be mobilized for use by peripheral tissues. The release of metabolic energy, in the form of fatty acids, is controlled by a complex series of interrelated cascades that results in the activation of hormone-sensitive lipase (HSL). The stimulus to activate this cascade, in adipocytes, can be glucagon, epinephrine or beta-corticotropin (112). These hormones mediate their actions via four adrenergic receptors: beta1, beta2, beta3 and alpha2. These adrenergic receptors are members of the superfamily of G-protein-coupled receptors that are characterized by 7 transmembrane spans of 20-28 hydrophobic amino acids, an extracellular amino terminus with glycosylation sites, and intracellular carboxyl terminus that is palmitoylated for stabilization of the protein in the membrane. The extracellular surface is critical for ligand binding, while the intracellular surface is involved in G-protein recognition and activation (113). Upon ligand binding, these receptors are coupled to the activation of adenylate cyclase. The resultant increase in cAMP leads to activation of PKA (112). The two main targets of PKA-mediated phosphorylation in the adipocyte are HSL and the perilipins, and the phosphorylation of these proteins dramatically increases lipolysis (114). Stimulation of adipocytes with catecholamines triggers the translocation of

HSL from the cytoplasmic compartment to the surface of the lipid droplets, a phenomenon that has been demonstrated both by subcellular fractionation experiments on primary adipocytes (115, 116) and by direct immunocytochemistry on 3T3-L1 adipocytes (117). A complementary mechanism precluding HSL binding to the lipid droplets in nonstimulated intact cells seems to rely on the perilipins. These are a family of closely related proteins located on the surface of the lipid droplet (118). It has been proposed that perilipins may create a protective barrier for the interaction of HSL with the lipds (119). On stimulation of the adipocytes, perilipin phosphorylation would relieve the restraint and allow phosphorylated HSL free access to the lipid droplet substrate, leading to initiation of TG hydrolysis (114). HSL hydrolyzes fatty acids from carbon atoms 1 or 3 of triacylglycerols (112). The resulting diacylglycerols are substrates for either HSL or the non-inducible enzyme diacylglycerol lipase (112). Finally the monoacylglycerols are substrates for monoacylglycerol lipase. The net result of the action of these enzymes is three fatty acids and one mole of glycerol (Fig 14). The free fatty acids diffuse from adipose cells, combine with albumin in the blood, and are thereby transported to other tissues, where they passively diffuse into cells (112).

Insulin, the most important physiological inhibitor of catecholamine-induced lipolysis, induces phosphorylation and activation of the phosphodiesterase type 3B (PDE3B), leading to a decrease in cAMP levels and concomitant decrease of PKA activity (121). Specific inhibition of PDE3B completely blocks the antilipolytic effect of insulin, indicating that cAMP degradation is the main mechanism whereby insulin antagonizes catecholamine-induced lipolysis (122) (Fig 14).

Figure 14: Hormone Induced Fatty Acid Mobilization in Adipocytes

Model for the activation of hormone-sensitive lipase by a catecholamine. Norepinephrine binds its' receptor and leads to the activation of adenylate cyclase. The resultant increase in cAMP activates PKA, which then phosphorylates and activates hormone-sensitive lipase. Hormone-sensitive lipase hydrolyzes fatty acids from triacylglycerols and diacylglycerols. The final fatty acid is released from monoacylglycerol lipase, an enzyme active in the absence of hormonal stimulation. Insulin inhibits the phosphorylation of adenylate cyclase to inhibit fat mobilization.

Hormone sensitive lipase

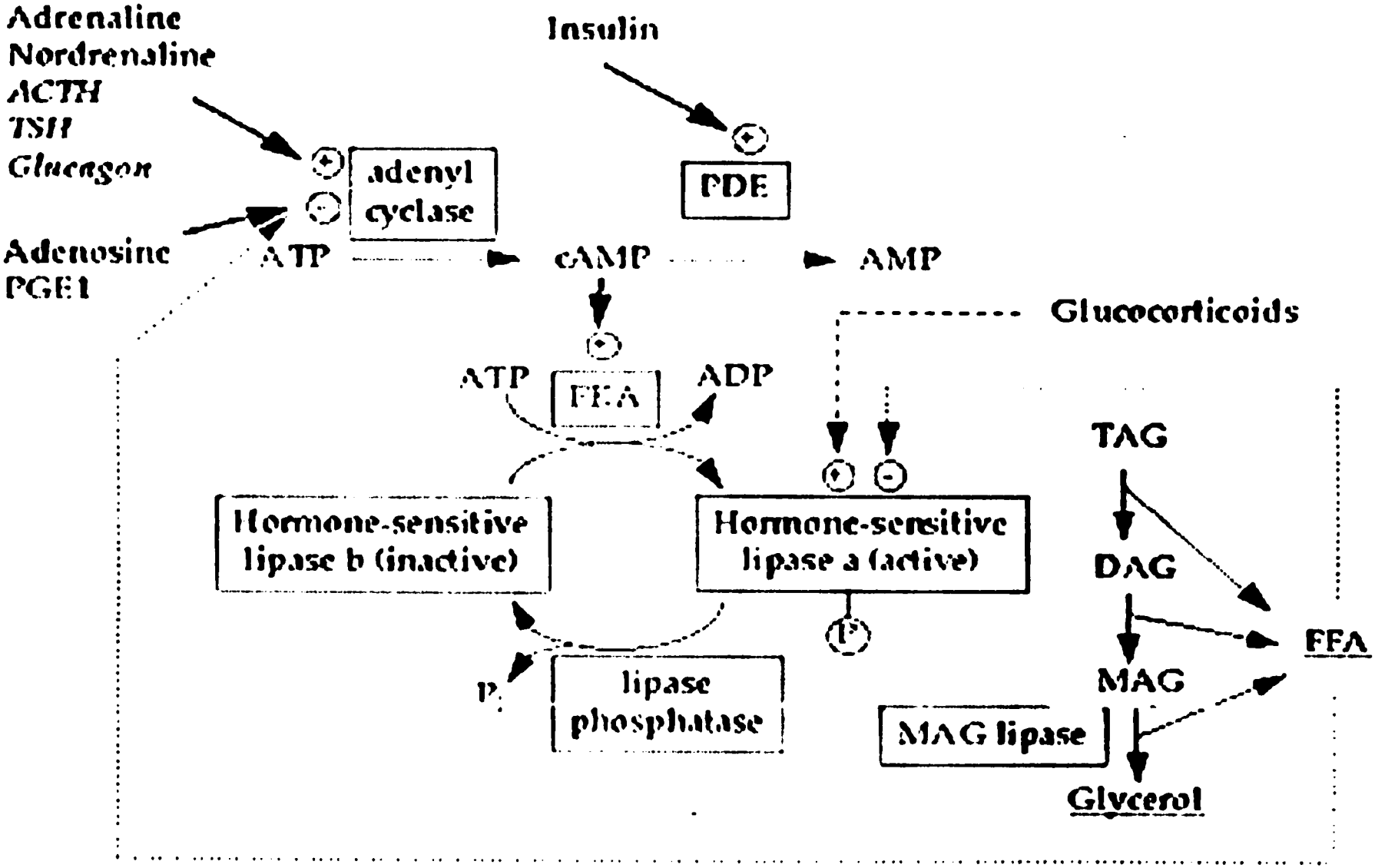

MATERIALS AND METHODS

1. Materials

Insulin (bovine pancreas) from Sigma (cat# I-5500). 3-Isobutyl-1-methyl-xanthine from Sigma (cat# I-5879). Dexamethasone and norepinephrine from Sabex. Humulin from Lilly. Glut 4 antibody from Alpha diagnostics International. IRS-1 and PI3-kinase antibodies from Upstate Biotechnology. Indinavir from Merck & Co.. Ritonavir from Abbott Laboratories. Saquinavir from Roche.

2. Cell Culture

3T3-L1 preadipocytes were cultured in 10% DMEM (containing 10% [v/v] fetal calf serum, pencillin [100 U/ml], and streptomycin [100 U/ml] at 37°C in a 5% CO_2 humidified incubator. 3T3-L1 fibroblasts were maintained and split before reaching 80% confluence. Upon reaching confluence, cells were subjected to differentiation with 1 ug/ml insulin, 0.5 mM isobutylmethylxanthine (IBMX), and 0.25 uM dexamethasone (Dex), in 10% DMEM for 4 days. The cells were then incubated in 10% DMEM and 1 ug/ml insulin for another 3 days, after which they were maintained in 10% DMEM for 4 days. All HIV protease inhibitors were dissolved in dimethylsulfoxide (DMSO) and then diluted with 10% DMEM. Since the compounds used in this study were solubilized in DMSO, control cells were treated with matching concentrations of DMSO and the final concentrations of DMSO were kept below 0.1%. HIV protease inhibitors were added throughout differentiation of 3T3-L1 preadipocytes as well as short- term during experiments, unless otherwise noted.

3. Oil Red Staining

3T3-L1 adipocytes were washed twice with PBS, and then fixed with 4% paraformaldehyde for 12 minutes. The cells were then washed again with PBS. The oil red stain (5% oil red in 70% pyridine) was applied for 30 minutes, and cells were washed three times with PBS (119).

4. Toxicity

The CellTiter 96 Aqueous Non-Radioactive Cell Proliferation Assay (Promega) is a colometric method determining the number of viable cells in proliferation. The assay is composed of solutions of a novel tetrazolium compound (3-(4,5-dimethylthiazol-2-yl)-5-(3-carboxymethoxyphenyl)-2-(4-sulphonyl)-2H-tetrazolium, inner salt;MTS) and an electron coupling reagent (phenazine methosulfate; PMS). MTS is bioreduced by cells into formazan that is soluble in tissue culture medium. The absorbance of the formazan at 490nm can be measured directly from 96 well plates. Dehydrogenase enzymes found in metabolically active cells accomplish the conversion of MTS into the aqueous soluble formazan. The amount of formazan product measured by the amount of 490nm absorbance is directly proportional to the number of living cells.

3T3-L1 preadipocytes were cultured and differentiated in 96-well plates. A volume of 20 ul of the MTS/PMS solution was added to each well. The plate was then incubated for 1-4 hours at 37°C in a humidified 5% CO_2 atmosphere. At this point, the absorbance at 490nm was recorded using an Elisa plate reader.

5. Insulin-Stimulated Triacylglycerol Synthesis

3T3-L1 preadipocytes were cultured and differentiated in 24 well plates at 1 x 10^4 cells/mL. At precisely 3 or 11 days post induction, 3T3-L1 cells were serum starved overnight in MEM, 5 mM glucose, and 0.1% BSA. The cells were then incubated with 3.35 nM insulin in MEM, 5mM glucose, and 0.1% BSA for 6 hrs. ^{14}C(U)-Glucose (2.21 dpm/pmole) was then added for 18 hrs at 37°C in a 5% CO_2 humid incubator (120). The cells were the placed on ice and the medium was removed, after which the cells were washed three times with PBS. Triglycerides were then extracted for 30 minutes with 2 X 1 mL of isopropanol:heptane (2:3 vol/vol) and collected (121). The incorporated ^{14}C(U)-glucose into triacylglycerols was then determined by scintillation counting. Soluble cell protein was then dissolved in 1 mL 1N NaOH and measured by the method of Lowry (121).

6. Lipolysis

Lipolysis experiments were conducted using a glycerol assay from Sigma Diagnostics (procedure No.337). Triglycerides are hydrolyzed to glycerol and fatty acids. The glycerol produced is then measured by coupled enzyme reactions catalyzed by glycerol kinase, glycerol phosphate oxidase and peroxidase. 3T3-L1 adipocytes were incubated for 24 hours with or without 100 nM norepinephrine. At that point, 10 ul of media from each sample was added to 1 mL of Triglyceride (GPO-Trinder) Reagent in a cuvet. The absorbance at 540 nm of blank, glycerol standard, and sample was recorded. To obtain the change in absorbance due to glycerol, the absorbance of the blank was subtracted from the absorbance of the standard and each sample. The glycerol

concentration in each sample was determined using the calculation given. Soluble cell protein was then dissolved in 1 mL 1N NaOH and measured by the method of Lowry.

7. Insulin Binding

3T3-L1 cells throughout differentiation were serum starved with 0% DMEM + 0.1% BSA for 2 hours and then washed twice with Hank's Hepes Balanced Salt Solution (HHBS + 0.2% BSA). The cells were then exposed to labeled ^{125}I-insulin (1 ng/mL) alone (total binding) or labeled ^{125}I-insulin (1 ng/mL) plus a large excess of unlabeled insulin (40 ug/mL) (non-specific binding) for 2 hours on a rotary shaker at room temperature. At this point, the cells were washed four times with 4°C HHBS. Samples were solubilzed in 1 mL of 1N NaOH and counted in a gamma-counter. Protein analysis was performed on separate cell samples employing the method of Lowry.

8. Insulin Binding Reversal

Binding experiments were performed as described previously with slight modifications. Changes were made during the exposure to ^{125}I-labeled insulin relative to the presence or absence of indinavir. There were a total of four groups. Group 1 was the control group. Group 2 had indinavir present only during exposure to ^{125}I-labeled insulin. In-group 3, indinavir was present during cell culture, differentiation, and serum starvation but absent during exposure to ^{125}I-labeled insulin. Group 4 had indinavir present during all stages of the experiment.

9. Competitive Displacement Profile of Insulin Binding

Binding experiments were performed as above with slight modifications. The amount of ^{125}I-insulin bound was measured in the presence of increasing concentrations of unlabeled insulin (range 0.6 ng/mL - 4000 ng/mL).

10. Insulin Binding, Internalization and Degradation

Binding experiments were performed as above with slight modifications. 3T3-L1 adipocytes were pre-incubated with ^{125}I-insulin at 4°C for 4 hours to allow steady-state equilibrium. ^{125}I-insulin was then removed by washing the cells four times with HHBS containing 0.2% BSA at 4°C. At zero time the medium was replaced with 1 mL of 37°C buffer. To stop ^{125}I-insulin internalization, cells were washed rapidly four times with 4°C HHBS + 0.2% BSA buffer and placed at 4°C. Internalized ^{125}I-insulin was assessed by incubating the cells with 0.2 M acetic acid (pH 2.7) containing 0.5 M NaCl for 6 minutes at 4°C. Under these conditions greater than 95% of all surface bound insulin was removed. Cells were then solubilized with NaOH to determine the amount of ^{125}I-insulin incorporated. The amount of surface bound ^{125}I-insulin was determined by substracting the amount-internalized insulin from the amount of total insulin bound (plates not treated with acetic acid) at each time frame.

In order to determine the amount of ^{125}I-insulin that was degraded both intracellularly and extracellularly, the above procedure was performed with two additional steps. First, after the indicated time points for incubation at 37°C, the media for each sample was stored in microcentrifuge tubes pre-chilled at 4°C. Cells were then rinsed and

placed at 4°C. Second, cells, which were stripped of their surface bound insulin, were exposed to 1 mL of Triton X-100 for one hour. Media aliquots of 0.4 mL were directly counted for ^{125}I in a gamma-counter and an additional 0.4 mL was incubated with 0.4 mL of 20% TCA for one hour at 4°C. These samples were centrifuged at 14,000 rpm for five minutes and protein pellets were dissolved in 1mL of 1N NaOH and counted. The amount of TCA soluble material was determined by substraction of TCA precipitable material and the total amount counted in 0.4 mL. To determine the amount of TCA soluble material in the medium, 0.4 mL media aliquots were collected and subjected to the same process as for Trix aliquots. (122).

11. Preparation of Whole Cell Extracts

3T3-L1 cells were washed twice with 4°C PBS. A volume of 0.5mL RIPA buffer (1X PBS, 1%Nonidet P-40, 0.5% sodium deoxycholate, 0.1% SDS, 1mM PMSF, 1 ug/mL aprotinin, 1 ug/mL leupeptin, 1 ug/mL pepstatin, 1mM sodium vanadate, and 1mM sodium fluoride) was added to each sample and cells were scraped using a cell scraper. The samples were gently rocked for 15 minutes at 4°C. The lysates were then centrifuged at 14,000-x g for 15 minutes at 4°C. The supernatant fluid was the total cell lysate and proteins were determined using the Modified Lowry method.

12. Immunoprecipitation

A 250-ug-cell lysate was placed in a microcentrifuge tube. Antibody, 2 ug of rabbit anti-IRS-1 was added. The reaction was rocked overnight at 4°C. The immunocomplex was captured by adding 50 ul of Protein A agarose bead slurry (25%).

The reaction mixture was again rocked for 2 hours at 4°C. The agarose beads were collected by centrifugation at 2,500 rpm at 4°C for five minutes. The beads were washed three times with PBS. The agarose beads were resuspended in 50 ul 2X Laemmli sample buffer (0.2 M Tris-Cl pH 6.8, 4% SDS, 20% glycerol, 0.008% bromophenol blue, and 8% mercaptoethanol) and boiled for five minutes. A microcentrifuge pulse collected the beads and SDS-polyacrylamide gel electrophoresis (SDS-PAGE) was then performed using the supernanant. Proteins were probed with a rabbit anti-mouse tyrosine phosphorylated primary antibody followed by a goat anti-rabbit HRP-labeled secondary antibody.

13. Western Blotting

Cell lysate proteins (40 ug of protein) were mixed with 4X Laemmli buffer (8% SDS, 400mM DTT, 0.24 M Tris (pH 6.8), 0.04% bromophenol blue, 40% glycerol, 4mM EDTA) in a 1:4 ratio. Samples were separated by SDS-PAGE (200V, 30 miuntes) on a 6% gel. Proteins were transferred (100V, 1 hour) to nitrocellulose (0.2 μm) sheets and blocked in 5% milk in PBST. The blots were then washed with PBST (0.1% Tween) and subsequently probed with a rabbit anti-mouse IRS-1 polyclonal antibody (1:1000 dilution) dissolved in 5% milk for 1 hour at room temperature. The membrane was again washed with PBST and then incubated with a goat anti-rabbit HRP-labeled secondary antibody diluted 1:1000 in blocking reagent. Following washing with PBST, the blot was incubated with the chemiluminescence detection reagents (ECL Amersham) prior to exposure to film (Kodak X-Omat Blue). The intensity of the bands was quantitated using UN-SCAN-IT computer software (Silk Scientific).

14. Statistics

All analyses were done with triplicates experiments, with triplicate samples in each experiment. The statistical analyses employed herein include column statistics and one-way analysis of variance (ANOVA). The lowest level of significance was set at $p<0.05$.

Results

1. The Effect of Saquinavir on 3T3-L1 Adipocyte Diffentiation

Under appropriate culture conditions, including incubation with a hormonal mixture, 3T3-L1 preadipocytes undergo differentiation and assume adipocyte characteristics that include a specific pattern of gene expression and accumulation of cytoplasmic, triacylglycerol-rich lipid droplets. Experiments were conducted to determine whether HIV protease inhibitors (PIs) affect this process. Preadipocytes were induced to differentiate in the absence or presence of 1 and 10 uM Saquinavir (Saq). Eleven days after the onset of differentiation, when cytoplasmic lipid droplets are normally abundant, adipocytes were fixed with 4% paraformadelhyde and stained with oil red. Plates were photographed microscopically and compared for differences in cell size and lipid content.

Figure 15 shows the results for the control, 1 uM Saq and 10 uM Saq adipocyte cell models. Adipocytes that were differentiated in the presence of 1 and 10 uM saquinavir showed slight differences in lipid content when compared to the control group. The photographs portray a concentration dependent inhibition of lipid accumulation with increasing concentrations of saquinavir. The size of the fat cell and the quantity of lipid droplets in the drug treated samples were smaller and fewer, respectively.

Figure 15 : The Effect of Saquinavir on 3T3-L1 Adipocyte Differentiation
The following depicts photographs of differentiated 3T3-L1 adipocytes in the absence and presence of 1 uM saquinavir and 10 uM saquinavir.

2. The Effect of Indinavir on 3T3-L1 Adipocyte Differentiation

3T3-L1 fibroblasts were cultured and subjected to adipocyte differentiation in 10% DMEM. Indinavir (Ind) was present at varying concentrations of 1 and 10 uM during all stages of culture. Adipocytes were fixed with 4% paraformadelhyde and stained with oil red. Plates were photographed microscopically and compared for differences in cell size and lipid content.

Figure 16 shows the results for the control, 1 uM Ind and 10 uM Ind adipocyte cell models. Adipocytes that were differentiated in the presence of 1 uM indinavir showed little differences in lipid content when compared to the control group. However, cells differentiated in 10 uM indinavir showed extensive differences in cell morphology when compared to the control group. It seems that indinavir has detrimental effects on 3T3-L1 adipocyte differentiation with regards to the size of the fat cell and the quantity of lipid droplets in the drug treated samples, being smaller and fewer, respectively.

Figure 16 : The Effect of Indinavir on 3T3-L1 Adipocyte Differentiation
The following depicts photographs of 3T3-L1 differentiated adipocytes in the absence and presence of 1 and 10 uM indinavir.

3. The Effect of Ritonavir on 3T3-L1 Adipocyte Differentiation

3T3-L1 fibroblasts were cultured and subjected to adipocyte differentiation in 10% DMEM. Ritonavir (Rit) was present at varying concentrations of 1 and 10 uM during all stages of culture. Adipocytes were fixed with 4% paraformadelhyde and stained with oil red. Plates were photographed microscopically and compared for differences in cell size and lipid content.

Figure 17 shows the results for the control, 1 uM Rit and 10 uM Rit adipocyte cell models. Adipocytes that were differentiated in the presence of 1 and 10 uM ritonavir showed moderate differences in lipid content when compared to the control group. The photographs portray a concentration dependent inhibition of lipid accumulation with increasing concentrations of ritonavir. The size of the fat cell and the quantity of lipid droplets in the drug treated samples were smaller and fewer, respectively. Both saquinavir and ritonavir have similar effects on adipocyte differentiation with ritonavir having a slightly greater efficacy.

Figure 17 : The Effect of Ritonavir on 3T3-L1 Adipocyte Differentiation
The following depicts photographs of differentiated 3T3-L1 adipocytes in the absence and presence of 1 and 10 uM ritonavir.

4. The Incorporation of ^{14}C-Glucose into the Glycerol Backbone of Triacylglycerols Over Various Time Frames in 3T3-L1 Cells

3T3-L1 fibroblasts were cultured and subjected to adipocyte differentiation in 10% DMEM. At 3 days post-induction (pre-adipocytes) and at 11 days post-induction (full blown adipocytes) cells were stimulated 3.35nM insulin for 6 hrs and pulsed with ^{14}C-glucose (2.21 dpm/pmole) for various time frames. Triglycerides were extracted using isopropanol:heptane and aliquots were counted using a scintillation counter to determine the amounts of triacylglycerols containing ^{14}C in their glycerol backbone.

Figure 18 shows a linear increase in ^{14}C-glucose incorporation into triacylglycerols over time at basal as well as insulin-stimulated levels. This control experiment was carried out to find the optimum time frame for the greatest generation of triacylglycerols. As the graph demonstrates, an 18-hour pulse with ^{14}C-glucose is the optimum time frame for both experiments involving pre-adipocytes and adipocytes.

An 18-hour pulse time was used for all future experiments regarding triacylglycerol synthesis. Analysis was done using triplicate experiments with triplicates plates in each experiment.

Figure 18 : The Incorporation of ^{14}C-Glucose into Triacylglycerols Over Various Time Frames in 3T3-L1 Cells

The following data depicts the incorporation of ^{14}C-glucose into the glycerol backbone of triacylglycerols over various time frames. Cells were stimulated with 3.35 nM insulin and pulsed with ^{14}C-glucose. Triacylglycerol synthesis was observed at basal (Δ) and insulin-stimulated (▲) for pre-adipocytes, 3 days post-induction. The same treatments were performed for adipocytes (11 days post-induction) at basal (□) and insulin-stimulated (■) conditions. The results are a summary of three experiments with triplicates plates in each experiment.

The Incorporation of ^{14}C-Glucose into Triglycerides Over Time in 3T3-L1 Cells

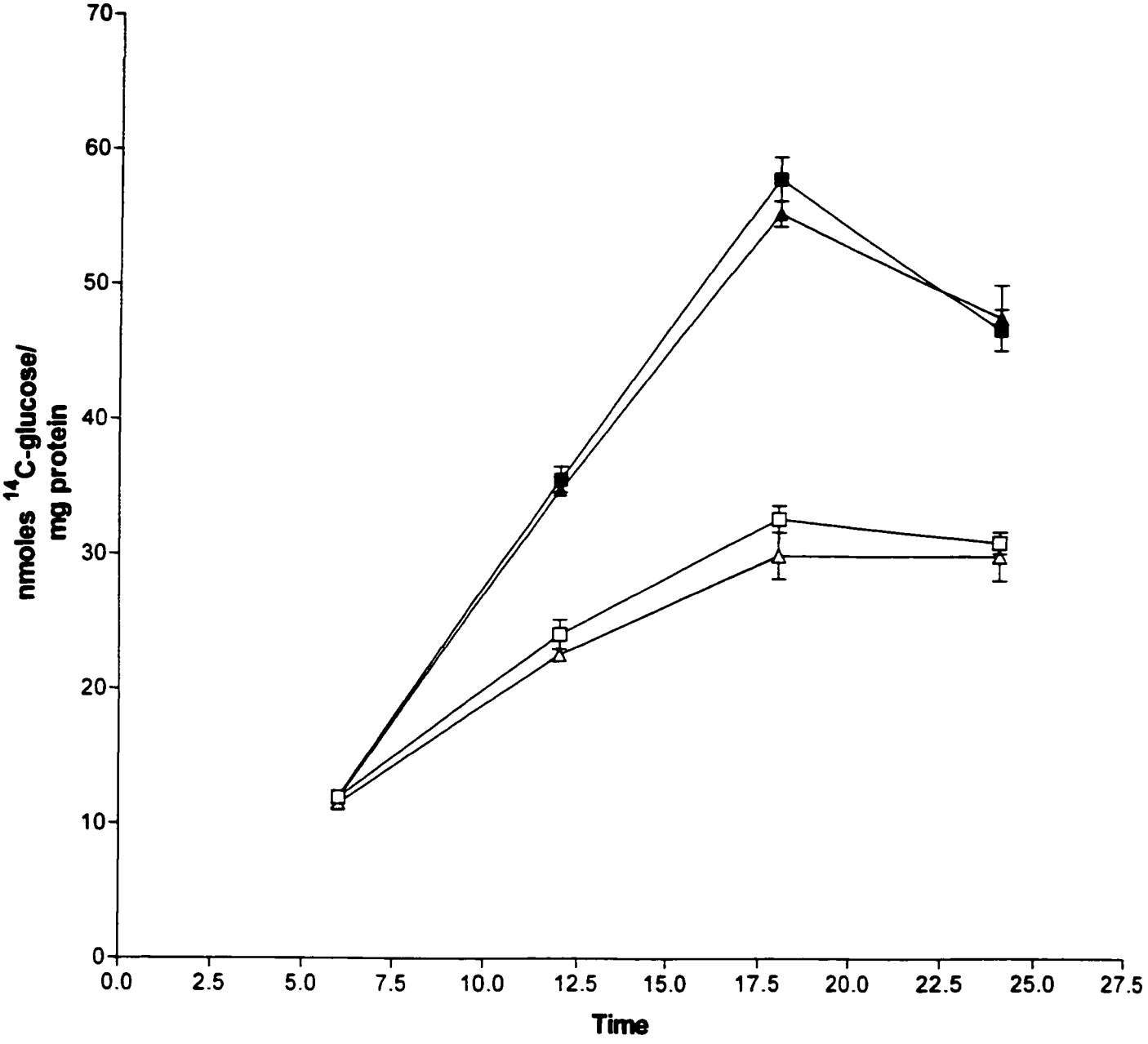

5.The Incorporation of ^{14}C-Glucose into Triacylglycerols Using Various Concentrations of Insulin in 3T3-L1 Cells

3T3-L1 fibroblasts were cultured and differentiated in 10 % DMEM as previously described. Upon reaching the desired level of differentiation pre-adipocytes and adipocytes were insulin-stimulated for 6 hours with various concentrations of insulin and pulsed for another 18 hours with ^{14}C-glucose (2.21 dpm/pmole). Triacylglycerols produced were extracted using isopropanol:heptane and aliquots were measured by scintillation counting.

The purpose of this control experiment was to find the optimum insulin concentrations at which the greatest amounts of triacylglycerols were produced. The results are shown in figure 19. We observed an increase in triacylglycerol synthesis with a maximal production at 3.35 nM insulin followed by triglyceride synthesis slowly tapering off with increasing concentrations of insulin. This effect was observed with pre-adipocytes with a maximal of 25 nmoles ^{14}C-glucose/mg protein at 3.35 nM insulin, as well as with adipocytes, 53 nmoles ^{14}C-glucose/mg protein.

Therefore, an insulin concentration of 3.35 nM was chosen for all future experiments involving triglyceride synthesis. Analysis was done on triplicate experiments with triplicate plates in each experiment.

Figure 19 : Monitoring the Incorporation of ^{14}C-Glucose into Triacylglycerols Using Various Concentrations of Insulin in 3T3-L1 Cells

The following data demonstrates the optimum insulin concentration at which the greatest amount of triacylglycerol is produced in vitro in 3T3-L1 cells. This experiment was conducted with 3T3-L1 cells at different stages of adipocyte differentiation; pre-adipocytes. 3 days post-induction (■), and adipocytes, 11 days post-induction (▲). Cells were stimulated with increasing concentrations of insulin and pulsed with ^{14}C-Glucose. Maximum triacylglycerol synthesis occurs at 3.35 nM insulin. Analysis was done using triplicate experiments with triplicate plates in each experiment.

The Incorporation of ^{14}C-Glucose into Triglycerides Using Various Concentrations of Insulin in 3T3-L1 Cells

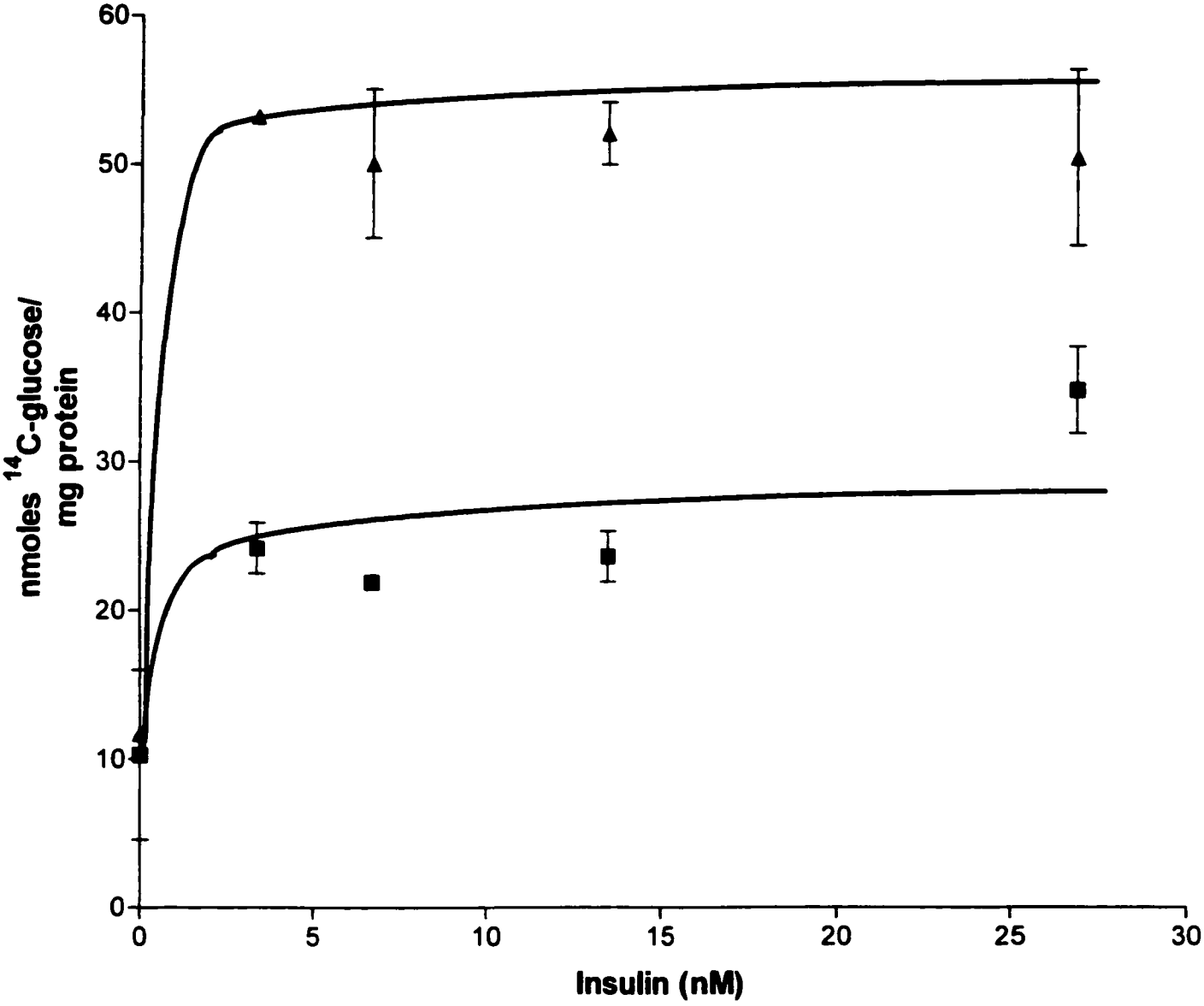

6. The Effect of Saquinavir on Basal and Insulin Stimulated Triacylglycerol Synthesis in 3T3-L1 Pre-adipocytes (3 days post-induction)

The following experiments will be conducted to determine the effects of HIV protease inhibitors on triacylglycerol synthesis in vitro. This is to assess if there are any perturbations in triglyceride synthesis, and if it can explain what is observed in lipodystrophy patients.

3T3-L1 fibroblasts were cultured and subjected to adipocyte differentiation in 10 % DMEM as previously described. Saquinavir was present throughout all stages of the experiment at concentrations of 0.1 uM, 1 uM and 10 uM. At 3 days post-induction, pre-adipocytes were stimulated for 6 hours with 3.35 nM insulin and pulsed for an additional 18 hours with ^{14}C-glucose (2.21 dpm/pmole). Triacylglycerols were extracted using isopropanol:heptane and aliquots were measured by scintillation counting to determine the amount of ^{14}C-glucose incorporated into the glycerol backbone of triglycerides.

Figure 21 (top panel) shows a concentration dependent increase in basal triacylglycerol synthesis in drug treated samples when compared to the control group. The differences between treated and control groups was found to be statiscally significant ($p<0.05$). Analysis of the data gave increases of 33.35% ± 0.03, 38.27% ± 0.05, and 45.04% ± 1.26 for 0.1 uM, 1 uM and 10 uM saquinavir respectively.

In figure 20 (lower panel), we observed an overall decrease in insulin-stimulated triglyceride synthesis in the drug treated samples. The values, when compared to the control group, decreased by 29.24% ± 0.07, 29.93% ± 0.83, and 34.70% ± 2.218 for 0.1uM, 1 uM, and 10 uM saquinavir respectively. These differences were also all statistically significant ($p<0.05$). The results are expressed as ± SEM for n=3.

Figure 20 : The Effect of Saquinavir on Basal and Insulin-Stimulated Triacylglycerol Synthesis in 3T3-L1 Pre-Adipocytes

The following data depicts the effect of the HIV protease inhibitor saquinavir on triacylglycerol synthesis in vitro using 3T3-L1 pre-adipocytes. 3T3-L1 fibroblasts were differentiated as previously described and stimulated with 3.35 nM insulin and pulsed with ^{14}C-glucose. The upper panel, A, shows basal triacylglycerol synthesis and the lower panel, B, shows insulin-stimulated triacylglycerol synthesis. Saquinavir, at concentrations of 0.1uM, 1 uM, and 10 uM were present at all stages of the experiment. Data is presented as nmoles of ^{14}C-glucose incorporated into a triglyceride backbone per mg protein. The results are expressed as +SEM for n=3. Statistical significance determined by one-way anova ($p<0.05$).

The Effect of Saquinavir on Basal Incorporation of ^{14}C-Glucose into Triglycerides in 3T3-L1 Preadipocytes (3 Days Post-Induction)

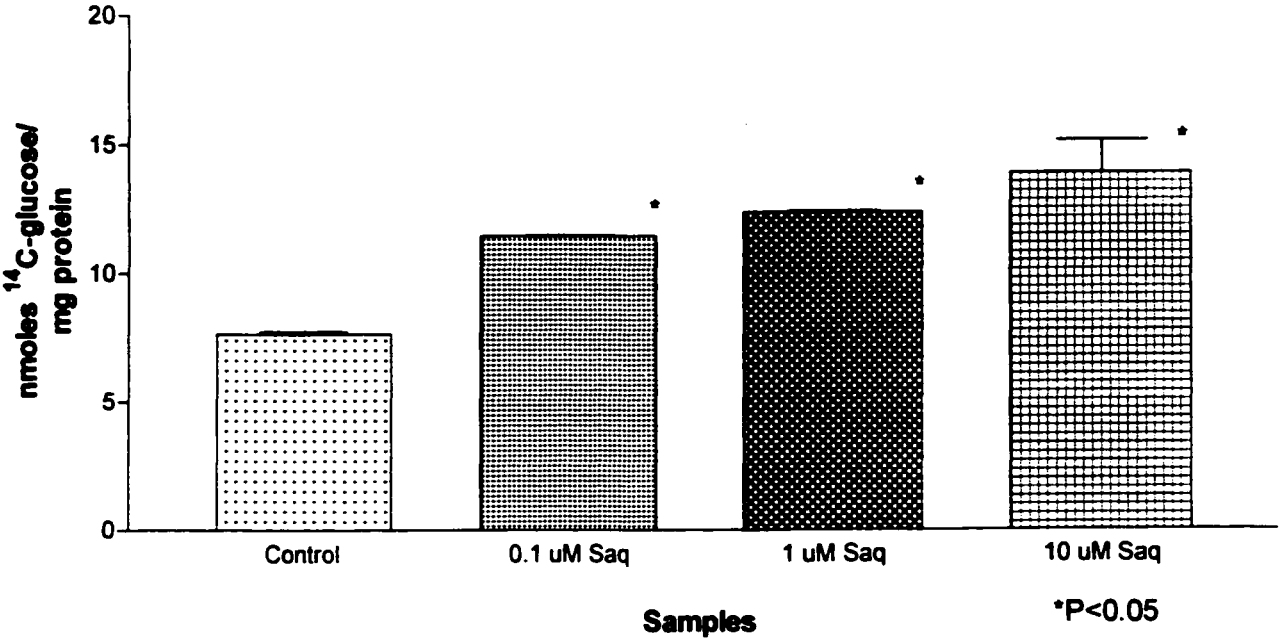

The Effect of Saquinavir on Insulin-Stimulated Incorporation of ^{14}C-Glucose into Triglycerides in 3T3-L1 Preadipocytes (3 Days Post Induction)

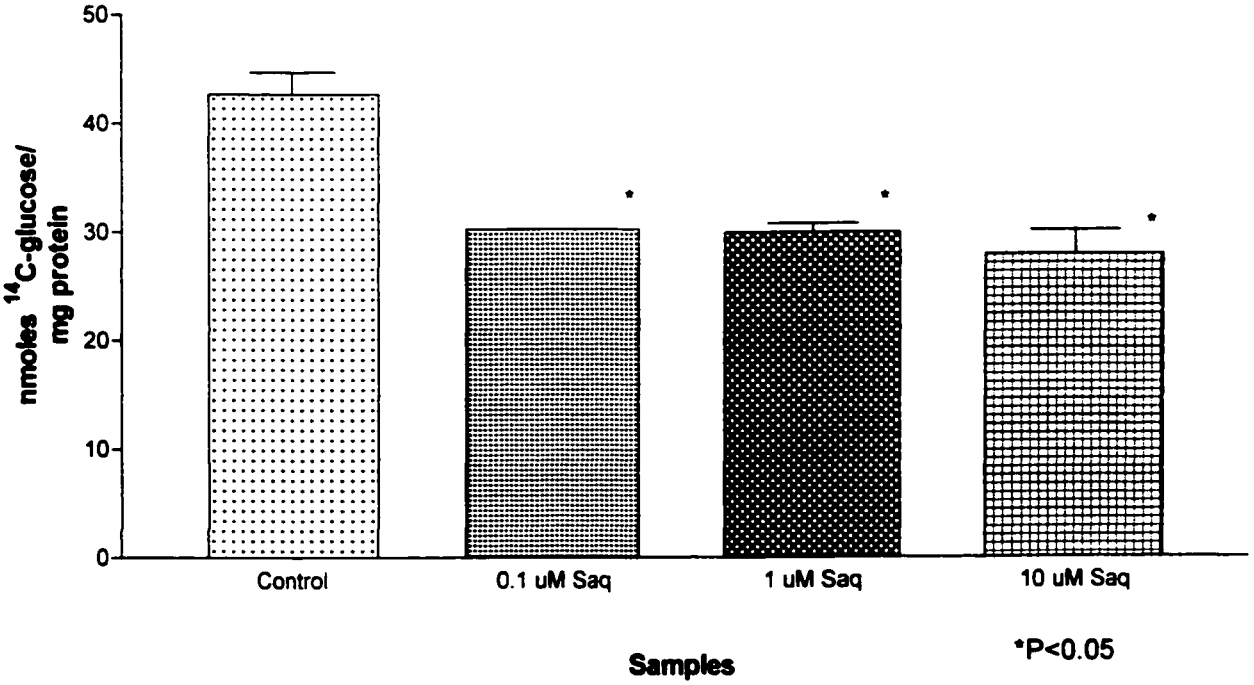

7. The Effect of Indinavir on Basal and Insulin-Stimulated Triacylglycerol Synthesis in 3T3-L1 Pre-Adipocytes (3 days post-induction)

3T3-L1 fibroblasts were cultured and subjected to adipocyte differentiation in 10 % DMEM as previously described. Indinavir was present throughout all stages of the experiment at concentrations of 0.1 uM, 1 uM and 10 uM. At 3 days post-induction, pre-adipocytes were stimulated for 6 hours with 3.35 nM insulin and pulsed for an additional 18 hours with ^{14}C-glucose (2.21 dpm/pmole). Triacylglycerols were extracted using isopropanol:heptane and aliquots were measured by scintillation counting to determine the amount of ^{14}C-glucose incorporated into the glycerol backbone of triglycerides.

Figure 21 (top panel) shows a concentration dependent increase in basal triacylglycerol synthesis in drug treated samples when compared to the control group. The differences between treated and control groups was found to be statiscally significant ($p<0.05$). Analysis of the data gave increases of 26.82% ± 0.02, 42.25% ± 0.03, and 55.94% ± 0.01 for 0.1 uM, 1 uM and 10 uM indinavir respectively.

In figure 21 (lower panel), we observed an overall decrease in insulin-stimulated triglyceride synthesis in the drug treated samples. The values, when compared to the control group, decreased by 32.77% ± 0.11, 34.26% ± 1.02, and 33.27% ± 0.64 for 0.1 uM, 1 uM, and 10 uM indinavir respectively. These differences were also all statistically significant ($p<0.05$). The results are expressed as ± SEM for n=3.

Figure 21 : The Effect of Indinavir on Basal and Insulin-Stimulated Triacylglycerol Synthesis in 3T3-L1 Pre-Adipocytes

The following data depicts the effect of the HIV protease inhibitor indinavir on triacylglycerol synthesis in vitro using 3T3-L1 pre-adipocytes. 3T3-L1 fibroblasts were differentiated as previously described and stimulated with3.35 nM insulin and pulsed with ^{14}C-glucose for 18 hours. The upper panel, A, shows basal triacylglycerol synthesis and the lower panel, B, shows insulin-stimulated triacylglycerol synthesis. Indinavir, at concentrations of 0.1 uM, 1 uM, and 10 uM were present at all stages of the experiment. Data is presented as nmoles of ^{14}C-glucose incorporated into a triglyceride backbone per mg protein. The results are expressed as +SEM for n=3. Statistical significance determined by one-way anova ($p<0.05$).

The Effect of Indinavir on Basal Incorporation of ^{14}C-Glucose into Triglycerides in 3T3-L1 Preadipocytes (3 Days Post-Induction)

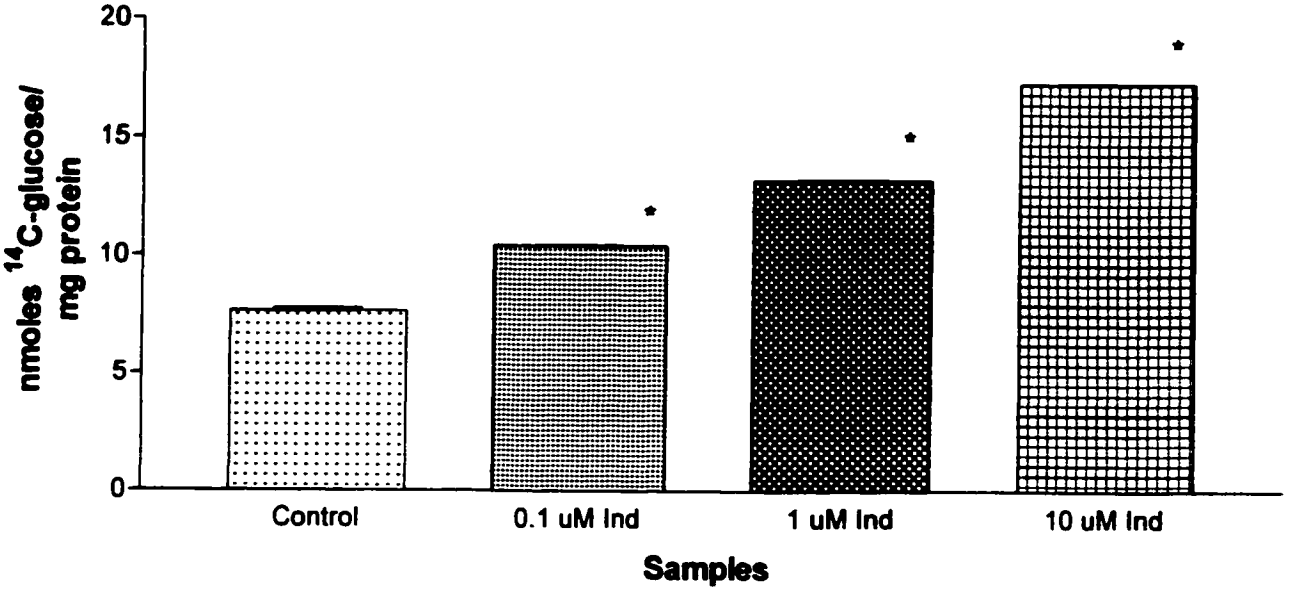

The Effect of Indinavir on Insulin-Stimulated Incorporation of ^{14}C-Glucose into Triglycerides in 3T3-L1 Preadipocytes (3 Days Post Induction)

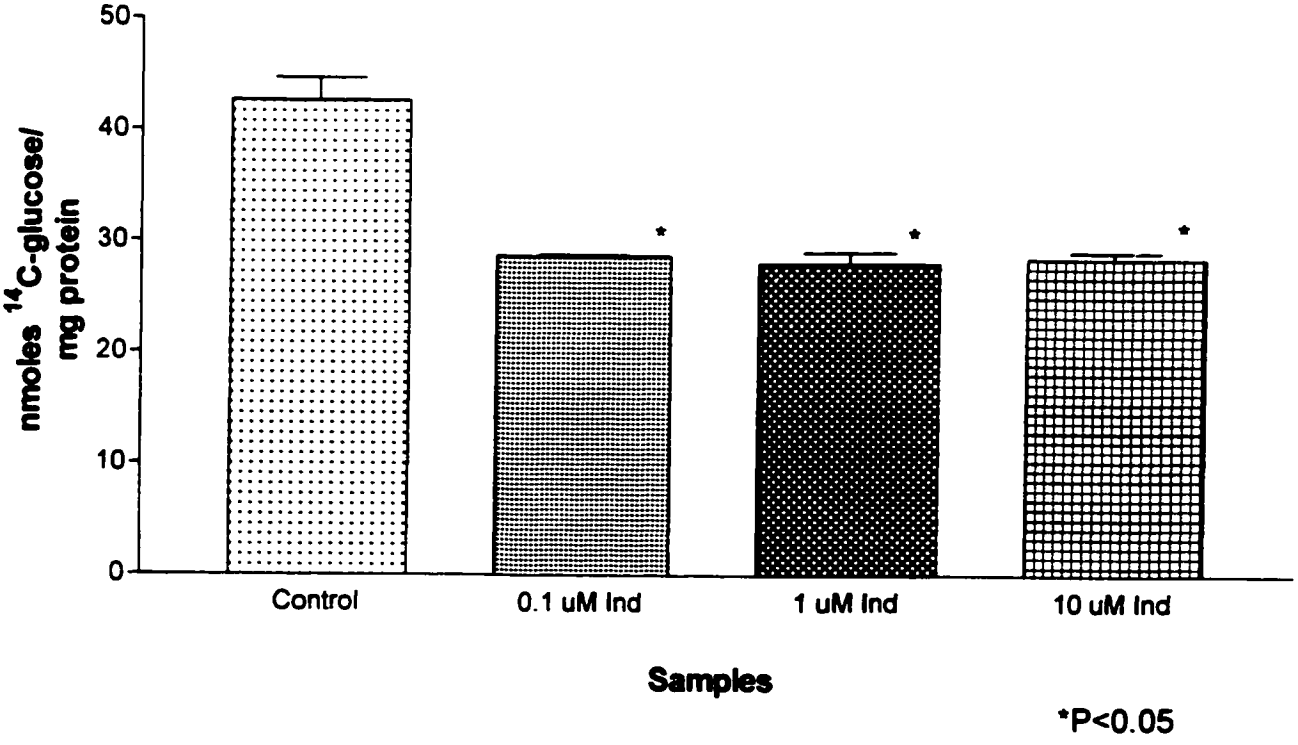

8. The Effect of Ritonavir on Basal and Insulin-Stimulated Triacylglycerol Synthesis in 3T3-L1 Pre-Adipocytes (3 days post-induction)

3T3-L1 fibroblasts were cultured and subjected to adipocyte differentiation in 10 % DMEM as previously described. Ritonavir was present throughout all stages of the experiment at concentrations of 0.1 uM, 1 uM and 10 uM. At 3 days post-induction, pre-adipocytes were stimulated for 6 hours with 3.35nM insulin and pulsed for an additional 18 hours with ^{14}C-glucose (2.21 dpm/pmole). Triacylglycerols were extracted using isopropanol:heptane and aliquots were measured by scintillation counting to determine the amount of ^{14}C-glucose incorporated into the glycerol backbone of triglycerides.

Figure 22 (top panel) shows a concentration dependent increase in basal triacylglycerol synthesis in drug treated samples when compared to the control group. The differences between treated and control groups was found to be statiscally significant ($p<0.05$) at 1 uM and 10 uM ritonavir only. Analysis of the data gave increases of 26.12% ± 0.56, 32.71% ± 0.04, and 55.46% ± 1.12 for 0.1 uM, 1 uM and 10 uM ritonavir respectively.

In figure 22 (lower panel), we observed an overall decrease in insulin-stimulated triglyceride synthesis in the drug treated samples. The values, when compared to the control group, decreased by 33.51% ± 2.02, 29.21% ± 2.17, and 54.45% ± 2.58 for 0.1 uM, 1 uM, and 10 uM ritonavir respectively. These differences were also all statistically significant ($p<0.05$). The results are expressed as ± SEM for n=3.

Figure 22 : The Effect of Ritonavir on Basal and Insulin-Stimulated Triacylglycerol Synthesis in 3T3-L1 Pre-Adipocytes

The following data depicts the effect of the HIV protease inhibitor ritonavir on triacylglycerol synthesis in vitro using 3T3-L1 pre-adipocytes. 3T3-L1 fibroblasts were differentiated as previously described and stimulated 3.35 nM and pulsed with ^{14}C-glucose for 18 hours. The upper panel, A, shows basal triacylglycerol synthesis and the lower panel, B, shows insulin-stimulated triacylglycerol synthesis. Ritonavir, at concentrations of 0.1uM, 1 uM, and 10 uM were present at all stages of the experiment. Data is presented as nmoles of ^{14}C-glucose incorporated into a triglyceride backbone per mg protein. The results are expressed as +SEM for n=3. Statistical significance determined by one-way anova ($p<0.05$).

The Effect of Ritonavir on Basal Incorporation of ^{14}C-Glucose into Triglycerides in 3T3-L1 Preadipocytes (3 Days Post-Induction)

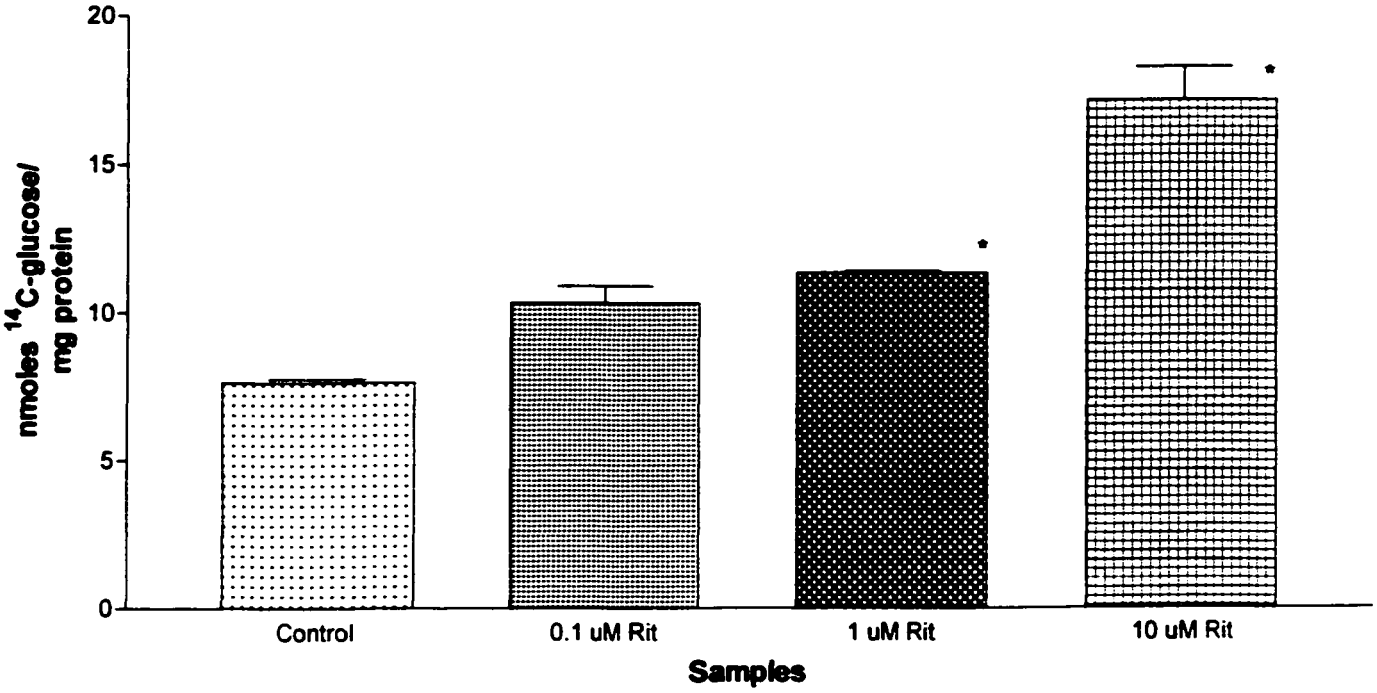

*P<0.05

The Effect of Ritonavir on Insulin-Stimulated Incorporation of ^{14}C-Glucose into Triglycerides in 3T3-L1 Preadipocytes (3 Days Post Induction)

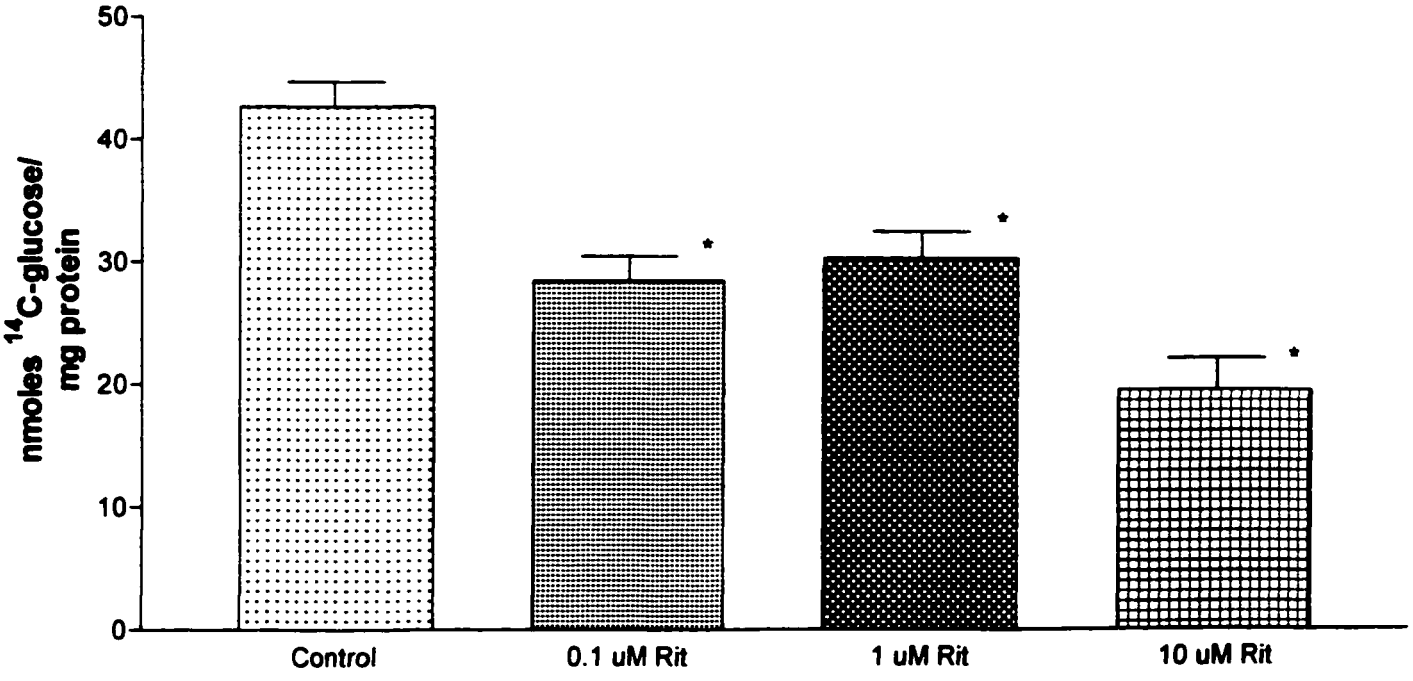

*P<0.05

9. The Effect of Ritonavir on Basal and Insulin-Stimulated Triacylglycerol Synthesis in 3T3-L1 Adipocytes (11 days post-induction)

In the three last experiments we assessed the effect of saquinavir, indinavir, and ritonavir HIV protease inhibitors on triacylglycerol synthesis, in vitro, in 3T3-L1 mouse pre-adipocytes. The results suggested significant effects under basal and insulin-stimulated conditions. Therefore, this next experiment was conducted to assess the effects of protease inhibitors on completely differentiated adipocytes, 11 days post-induction. Due to its superior adverse effects, when compared to the other two HIV protease inhibitors used previously, ritonavir was chosen as a drug for this experiment.

3T3-L1 fibroblasts were cultured and subjected to adipocyte differentiation in 10 % DMEM as previously described. Ritonavir was present throughout all stages of the experiment at concentrations of 0.1 uM, 1 uM and 10 uM. At 11 days post-induction, adipocytes were stimulated for 6 hours with 3.35 nM insulin and pulsed for an additional 18 hours with ^{14}C-glucose (2.21 dpm/pmole). Triacylglycerols were extracted using isopropanol:heptane and aliquots were measured by scintillation counting to determine the amount of ^{14}C-glucose incorporated into the glycerol backbone of triglycerides.

Figure 23, upper panel, shows small increases in basal triacylglycerol synthesis in ritonavir treated samples. Synthesis increased by 11.26% ± 10.41, 22.83% ± 15.63, and 2.03% ± 15.30 for 0.1 uM, 1 uM, and 10 uM ritonavir respectively. Adipocytes exposed to ritonavir did not show concentration dependent increases in triacylglycerol synthesis as seen in pre-adipocytes. Furthermore, the differences between treated and control samples were not statistically significant.

Figure 23, lower panel, displays the results for insulin-stimulated adipocytes. A concentration dependent decrease in triacylglycerol synthesis was observed with increasing concentrations of ritonavir when compared to the control group. Synthesis decreased by 3.34% ± 0.19 and 29.93% ± 1.29 for 1 uM and 10 uM ritonavir respectively. No decrease in triacylglycerol synthesis was observed at 0.1 uM ritonavir. The greatest decrease in synthesis was observed with 10 uM ritonavir and coincidently is the only one that was statistically significant ($p<0.05$) when compared to the control sample. The results are expressed as ± SEM for n=3.

Figure 23 : The Effect of Ritonavir on Basal and Insulin-Stimulated Triacylglycerol Synthesis in 3T3-L1 Adipocytes

The following data depicts the effect of the HIV protease inhibitor ritonavir on triacylglycerol synthesis in vitro using 3T3-L1 adipocytes. 3T3-L1 fibroblasts were differentiated as previously described and stimulated with 3.35 nM insulin and pulsed with ^{14}C-glucose for 18 hours. The upper panel, A, shows basal triacylglycerol synthesis and the lower panel, B, shows insulin-stimulated triacylglycerol synthesis. Ritonavir, at concentrations of 0.1uM, 1 uM, and 10 uM were present at all stages of the experiment. Data is presented as nmoles of ^{14}C-glucose incorporated into a triglyceride backbone per mg protein. The results are expressed as +SEM for n=3. Statistical significance determined by one-way anova ($p<0.05$).

The Effect of Ritonavir on Basal Incorporation of ^{14}C-Glucose into Triglycerides in 3T3-L1 Adipocytes

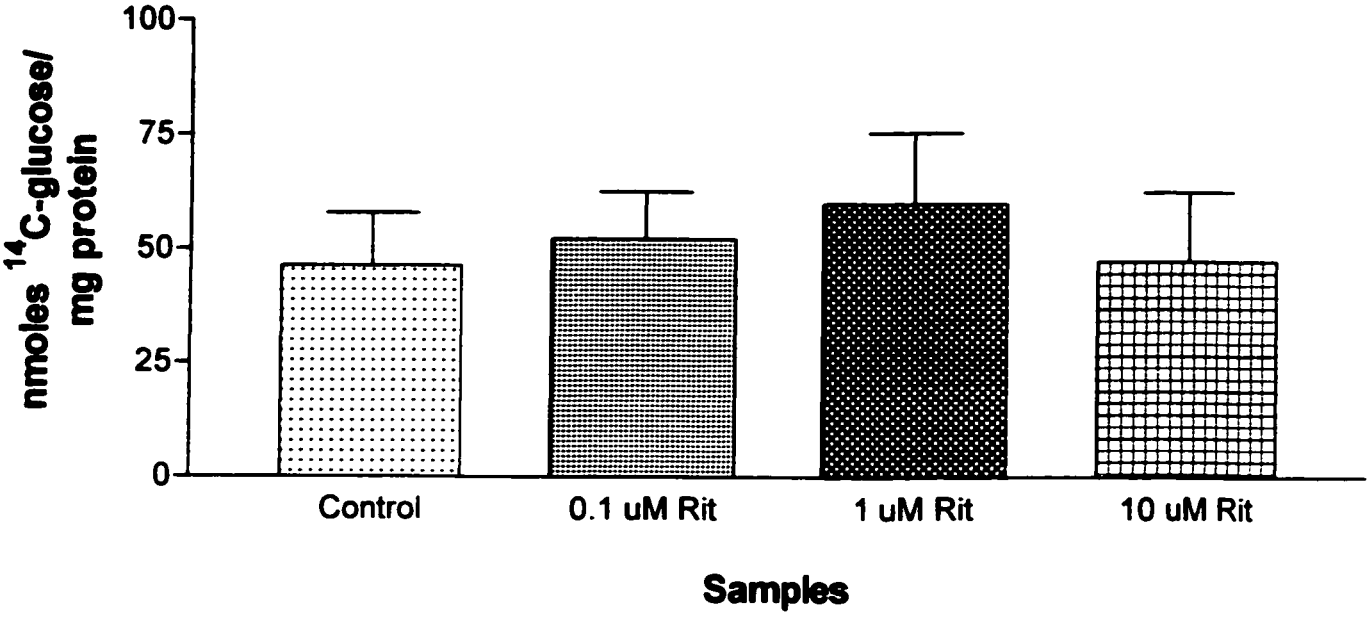

The Effect of Ritonavir on Insulin-Stimulated ^{14}C-Glucose Incorporation into Triglycrides in 3T3-L1 Adipocytes

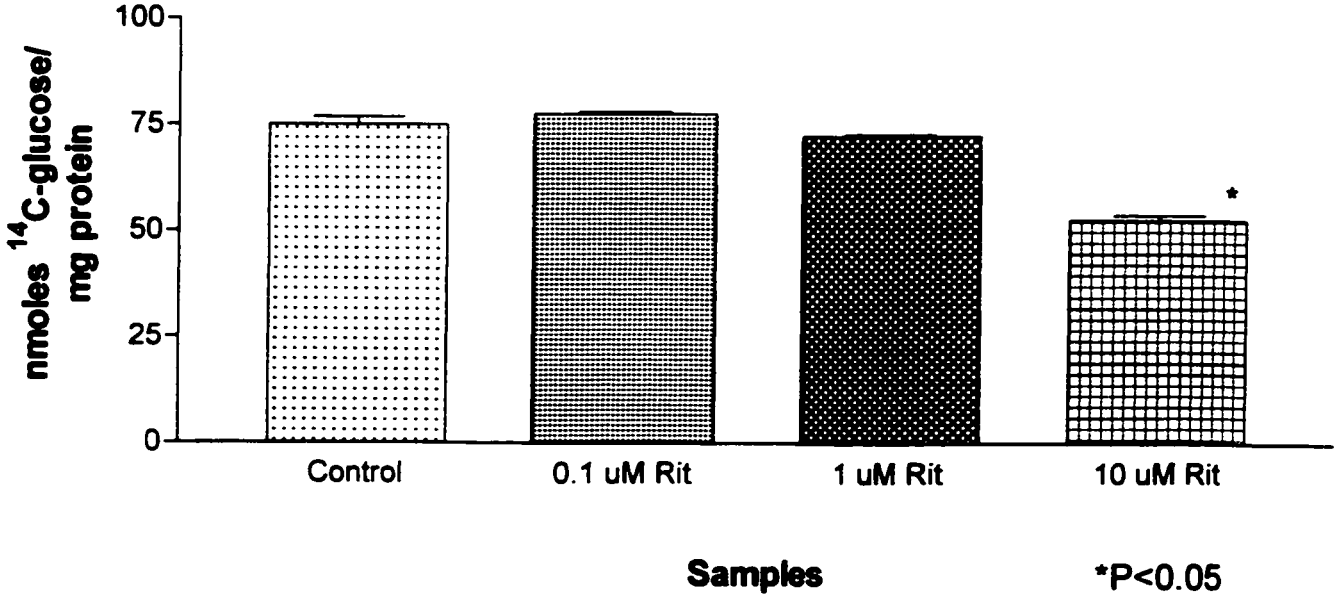

10. The Effect of Ritonavir on Triacylglycerol Synthesis Using Various Concentrations of Insulin in 3T3-L1 Pre-adipocytes (3 days post-induction)

3T3-L1 fibroblasts were cultured and subjected to adipocyte differentiation in 10% DMEM as previously described. Ritonavir was present throughout all stages of the experiment at concentrations of 1 uM and 10 uM. At 3 days post-induction, pre-adipocytes were stimulated for 6 hours with increasing concentrations of insulin and pulsed for an additional 18 hours with ^{14}C-glucose (2.21 dpm/pmole). Triacylglycerols were extracted using isopropanol:heptane and aliquots were measured by scintillation counting to determine the amount of ^{14}C-glucose incorporated into the glycerol backbone of triglycerides.

In figure 24 we notice that with increasing insulin concentrations there is a progressive decrease in triacylglycerol synthesis in both 1 uM and 10 uM ritonavir samples, when compared to the control group. Furthermore, decreases in synthesis are concurrent with the increasing concentrations of ritonavir from 1 to 10 uM. However, exposure to higher levels of insulin did not further stimulate triacylglycerol synthesis in these cells. Therefore, insulin could not alleviate the diminished insulin response brought about by ritonavir. The differences between treated and control group were all statistically significant ($p<0.05$). The results are expressed as ± SEM for n=3.

Figure 24 : The Effect of Ritonavir on Triaclyglycerol Synthesis Using Increasing Concentrations of Insulin in 3T3-L1 Pre-adipocytes

The following data depicts the effect of the HIV protease inhibitor ritonavir on triacylglycerol synthesis in vitro using 3T3-L1 pre-adipocytes. 3T3-L1 fibroblasts were differentiated as previously described and stimulated for 6 hours with various concentrations of insulin and pulsed with ^{14}C-glucose for 18 hours. Ritonavir, at concentrations of 1 uM, and 10 uM were present at all stages of the experiment. Data is presented as nmoles of ^{14}C-glucose per mg protein. Control samples are represented by (■), followed by 1 uM (▲) and 10 uM (▼) ritonavir. The results are expressed as ÷SEM for n=3. Statistical significance determined by one-way anova ($p<0.05$).

The Effect of Ritonavir on Triglyceride Synthesis with Increasing Concentrations of Insulin in 3T3-L1 Preadipocytes

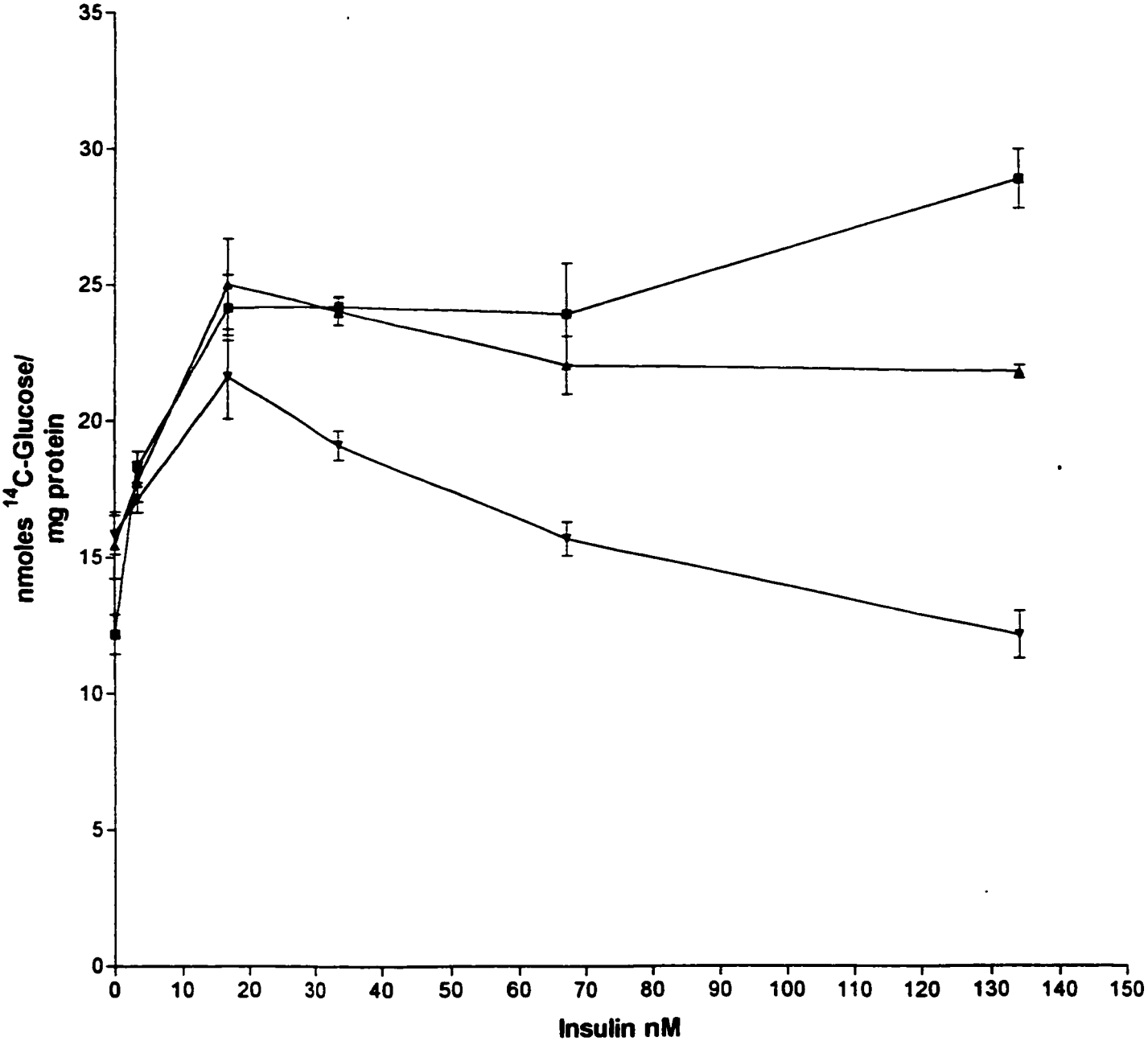

11. The Effect of Ritonavir on Triacylglycerol Synthesis Using Various Concentrations of Insulin in 3T3-L1 Adipocytes (11 days post-induction)

3T3-L1 fibroblasts were cultured and subjected to adipocyte differentiation in 10% DMEM as previously described. Ritonavir was present throughout all stages of the experiment at concentrations of 1 uM and 10 uM. At 11 days post-induction, adipocytes were stimulated for 6 hours with increasing concentrations of insulin and pulsed for an additional 18 hours with ^{14}C-glucose (2.21 dpm/pmole). Triacylglycerols were extracted using isopropanol:heptane and aliquots were measured by scintillation counting to determine the amount of ^{14}C-glucose incorporated into the glycerol backbone of triglycerides.

In figure 25 we notice that with increasing insulin concentrations there is an overall decrease in triacylglycerol synthesis in both 1 uM and 10 uM ritonavir samples. when compared to the control group. As previously observed, exposure to higher levels of insulin did not further stimulate triacylglycerol synthesis in these cells. Therefore, insulin could not alleviate the diminished insulin response brought about by ritonavir. The differences between treated and control group were all statistically significant ($p<0.05$).

Figure 25 : The Effect of Ritonavir on Triaclyglycerol Synthesis Using Increasing Concentrations of Insulin in 3T3-L1 Adipocytes

The following data depicts the effect of the HIV protease inhibitor ritonavir on triacylglycerol synthesis in vitro using 3T3-L1 adipocytes. 3T3-L1 fibroblasts were differentiated as previously described and stimulated for 6 hours with various concentrations of insulin and pulsed with ^{14}C-glucose for 18 hours. Ritonavir, at concentrations of 1 uM, and 10 uM were present at all stages of the experiment. Data is presented as nmoles ^{14}C-glucose per mg protein. Control samples are represented by (■), followed by 1 uM (▲) and 10 uM (▼) ritonavir. The results are expressed as +SEM for n=3. Statistical significance determined by one-way anova ($p<0.05$).

The Effect of Ritonavir on Triglyceride Synthesis with Increasing Concentrations of Insulin in 3T3-L1 Adipocytes (Day 11)

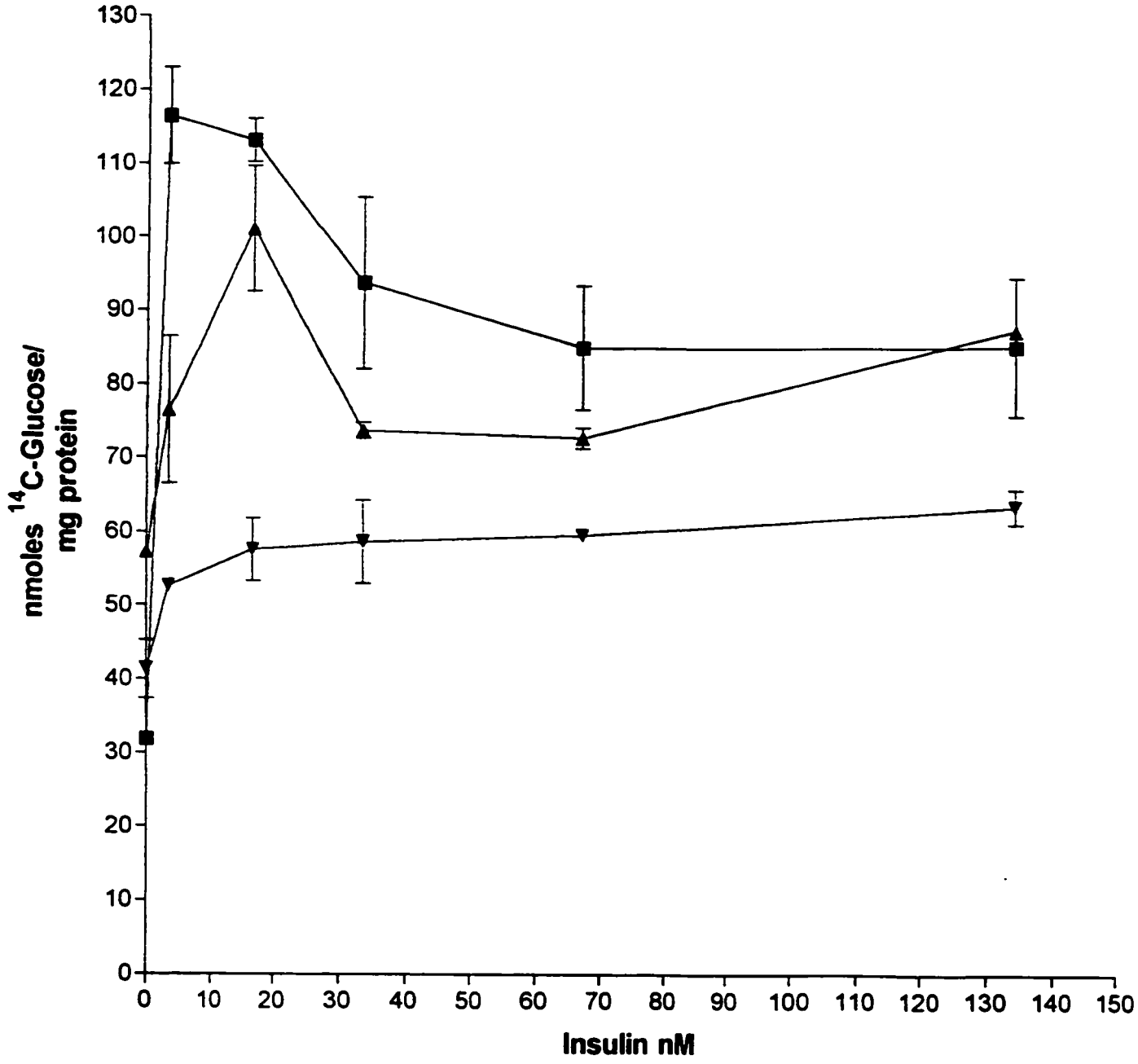

12. Investigating the Effects of HIV Protease Inhibitors in Stimulating Lipolysis in 3T3-L1 Adipocytes

Previous experiments have shown that HIV protease inhibitors cause an increase and decrease of triacylglycerol synthesis under basal and insulin-stimulated conditions respectively. Therefore, we assessed the effects of HIV protease inhibitors on stimulating catabolic metabolism, namely lipolysis, in 3T3-L1 adipocytes. Lipolysis was observed under basal and norepinephrine (NE) stimulated conditions.

3T3-L1 fibroblasts were cultured and subjected to adipocyte differentiation in 10% DMEM as previously described. Adipocytes were given fresh media with or without 100 nM NE and incubated for 24 hours at 37°C. HIV protease inhibitors, saquinavir, indinavir, and ritonavir were present at concentrations of 1 and 10 uM throughout all stages of the experiment. Glycerol expelled in the media, due to the metabolism of triacylglycerols to glycerol and fatty acids, was measured using TPO-Trinder Kit from Sigma (described under material and methods).

Table 1 shows the results in values expressed as mM glycerol released per mg protein per 24 hours. At basal levels, when compared to the control group, lipolysis was not affected when treated with saquinavir, indinavir, and ritonavir at 1 and 10 uM. Under NE stimulated conditions, lipolysis was stimulated 4-fold for all samples. However, there were no significant differences in triacylglycerol metabolism between control and treated samples. The results are expressed as ±SEM for n=3. Statistical significance was determined by one-way anova

($p>0.05$). Lipolysis experiments were also performed in the presence of 3.35nM insulin (data not shown), which showed no stimulation of lipolysis after 24 hours.

Table 1: The Effects of HIV Protease Inhibitors on Lipolysis in 3T3-L1 Adipocytes

The following shows the amount of glycerol (mM) released per mg during a 24 hours incubation period. Samples include adipocytes under basal and NE-stimulated conditions in the absence or presence of 1 and 10 uM saquinavir, indinavir, and ritonavir. Lipolysis was increased by the addition of 100 nM NE. No significant differences were observed between the protease inhibitor groups versus the control group (one-way anova; n=3, $P>0.05$). All data ±SEM.

Table 1. The Effects of Protease Inhibitors on Lipolysis in 3T3-L1 Adipocytes

Treatment	Lipolysis (mM glycerol released/mg protein/24 h)						
	0	Saq[a] 1 uM	Ind[b] 1 uM	Rit[c] 1 uM	Saq[a] 10 uM	Ind[b] 10 uM	Rit[c] 10 uM
Control	3.3 ± 0.13	3.5 ± 0.07	4.8 ± 0.80	3.7 ± 1.10	3.0 ± 0.80	3.6 ± 1.00	3.2 ± 0.33
NE (100 nM)	12.2 ± 0.50	11.3 ± 1.30	16.8 ± 4.00	10.4 ± 1.00	12.0 ± 1.80	13.0 ± 3.70	13.1 ± 0.10

[a]Saq = Saquinavir
[b]Ind = Indinavir
[c]Rit = Ritonavir

13. The Effect of HIV Protease Inhibitors on Specifec ^{125}I-Insulin Receptor Binding to the 3T3-L1 Murine Preadipocyte Cell Line

The previous experiments dealt with the effect of HIV protease inhibitors on triacylglycerol synthesis in 3T3-L1 at different stages of adipocyte differentiation. Due to the fact that these drugs had a profound effect on both basal and insulin-stimulated triacylglycerol synthesis, the next step was to assess the effect of these inhibitors on insulin receptor binding in these cells. This was to examine if the effects on triacylglycerol synthesis was a reflection of interferences in insulin being able to bind to its receptor.

3T3-L1 fibroblasts were cultured and subjected to adipocyte differentiation in 10% DMEM as previously described. Exposure to saquinavir, indinavir, and ritonavir was throughout all stages of the experimental procedure. At different stages of adipocyte diffrentiation, cells were serum starved for 2 hours in 0% DMEM + 0.1% BSA. Afterward, the cells were exposed to ^{125}I-insulin (1 ng/ml ^{125}I, 40 ug/ml human insulin) for 2 hours at room temperature. This was followed by solubilization in 1N NaOH and aliquots were measured for the amount of ^{125}I-insulin bound by scintillation counting (gamma counter).

Figure 27 (top panel) shows the results for insulin receptor binding at different stages of differentiation, namely at 0, 4, 7, and 11 days post-induction, in the presence of either 1 uM saquinavir, indinavir, or ritonavir. At each stage of differentiation, all three HIV protease inhibitors cause a decrease in specific ^{125}I-insulin receptor binding. The most profound effect is seen in fully differentiated adipocytes (11 days post-induction). Furthermore, the differences between treated and control samples were statistically significant ($p<0.05$). Insulin binding

decreased by 69.17% ± 0.80, 51.87% ± 0.83, and 39.6% ± 0.2 for saquinavir, indinavir, and ritonavir respectively, when compared to the control group.

The data in the bottom panel (figure 27) depicts the specific binding of ^{125}I-insulin in adipocytes when exposed to increasing concentrations of saquinavir, indinavir, and ritonavir, namely 1 and 10 uM. The overall observation was a concentration dependent decrease in insulin binding with increasing concentrations of HIV protease inhibitors. When compared to the control group, insulin binding was reduced by 32.5% ± 0.8, 42.66% ± 0.83, and 30.59% ± 0.2 for 1 uM saquinavir, indinavir, and ritonavir respectively. Consequently, insulin binding decreased by 54.99% ± 0.46, 87.47% ± 0.25, and 60.72% ±0.28 for 10 uM saquinavir, indinavir, and ritonavir respectively. The differences between treated and control group were all statistically significant ($p<0.05$).

Figure 27 : The Effect of HIV Protease Inhibitors on Specific ^{125}I-Insulin Receptor Binding in 3T3-L1 Cells

The following two graphs depicts the effects of HIV protease inhibitors on specific ^{125}I-insulin receptor binding. The upper panel shows ^{125}I-insulin binding at different stages of adipocyte differentiation, namely at 0, 4, 7, and 11 days post-induction. Cells were cultured in the absence (■) or presence of three different HIV protease inhibitors at a concentration of 1 uM, saquinavir (▲), indinavir (●), and ritonavir (*). Experiments consisted of exposing the cells to 1 ng/ml of ^{125} I-insulin (40 ug/ml human insulin) and measuring ^{125} I-insulin bound by scintillation counting. The bottom panel shows insulin receptor binding at increasing concentrations of saquinavir (▲) , indinavir (●), and ritonavir (*), 1 and 10 uM. The values for binding were measured as fmoles of specific ^{125}I-insulin bound per mg protein. The results are expressed as +SEM for n=3. Statistical significance determined by one-way anova ($p<0.05$).

The Effect of Protease Inhibitors on Specific Insulin Binding to 3T3-L1 Cells

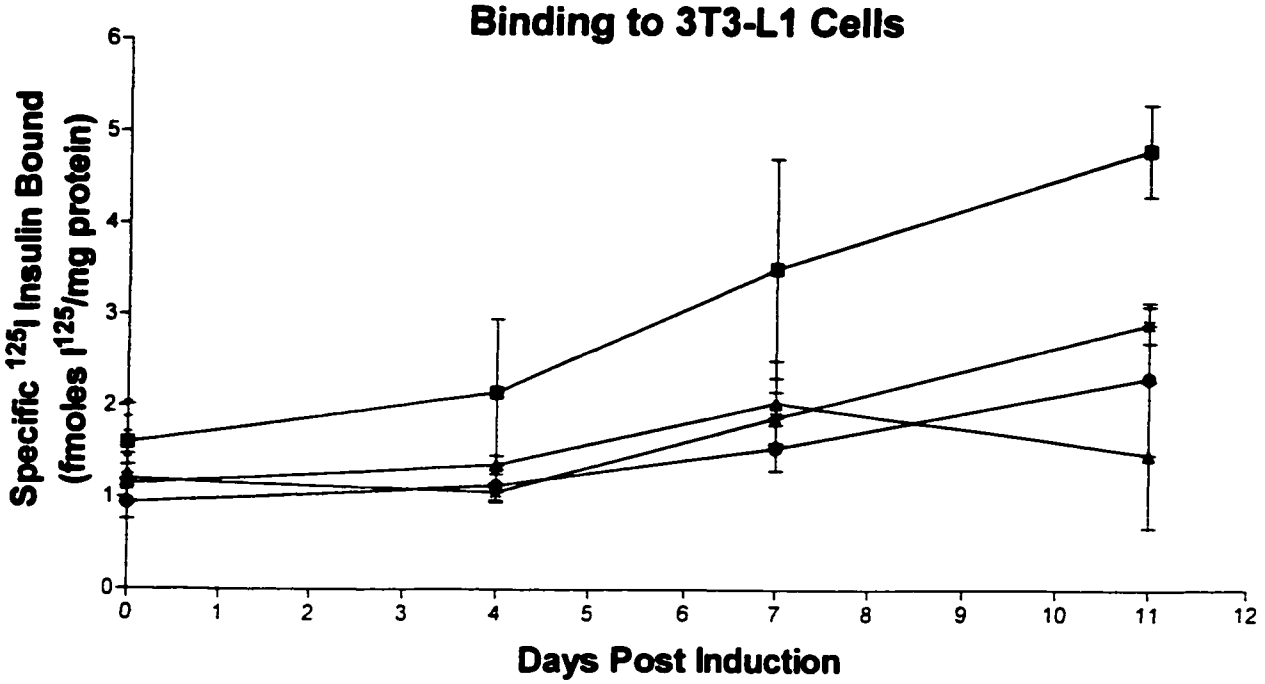

The Effect of Increasing Concentrations of Protease Inhibitors on Specific Insulin Binding in 3T3-L1 Adipocytes

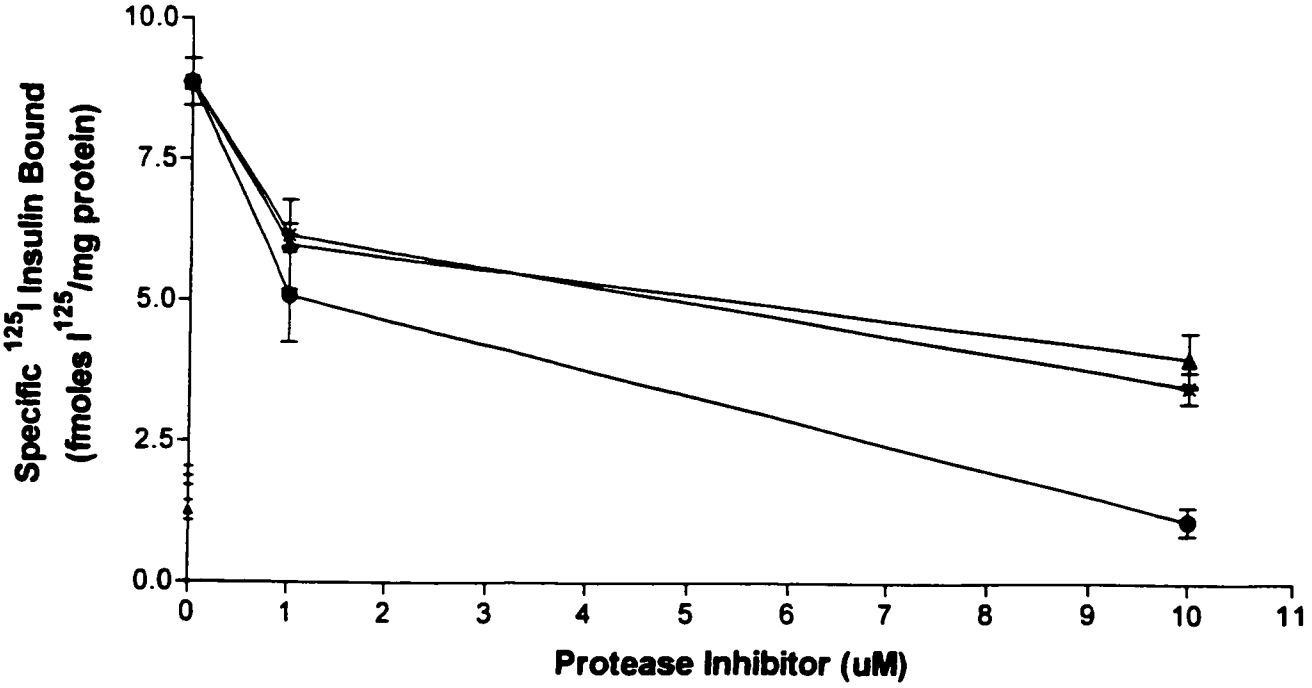

14. The Effect of Indinavir on the Displacement ^{125}I-Insulin Bound in the Presence Increasing Concentrations of Unlabeled Insulin Using 3T3-L1 Adipocytes as an *in vitro* Model

To determine whether the decrease in binding observed in drug treated samples was due to an altered receptor affinity, ^{125}I-insulin binding was measured in the presence of different competing concentrations of unlabeled insulin.

3T3-L1 fibroblasts were cultured and subjected to adipocyte differentiation in the absence and presence of 10 uM indinavir. The adipocytes were then conditioned to the same procedure for insulin binding as previously described. The only modification was an exposure to increasing concentrations of cold excess unlabeled insulin to constantly displace the ^{125}I-insulin bound to its receptor. Indinavir was present throughout all stages of the experiment.

Figure 28 shows the competitive displacement profile for 3T3-L1 adipocytes in the absence and presence of 10 uM indinavir. The data shows that the overall specific ^{125}I-insulin bound is significantly lower in indinavir treated cells compared to the control group. However, in both samples, the amount of unlabeled insulin required to cause a 50% displacement in the total amount of ^{125}I-insulin bound was approximately 300ng/ml, suggesting that the affinity for the insulin receptor to bind insulin was similar in both treated and control groups. Furthermore, 4000-ng/ml insulin was required for both samples to displace the entire ^{125}I-insulin bound. The inset depicts the percent of ^{125}I-insulin displaced with increasing concentrations of unlabeled insulin. The data points overlap showing little differences between control and drug treated samples. Therefore, insulin receptor affinities were not affected by indinavir. This data was based on one experiment with triplicate samples.

Figure 28 : The Effect of Indinavir on the Displacement of ^{125}I-Insulin Bound in the Presence of Increasing Concentrations of Unlabeled Insulin Using 3T3-L1 Adipocytes as an *in vitro* Model
The following shows the results for the competitive displacement profile for 3T3-L1 adipocytes in the absence (■) and presence of 10 uM indinavir (▲). ^{125}I-Insulin binding was performed in the presence of increasing concentrations of unlabeled insulin. Values are depicted as fmoles ^{125}I-insulin bound/mg protein versus the log of each insulin concentration. Unlabeled insulin concentrations used were as follows, 0, 0.6, 6, 60, 600, and 4000 ng /ml. The results are a summary of one experiment.

The Effect of Indinavir on the Displacement of ^{125}I-Insulin Bound in the Presence of Increasing Concentrations of Unlabeled Insulin in 3T3-L1 Adipocytes

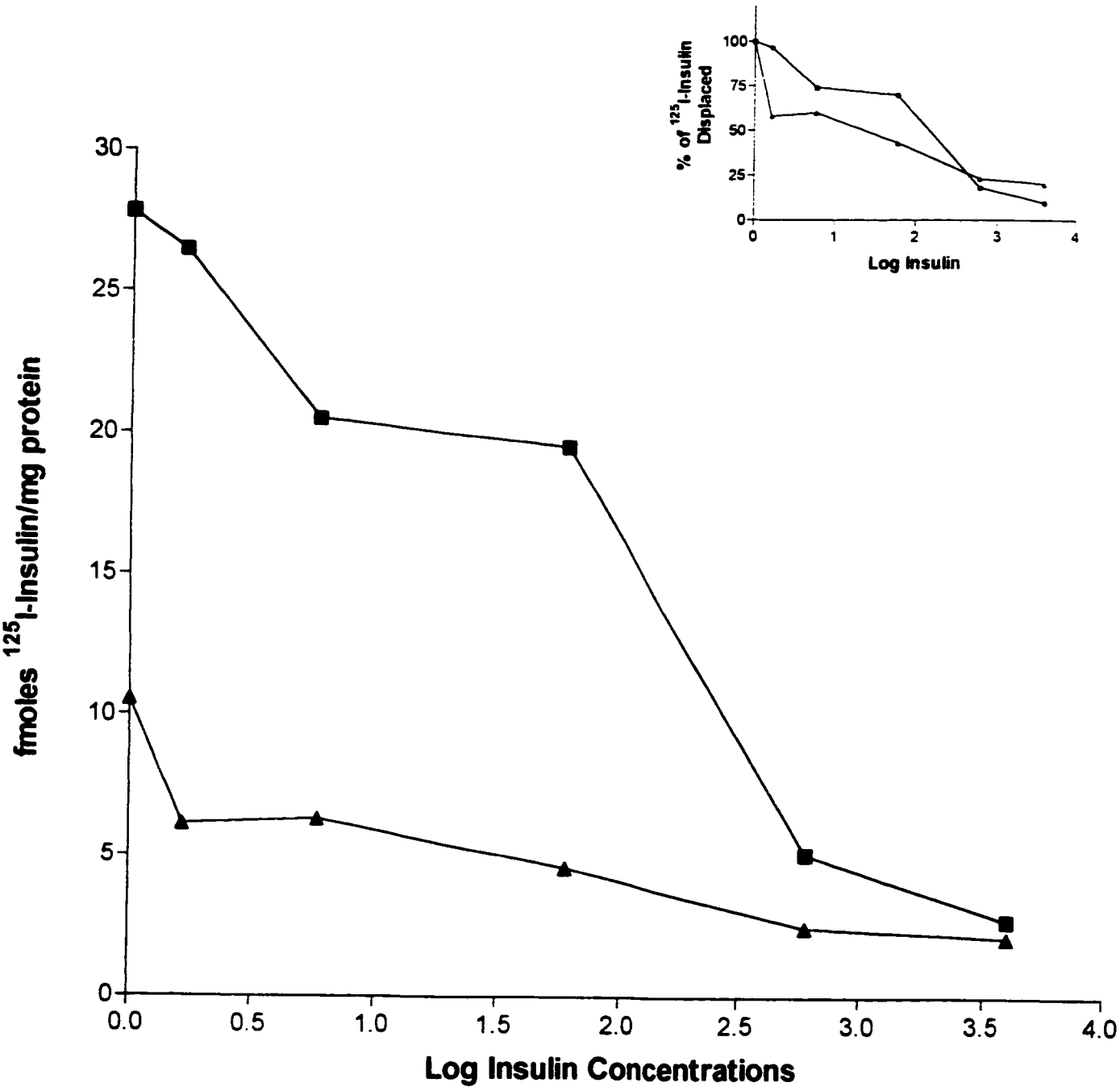

15. The Reversal of the Effect of Indinavir on Specific ^{125}I-Insulin Binding in 3T3-L1 Adipocytes

To determine if the effect of indinavir to decrease ^{125}I-insulin specific binding was reversable, insulin binding experiments were performed as previously described with a few modifications involving indinavir exposure. The modification was performed during ^{125}I-insulin binding. A total of four samples were prepared. Group 1 was labeled as the control sample. Group 2, were devoid of indinavir during culture but exposed to 1 uM indinavir during ^{125}I-insulin binding. Group 3 were exposed to 1 uM indinavir during culture, but the drug was removed during ^{125}I-insulin binding. And finally, group 4 were exposed to 1 uM indinavir during culture and during exposure to ^{125}I-insulin.

The data in figure 29 shows that the effect of indinavir on decreasing ^{125}I-insulin specific binding can indeed be reversed. Removal of the drug prior to exposing the cells to ^{125}I-insulin, in group 3, confirms this result by adipocytes binding similar amounts of fmoles of ^{125}I-insulin/mg protein to that of the control group 1. Group 2 depicts that indinavir interferes with insulin binding acutely. In other words, the drug was not required to be present during adipocyte differentiation for it to have an effect on insulin binding. The decreases for both group 2 and 4 were statistically significant (*$p<0.05$) when compared to the control group. Insulin binding declined by 32% ± 0.005 for group 2 and 42% ± 0.015 for group 4. Furthermore, although indinavir acutely affects binding, continual exposure does cause a slightly greater decrease in insulin binding.

Figure 29 : The Reversal of the Effects of Indinavir on Specific ^{125}I-Insulin Binding in 3T3-L1 Adipocytes

The following portrays the prospect of reversing the effects of indinavir on decreasing specific ^{125}I-insulin binding in 3T3-L1 adipocytes. Adipocytes were exposed to 1 ng/ml ^{125}I-insulin (40 ug/ml human insulin) for two hours. Scintillation counting was used to measure the amount of ^{125}I-insulin bound. Four samples were prepared. Group 1 was the control group. Group 2 had 1 uM indinavir present only during ^{125}I-insulin binding. Group 3 had 1 uM indinavir present during adipocyte culture only. And finally, group 4 had 1 uM indinavir present during all stages of the experiment. Values are expressed as specific ^{125}I-insulin bound per mg protein. The results are expressed as ± SEM for n=3. Statistical significance determined by one-way anova (*$p<0.05$).

The Reversal of the Effects of Indinavir on Specific ^{125}I-Insulin Binding in 3T3-L1 Adipocytes

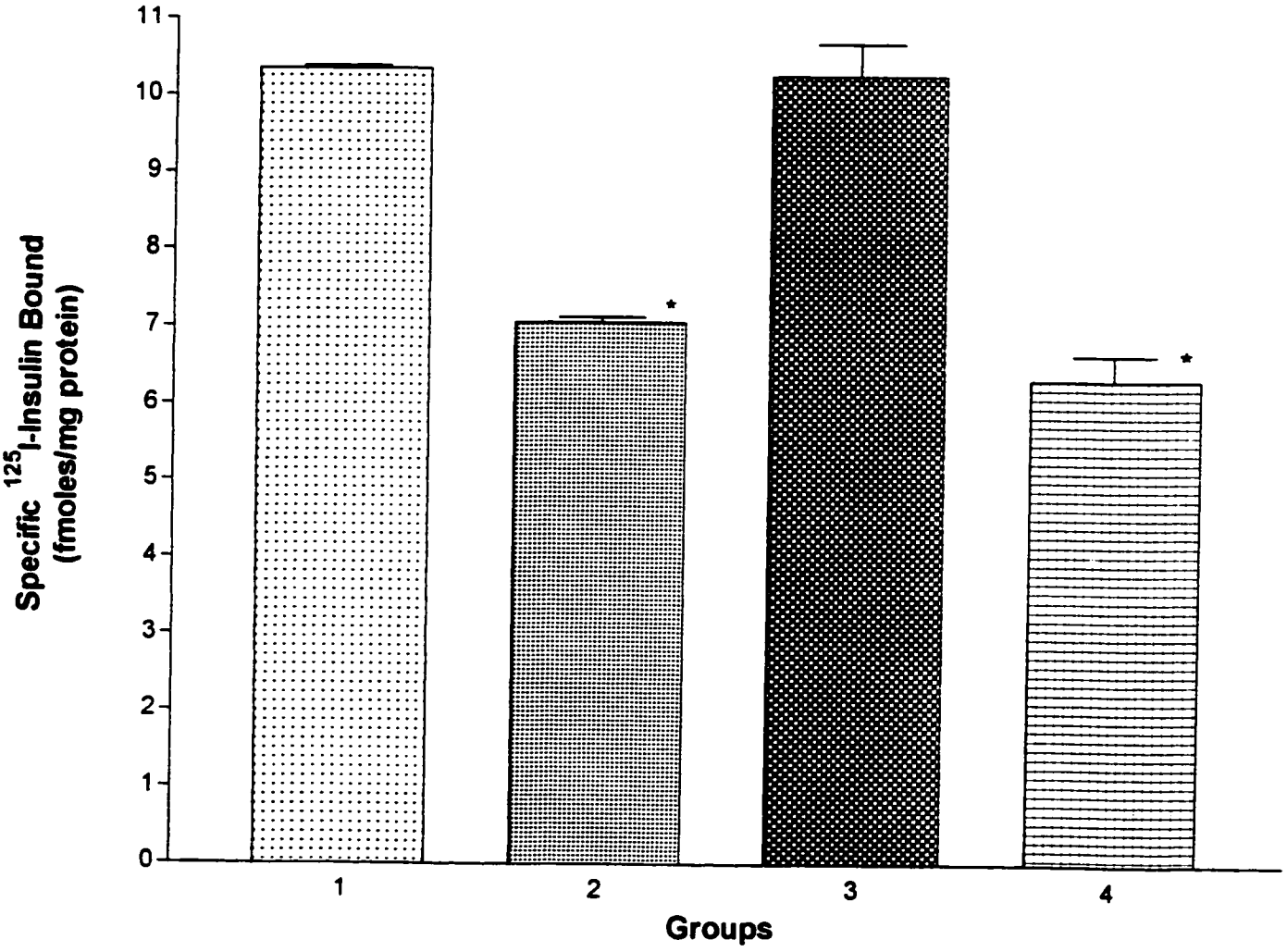

* P<0.05

16. The Effect of Indinavir on the Internalization of ^{125}I-Insulin in 3T3-L1 Adipocytes

To determine whether the decrease in triacylglycerol synthesis observed in the presence of HIV protease inhibitors was due to a defective mechanism in insulin/receptor internalization, leading to an interruption in insulin signaling, insulin internalization was assessed. 3T3-L1 fibroblasts were cultured and subjected to adipocyte differentiation in the absence or presence of 1 uM indinavir. The rate of insulin/receptor ligand internalization in both treated and control samples was measured by pre-incubating 3T3-L1 adipocytes with ^{125}I-insulin at 4°C for 4 hours and monitoring ligand uptake for various times at 37°C.

The results indicate that initially the control group adipocytes bound 31.46 fmoles ^{125}I-insulin/mg protein, where indinavir treated adipocytes only bound 22.2 fmoles ^{125}I-insulin/mg protein (data not shown). Figure 30 shows lower amounts of ^{125} I-insulin internalized over time in indinavir treated adipocytes than the control group. However, drug treated samples showed a decrease in total specific fmoles of ^{125} I-insulin bound per mg protein versus the control group. By normalizing the amount of ^{125}I-insulin bound between control and indinavir treated samples as an expression of the percent internalized from the total amount bound, it can be seen that the rates of internalization are nearly identical. Since internalization appeared unaffected, it could be assumed that the effect of indinavir on perturbing the insulin-stimulated response for triacylglycerol synthesis was occurring at a site distal to insulin receptor/ligand internalization. One possibility for indinavir's effect was that insulin could be degraded before reaching its site of action. Therefore, ^{125}I-insulin degradation was

assessed at various time frames (figure 31). The percent of the total insulin bound, which was degraded at 30 minutes, was 28.28% lower in indinavir treated adipocytes than for the control group (inset). The difference can be due to the fact that indinavir treated adipocytes bound less total ^{125} I-insulin than the control group. In conclusion, insulin internalization and degradation processes were not affected by indinavir. Data for these experiments are based on one experiment with triplicate samples.

Figure 30 : The Effect of Indinavir on the Internalization of ^{125}I-Insulin into 3T3-L1 Adipocytes

The following data depicts the effect of 1 uM indinavir on ^{125}I-insulin internalization in 3T3-L1 adipocytes. 3T3-L1 fibroblasts were subjected to adipocyte differentiation and incubated with ^{125}I-insulin for 4 hours at 4°C. The adipocytes were then washed to remove free ^{125}I-insulin, and incubated at 37°C for various time frames to assess differences in insulin internalization from surface bound insulin between control (■)and indinavir (●) treated samples. Values are given in fmoles specific ^{125}I-insulin bound per mg protein. Analyses was based on one experiment with single plates.

The Effect of Indinavir on the Internalization of ^{125}I-Insulin Following its Binding to 3T3-L1 Adipocytes

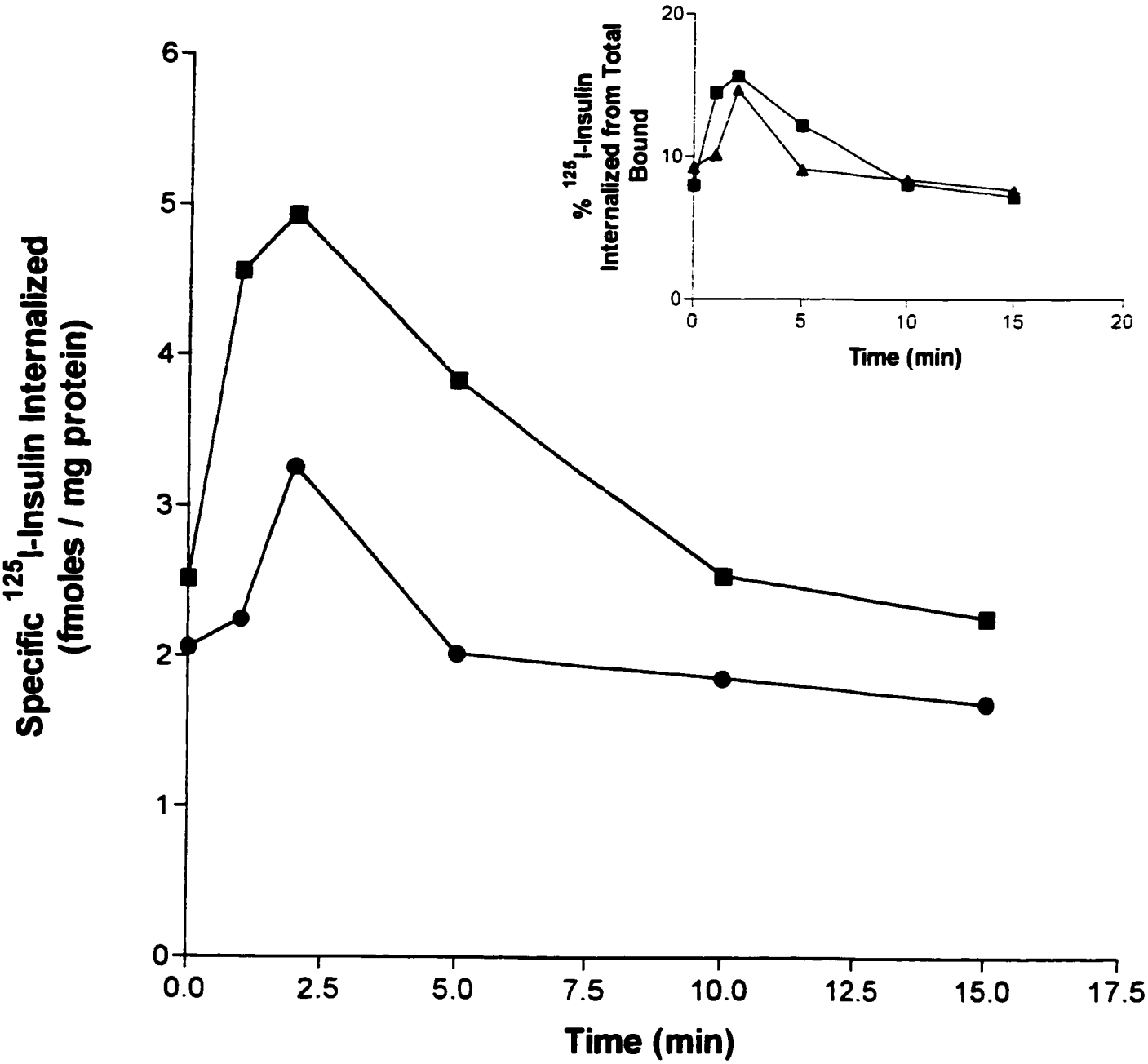

Figure 31 : The Effect of Indinavir on the Degradation of ^{125}I-Insulin Bound Following Uptake into 3T3-L1 Adipocytes

The following data depicts the effect of 1 uM indinavir on ^{125}I-insulin degradation following internalization in 3T3-L1 adipocytes. 3T3-L1 fibroblasts were subjected to adipocyte differentiation and incubated with ^{125}I-insulin (1 ng/ml). Following internalization, degradation was measued at various time frames to assess differences in ^{125}I-insulin degradation between control (■) and indinavir (●) treated samples. Values are expressed as fmoles of specific ^{125}I-insulin bound per mg protein. Analyses are based on one xperiment with individual samples.

The Effect of Indinavir on the Degradation of I^{125}-Insulin Following its Binding to 3T3-L1 Adipocytes

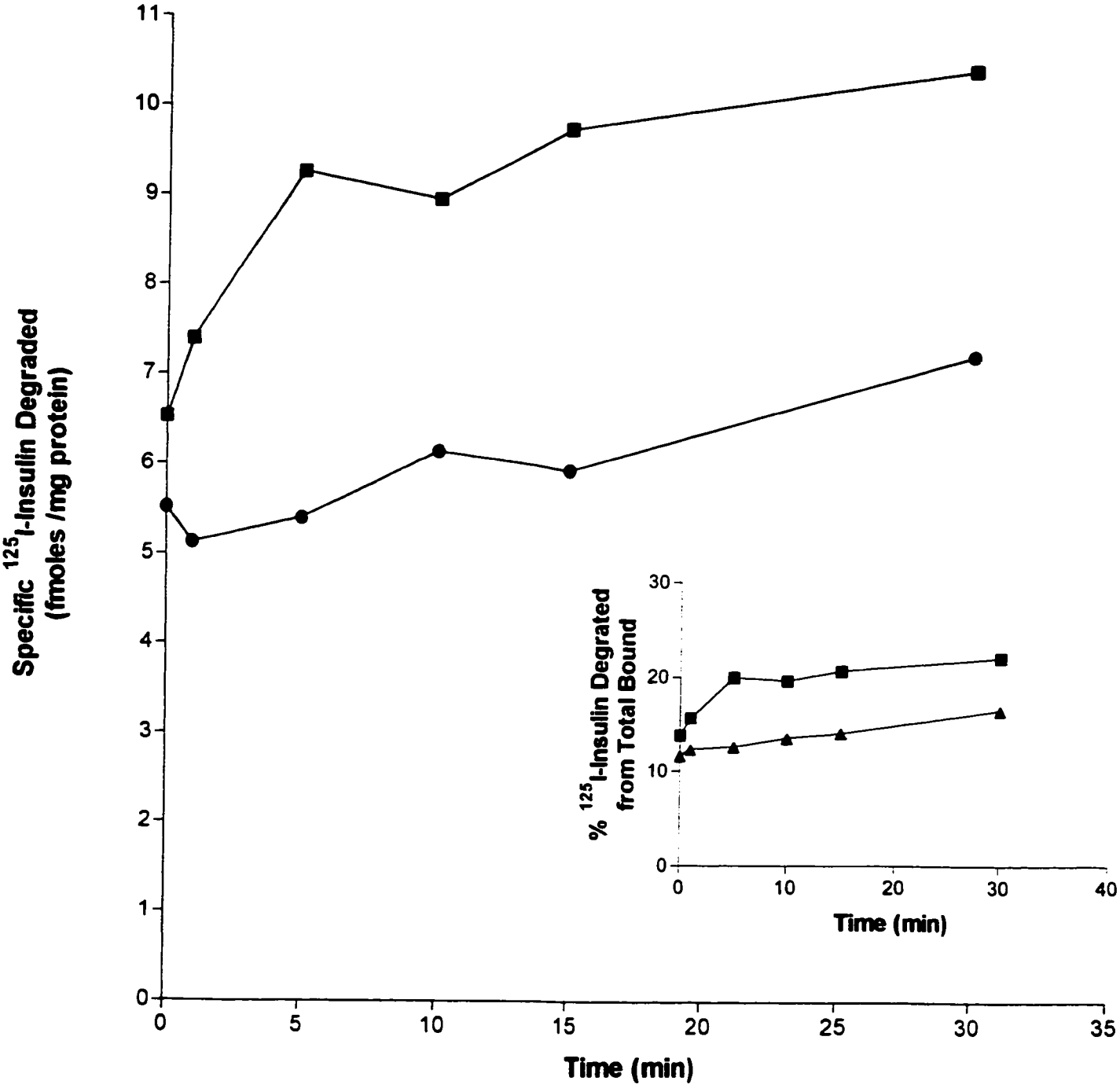

17. Investigating the Possibility of Toxicity in 3T3-L1 Fibroblasts Upon Exposure to HIV Protease Inhibitors

HIV protease inhibitors, namely saquinavir, indinavir, and ritonavir, cause some metabolic perturbations in 3T3-L1 preadipocytes and adipocytes. To determine whether exposure to these inhibitors caused a toxic effect leading eventually to increased cell death, and morphological deficiencies in adipocyte differentiation, toxicity experiments were performed using the Promega CellTiter 96 Aqueous Non-Radioactive Cell Proliferation Assay (described previously). 3T3-L1 fibroblasts were cultured in 10% DMEM and experiments were carried upon reaching confluence.

Using a range of HIV protease inhibitor concentration from 0-100 uM, table 2 shows no effect on cell viability at concentrations of 1 and 10 uM, those used in previous experiments involving adipocyte differentiation, triacylglycerol synthesis, insulin binding, and lipolysis. Furthermore, no significant differences were found between the treated and control groups (one-way anova; n=3, $P>0.05$). Cell death was only observed at concentrations 100 uM of saquinavir and ritonavir. Cell viability decreased by 48.3% ± 0.3 and 44% ± 3.2, respectively. These differences were statistically significant ($P<0.05$) when compared to the control group. Indinavir clearly had no effect on cell viability at any of the concentrations. Toxicity studies were also performed with 3T3-L1 adipocytes throughout differentiation (data not shown), and no cell death was observed in the drug treated samples.

Therefore, the metabolic effects of HIV protease inhibitors seen previously were not due to an increase in cell death by toxicity.

Table 2: Investigating the Possible Toxic Effects of HIV Protease Inhibitors on 3T3-L1 Cell Viability

The following shows the effects of saquinavir, indinavir, and ritonavir on 3T3-L1 fibroblast cell viability. Values are expressed as % cell viability versus increasing concentrations of protease inhibitors from 0-100 uM. Statistical significance determined by one-way anova, $P<0.05$ for n=3.

Table 2. The Possible Toxic Effects of HIV Protease Inhibitors in 3T3-L1 Fibroblasts
Values Expressed as % Cell Viability

[HIV PI] (uM)	Control	Saquinavir	Indinavir	Ritonavir
0	100	100 ± 0.0	100 ± 0.0	100 ± 0.0
1	100	92.7 ± 5.2	108.9 ± 2.5	94.8 ± 2.4
10	100	98.4 ± 12.8	108.1 ± 7.1	80.8 ± 2.2
50	100	86.6 ± 0.8	93.1 ± 5.7	69.3 ± 8.5
100	100	51.7 ± 0.3	96.4 ± 9.9	56.0 ± 3.2

18. The Effect of Ritonavir on Total IRS-1 Protein Levels in 3T3-L1 Cells

To determine if the effects of the HIV protease inhibitors on triacylglycerol synthesis and insulin binding were due to perturbations in the insulin signaling cascade, experiments were performed to assess any differences in IRS-1 protein levels in 3T3-L1 whole cell lysates. Western blots were performed for 3T3-L1 preadipocytes (3 days post-induction) and adipocytes (11 days post-induction). Experimental conditions consisted of samples existing under basal and insulin-stimulated (20 nM for 15 minutes) conditions in the absence or presence of 1 and 10 uM ritonavir. Whole cell extracts were prepared and subjected to SDS-PAGE. The membrane was treated with anti-IRS-1, incubated with a peroxidase-conjugated secondary antibody, and visualized by enhanced chemiluminescence (ECL).

The data in figure 33 indicates that preadipocytes exposed to ritonavir under basal conditions significantly increased the levels of total IRS-1 when compared to the control group. At 1 uM ritonavir the levels of IRS-1 increased by 38.69%. However, preadipocytes exposed to 10 uM ritonavir showed no changes in total IRS-1 levels. Under insulin-stimulated conditions, exposure to 1 and 10 uM ritonavir caused a 43.32% and 45.55% decrease in total IRS-1, respectively.

Figure 35 shows the changes in IRS-1 protein levels for adipocytes exposed to ritonavir. The same pattern as for preadipocytes was observed. Under basal conditions, exposure to 1 uM ritonavir increased total IRS-1 by 25.80% whereas no changes were observed at 10 uM. Under insulin-stimulated conditions, total IRS-1 levels decreased by 52.69% and 45.89%, respectively.

The results are representative of one experiment performed 3 times.

Figure 32 : The Effect of Ritonavir on Total IRS-1 Protein Levels in 3T3-L1 Preadipocytes

The following depicts a sample autoradiogram of a nitrocellulose membrane from a Western blot. The set of bands' show the changes observed in IRS-1 protein levels under basal and insulin-stimulated conditions and in the absence and presence of 1 and 10 uM ritonavir. At three days post-induction, assigned cell samples were exposed to 20 nM insulin for 15 minutes, extracted, and subjected to SDS-PAGE.

The Effect of Ritonavir on Total IRS-1 Protein Levels
in 3T3-L1 Preadipocytes

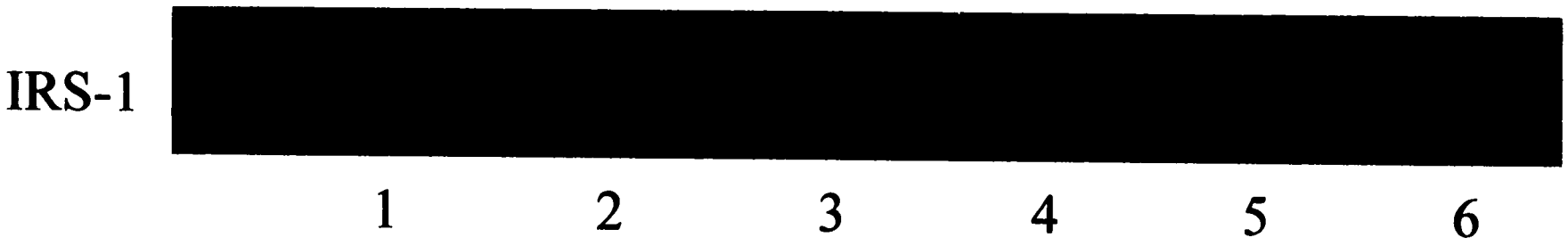

Lane 1 : Control
Lane 2 : Insulin 20 nM
Lane 3 : Ritonavir 1 uM
Lane 4 : Ritonavir 1 uM + Insulin 20 nM
Lane 5 : Ritonavir 10 uM
Lane 6 : Ritonavir 10 uM + Insulin 20 nM

Figure 33 : The Effect of Ritonavir on Total IRS-1 Protein Levels in 3T3-L1 Preadipocytes

The following is a chart showing differences in IRS-1 protein levels in 3T3-L1 cells at 3 days post-induction, following exposure to 1 and 10 uM ritonavir. Values for each sample are expressed as intensity in pixels (arb. units). Samples 1 through 6 are as follows; control, insulin, 1 uM ritonavir, insulin + 1 uM ritonavir, 10 uM ritonavir, and insulin + 10 uM ritonavir. Values are expressed as ± SEM for n=3. Statistical significance determined by one-way anova ($p<0.05$).

The Effect of Ritonavir on Total IRS-1 Protein Levels in 3T3-L1 Preadipocytes (3 days post-induction)

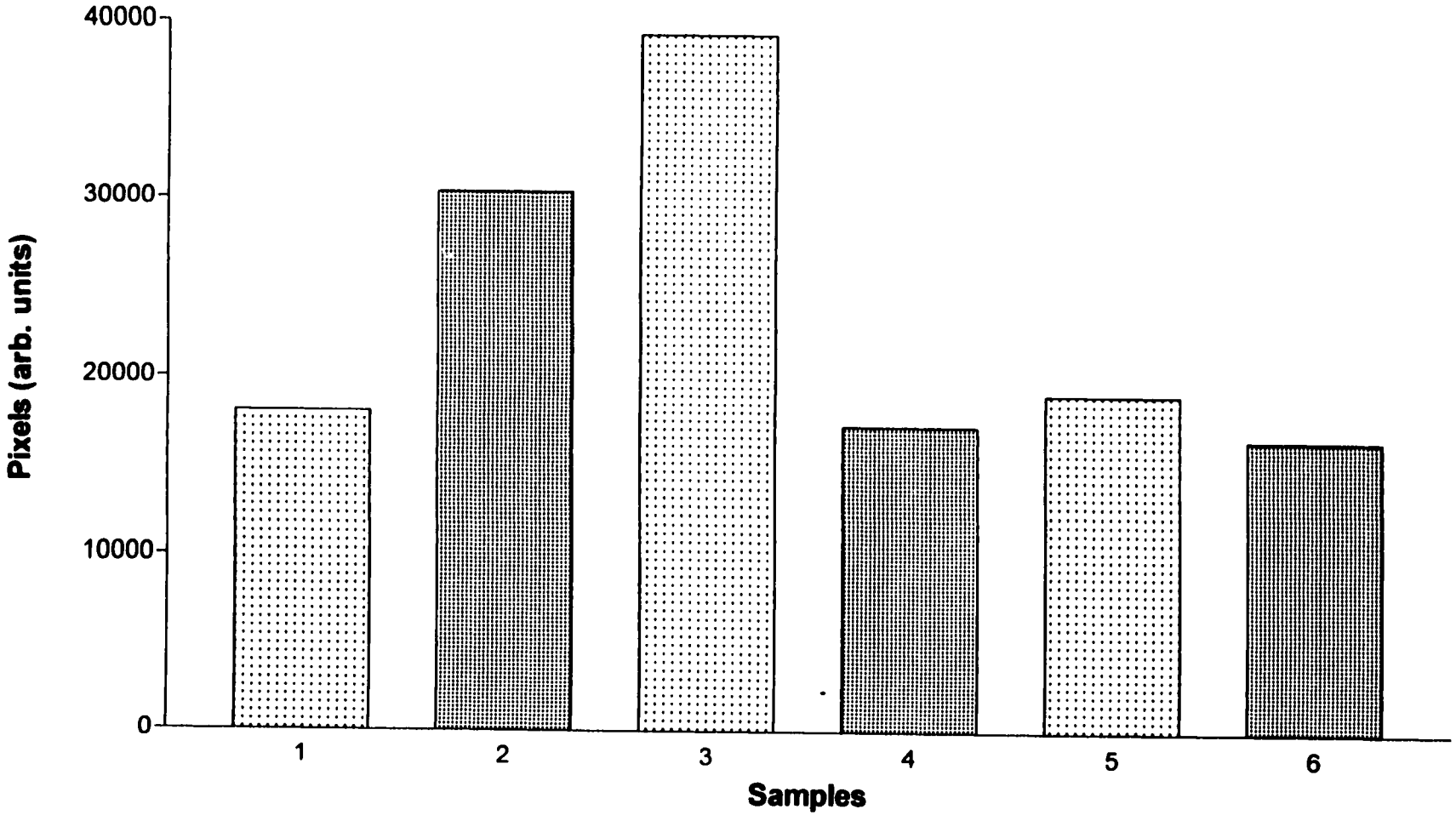

Figure 34 : The Effect of Ritonavir on Total IRS-1 Protein Levels in 3T3-L1 Adipocytes

The following depicts a sample autoradiogram of a nitrocellulose membrane from a Western blot. The set of bands' show the changes observed in IRS-1 protein levels under basal and insulin-stimulated conditions and in the absence and presence of 1 and 10 uM ritonavir. At 11 days post-induction, assigned cell samples were exposed to 20 nM insulin for 15 minutes, extracted, and subjected to SDS-PAGE.

The Effect of Ritonavir on Total IRS-1 Protein Levels in 3T3-L1 Adipocytes

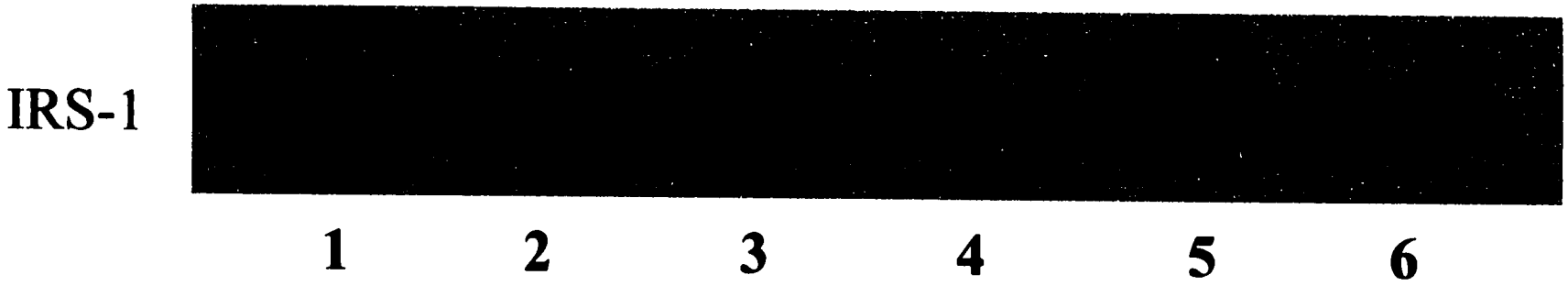

Lane 1 : Control
Lane 2 : Insulin 20 nM
Lane 3 : Ritonavir 1 uM
Lane 4 : Ritonavir 1 uM + Insulin 20 nM
Lane 5 : Ritonavir 10 uM
Lane 6 : Ritonavir 10 uM + Insulin 20 nM

Figure 35 : The Effect of Ritonavir on Total IRS-1 Protein Levels in 3T3-L1 Adipocytes

The following is a chart showing differences in IRS-1 protein levels in 3T3-L1 cells at 11 days post-induction, following exposure to 1 and 10 uM ritonavir. Values for each sample are expressed as intensity in pixels (arb. units). Samples 1 through 6 are as follows; control, insulin, 1 uM ritonavir, insulin + 1 uM ritonavir, 10 uM ritonavir, and insulin + 10 uM ritonavir. Values are expressed as ± SEM for n=3. Statistical significance determined by one-way anova ($p<0.05$).

The Effect of Ritonavir on Total IRS-1 Protein Levels in 3T3-L1 Adipocytes

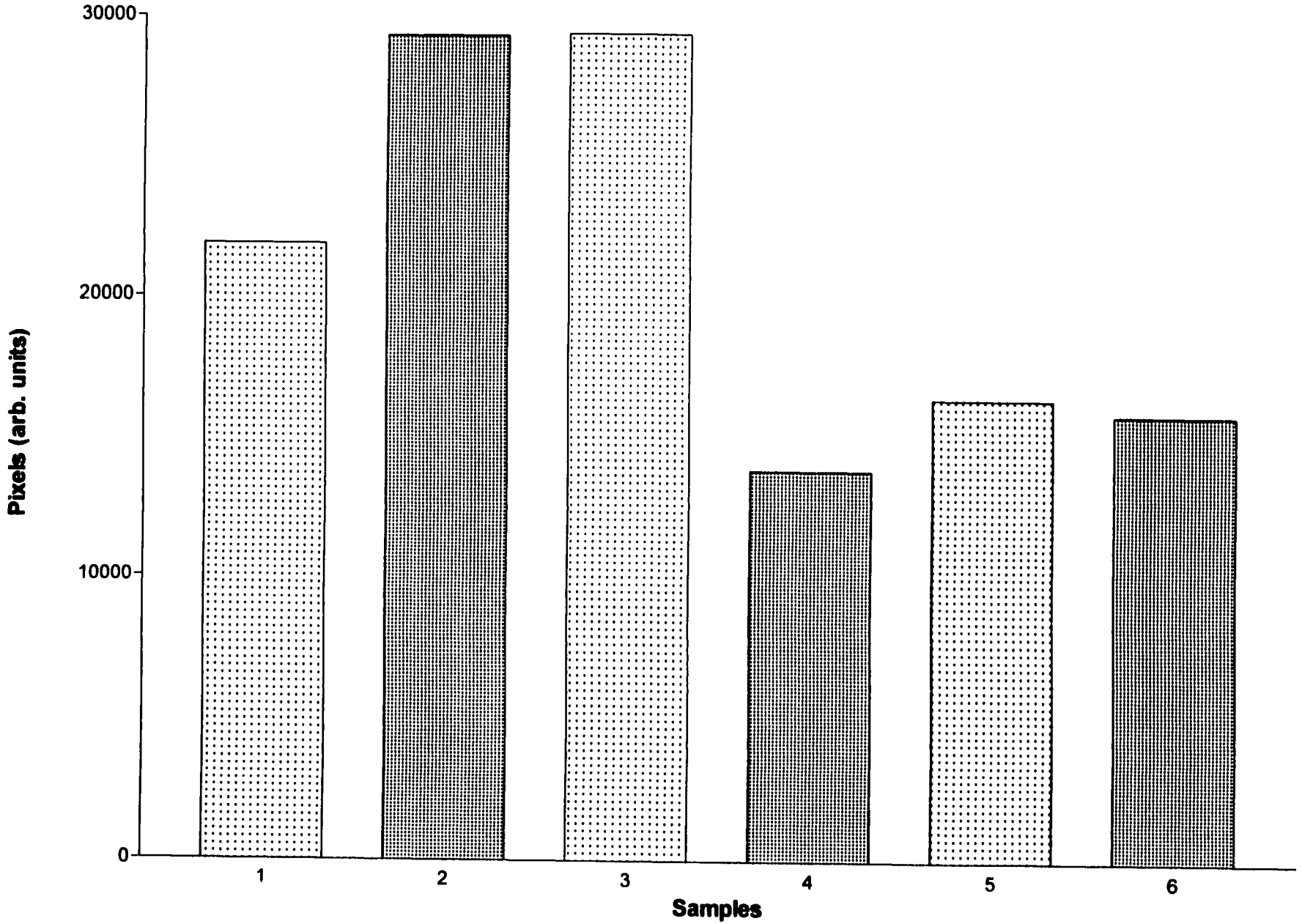

19. The Effect of Ritonavir on Tyrosine Phosphorylation of IRS-1 in 3T3-L1 Adipocytes

To further investigate the effect of ritonavir on IRS-1, immunoprecipitation experiments were performed to observe any differences in tyrosine phosphorylated IRS-1 under basal and insulin-stimulated conditions when exposed to 1 and 10 uM concentrations of ritonavir. Adipocytes were exposed to 20 nM insulin for 15 minutes followed by preparation of whole cell extracts. Sample extracts were mixed with a polyclonal rabbit anti-mouse IRS-1 antibody followed by the addition of Protein-A agarose bead slurry. Samples were then subjected to SDS-Page and probed with a tyrosine-phosphorylated antibody followed by an HRP-labeled secondary antibody, and visualized by enhanced chemiluminescence (ECL).

The data in figure 37 indicates that firstly, insulin rapidly increases IRS-1 phosphorylation and that exposure to ritonavir significantly decreases the levels of tyrosine phosphorylated IRS-1 when compared to the control group. Under basal conditions, 1 uM ritonavir significantly increased the levels of tyrosine phosphorylated IRS-1 by 60%. However, no changes were observed at 10 uM of drug. Under insulin-stimulated conditions, adipocytes exposed to 1 and 10 uM ritonavir showed a concentration dependent decrease in tyrosine phosphorylated IRS-1, by 40% and 50% respectively, when compared to the control group. These differences were statistically significant ($P<0.05$) when compared to the control group.

The results clearly show that ritonavir affects either the overall tyrosine phosphorylation of IRS-1, or its regulation by and serine/threonine kinases.

Figure 36 : Changes in Levels of Tyrosine Phosphorylated IRS-1 in the Presence of Ritonavir in 3T3-L1 Adipocytes

The following depicts a sample autoradiogram of a nitrocellulose membrane from a Western blot. The set of bands' show the changes observed in IRS-1 tyrosine phosphorylation levels under basal and insulin-stimulated conditions and in the absence and presence of 1 and 10 uM ritonavir. At 11 days post-induction, assigned cell samples were exposed to 20 nM insulin for 15 minutes, extracted, immunoprecipitated with an IRS-1 antibody and subjected to SDS-PAGE.

Changes in Levels of Tyrosine Phosphorylated IRS-1
in the Presence of Ritonavir in 3T3-L1 Adipocytes

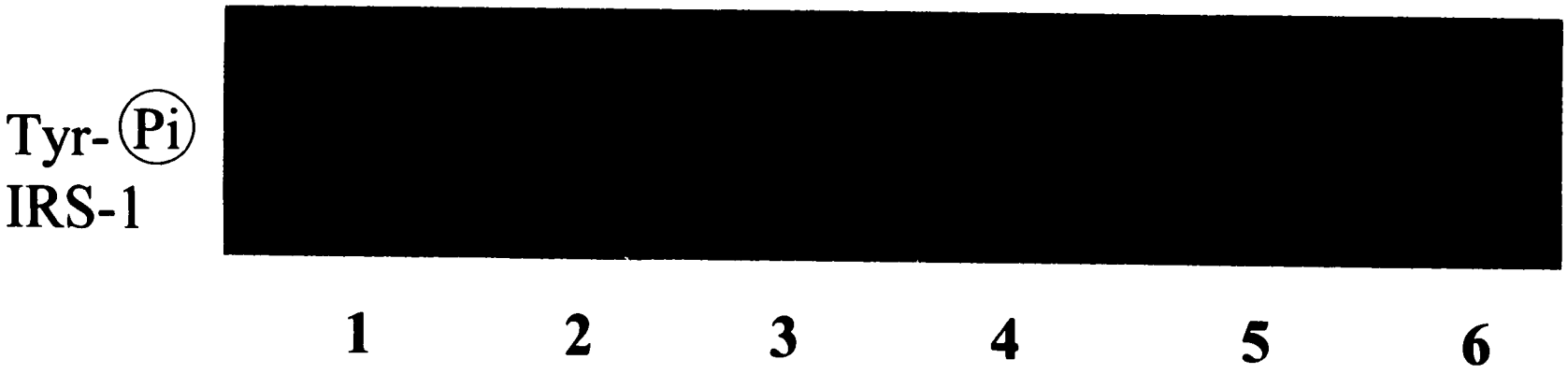

Lane 1 : Control
Lane 2 : Insulin 20 nM
Lane 3 : Ritonavir 1 uM
Lane 4 : Ritonavir 1 uM + Insulin 20 nM
Lane 5 : Ritonavir 10 uM
Lane 6 : Ritonavir 10 uM + Insulin 20 nM

Figure 37 : Changes in Levels of Tyrosine Phosphorylated IRS-1 in the Presence of Ritonavir in 3T3-L1 Adipocytes

The following is a chart showing differences in tyrosine phosphorylated IRS-1 in 3T3-L1 cells at 11 days post-induction, following exposure to 1 and 10 uM ritonavir, in the absence and presence of 20 nM insulin. Values for each sample are expressed as intensity in pixels (arb. units). Samples 1 through 6 are as follows; control, insulin, 1 uM ritonavir, insulin + 1 uM ritonavir, 10 uM ritonavir, and insulin + 10 uM ritonavir. Values are expressed as ± SEM for n=3. Statistical significance determined by one-way anova ($p<0.05$).

Changes in Tyrosine Phosphorylated IRS-1 in the Presence of Ritonavir in 3T3-L1 Adipocytes

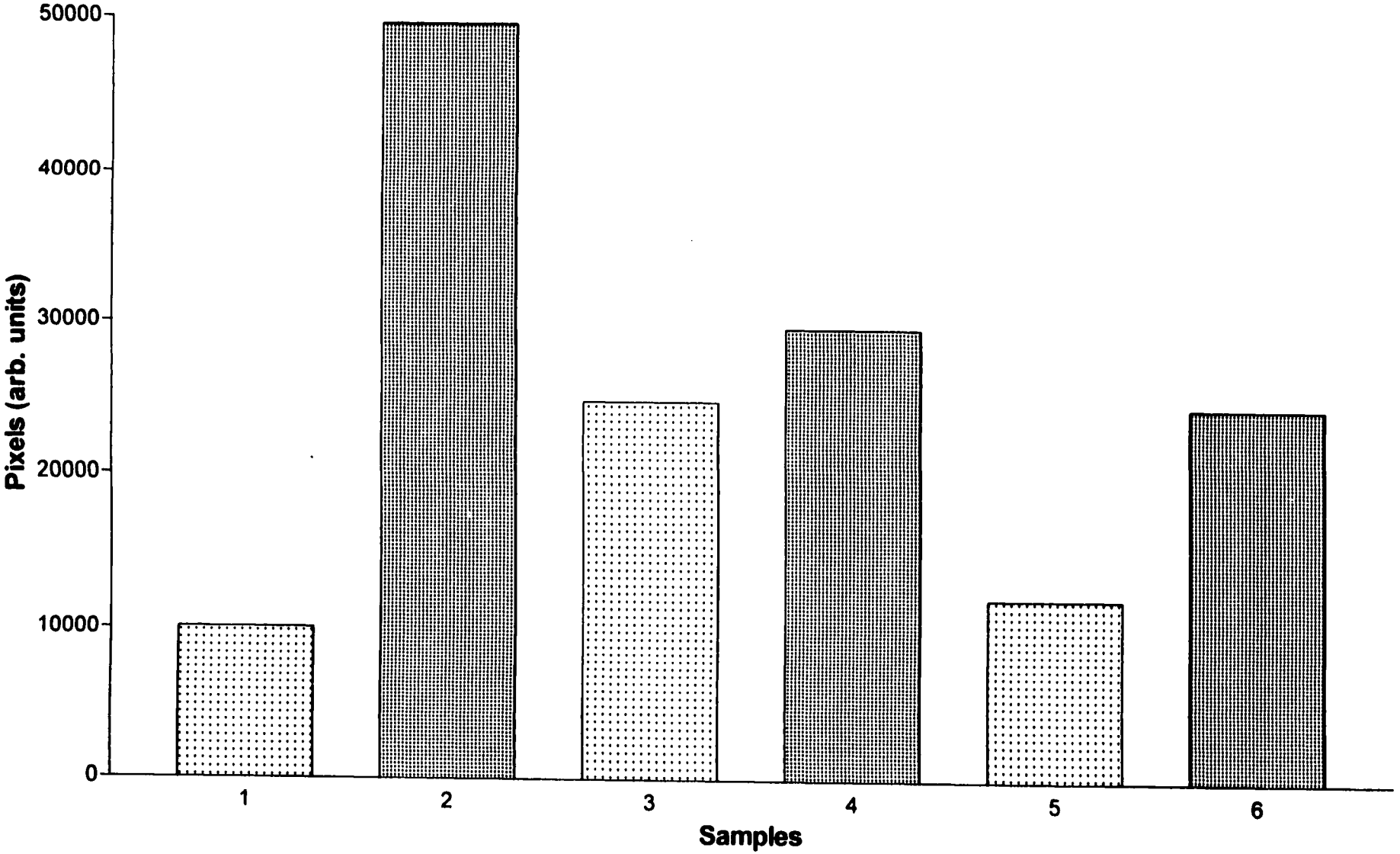

DISCUSSION

HIV protease inhibitor treatment, which dramatically improved the prognosis of HIV-infected patients, appears to cause or aggravate a metabolic syndrome with potentially severe consequences. The cellular mechanisms underlying the appearance of this syndrome are largely unknown. The clinical evidence of systemic peripheral insulin resistance, as well as the high prevalence of peripheral lipodystrophy and central adiposity, suggested that altered adipose tissue metabolism may have a central role in the development of the syndrome.

Foremost, all three HIV protease inhibitors used in this study did not alter cell viability in 3T3-L1 preadipocytes at concentrations used in all experiments (Table 2). Evidence is presented to suggest that the HIV protease inhibitors (PIs), saquinavir, indinavir, and ritonavir can inhibit *in vitro* murine preadipocyte differentiation (Figure 16, 17, & 18). All three PIs were capable of reducing the amount of total cytoplasmic triacylglycerol in 3T3-L1 adipocytes as measured by oil red staining and this effect was more pronounced at higher drug concentrations. At 10 uM, indinavir had the greatest inhibitory effect on adipocyte differentiation than both saquinavir and ritonavir. The concentrations of saquinavir, indinavir, or ritonavir, required to elicit these effects *in vitro* is within the range of that observed in plasma from patients administered therapeutic doses of PIs (127). Thus, it is possible that the effects of these PIs on the 3T3-L1 cell line observed *in vitro* may reflect *in vivo* events. Using the 3T3-L1 adipocyte cell line, Zhang *et al.* (128) have validated a portion of our observations showing that nelfinavir and ritonavir inhibit lipid accumulation *in vitro*. In contrast to our findings, Gagnon *et al.* (129) reported that they observed potentiation of 3T3-L1 preadipocyte differentiation by

indinavir and ritonavir. This effect was apparent by oil red staning and estimated to be 10-40%. As we have failed to observe any potentiation of 3T3-L1 preadipocyte differentiation by protease inhibitors in experiments where culture conditions were very similar to those reported by Gagnon, the reason for this discrepancy is unclear. Furthermore, no other laboratory has demonstrated PI effects as seen by Gagnon *et al.* Other effects of PIs on 3T3-L1 adipocytes were shown by Dowell *et al.* (127). He reported that 3T3-L1 adipocytes treated with ritonavir and saquinavir (20uM) exhibited signs of cell death and apoptosis. One other previous study revealed similar inhibitory effects on adipocyte differentiation in primary human preadipocytes. They showed that both indinavir and saquinavir inhibited human preadipocyte differentiation with the latter having a greater inhibitory effect (130). While the rank order of potency of these two agents has not been directly compared in clinical studies, patients treated with a ritonavir/saquinavir combination are more prone to develop lipodystrophy than those treated with indinavir alone (41). Therefore, evidence suggests that HIV PIs may contribute to adipose tissue atrophy by promoting adipocyte cell death and preventing replacement of lost adipocytes by inhibiting preadipocyte differentiation.

Treatments with certain PIs are often accompanied by atrophy of subcutaneous adipose tissue and accumulation of abdominal and breast fat. To determine if these changes were due to alterations in glucose and lipid metabolism, we studied the effects of PIs on de novo lipid synthesis in 3T3-L1 cells. It has been shown that saquinavir, indinavir, and ritonavir increased basal triacylglycerol synthesis yet decreased insulin-stimulated triacylglycerol synthesis in a dose-dependent fashion in murine 3T3-L1 preadipocytes at distinct stages of differentiation. Three days after the onset of

differentiation, at concentrations of up to 10 uM, 3T3-L1 preadipocytes showed an increase of approximately 50% in triacylglycerol synthesis under basal conditions. Additionally, a 50% decrease in triacylglycerol synthesis was observed for all three PIs at concentrations of 10 uM under insulin-stimulated conditions (Fig 21, 22, 23). However, eleven days after the onset of differentiation, when cytoplasmic lipid droplets are more abundant, ritonavir caused only slight changes in lipid synthesis. At 10 uM of drug, we observed only a 2% increase in basal triacylglycerol synthesis and a 30% significant decrease under insulin-stimulated conditions (Fig 24). The results suggest differences in de novo lipid synthesis at two distinct stages of adipocyte differentiation. Early on, preadipocytes, during differentiation, are under stress and seem to be more susceptible to the effects of the PIs while mature adipocytes are able to resist and maintain characteristic lipid synthesis and accumulation into lipid droplets. Since these PIs inhibit adipocyte differentiation in a dose-dependent fashion, one would assume that alterations in differentiation would cause a decrease in the degree of lipid synthesis under insulin-stimulated conditions due to the reduction of insulin receptors on the surface. However, indinavir was the only PI that caused the greatest inhibitory effect on differentiation, and lipid synthesis for fully differentiated adipocytes was only assessed with ritonavir. Therefore, exposure to ritonavir affects lipid synthesis in preadipocytes but is slightly effective in mature adipocytes. To explain the reason for increased lipid synthesis under basal conditions, PIs must be stimulating a pathway that mimics lipid synthesis derived from glucose, such as insulin does. PIs are either affecting the insulin signaling pathway or another distinct pathway such as the acylation-stimulating protein (ASP) pathway. Both human and murine adipocytes express the complement components C3, factor B and factor

D (adipsin). The combined activity of these components generates the acylation-stimulating protein, which stimulates lipogenesis. If PIs were affecting a different pathway (e.g. ASP), there would be an additive synthesis of triacylglycerols in the presence of insulin. Taking into account that PIs decrease lipid synthesis in the presence of insulin, PIs must be interfering with the insulin-signaling cascade. Clearly, in vitro, HIV PIs inhibit insulin-stimulated de novo triacylglycerol synthesis whereby the adipocytes exhibited a decreased response to insulin. This inhibition could contribute to the insulin resistance seen in HIV patients taking PIs as part of their regimens. On the same note, Ranganathan *et al.* (131) recently observed similar results in 3T3-F442A regarding sugar transport. They found that both saquinavir and indinavir increased basal glucose transport 2.7 fold and that saquinavir but not indinavir decreased insulin-stimulated glucose transport by 30%.

Correlating with the fact that 3T3-L1 adipocytes might be insulin resistant in the presence of PIs due to the decreased insulin response, lipid synthesis was performed with increasing concentrations of insulin. This was to assess whether higher insulin concentrations could compensate for the decreased insulin response and stimulate the cells to synthesize triacylglycerols. Insulin concentrations above physiological levels could not alleviate the inhibition of insulin-stimulated triacylglycerol synthesis by ritonavir (Fig 25,26). In vivo, the perturbed insulin response (insulin resistance) would cause the increased release of pancreatic insulin (hyperinsulinnemia) to regulate glucose levels in the blood. Therefore, it is not surprising that HIV patients exhibit hyperinsulinemia, hyperglycemia and eventually type 2 diabetes when given PI as part of their regimens.

This study has also demonstrated whether the effect of PIs on subcutaneous fat loss is a result of an increase in adipocyte lipolysis. The results showed that following a 24-hour exposure to the PIs, they had little effect on stimulating lipolysis in 3T3-L1 adipocytes (Table 1). In contrast to our findings, Lenhard *et al.* (132) found that PIs (10uM) stimulated lipolysis in C3H10T1/2 mesenchymal stem cells. Differences between the cell lines may account for disparity between these results. 3T3-L1 cells are committed to undergo differentiation into adipocytes independently or through induction with a hormonal cocktail, whereas C3H10T1/2 cells are stem cells that are not committed to the adipocyte lineage, but have the capacity to do so when appropriately induced. Moreover, 3T3-L1 cells express a phenotype similar to white adipose tissue (132) whereas C3H10T1/2 cells express a phenotype similar to brown adipose tissue (132).

In an effort to understand the mechanism underlying the effect of PIs on adipocyte differentiation and lipid metabolism, several studies were conducted to identify changes in gene expression when 3T3-L1 adipocytes were exposed to PIs. Stevens et al (133) showed that several genes associated with glucocorticoid metabolism and signaling were changed. The gene expression profile of PI-treated 3T3-L1 exhibited suppression of key transcription factors, lipogenic enzymes, and differentiation-related proteins. This is consistent with a partial block in early stages of preadipocyte differentiation to mature adipocytes. Previous hypothesis suggested PIs inhibit differentiation through alteration in PPAR-γ and RXR (41); however Stevens (134) showed that neither gene transcript changed with PI treatment. Furthermore, other studies confirmed that alteration in PPAR-γ/RXR signaling, regulation or antagonisms of ligand binding are not responsible for the inhibitory effect on adipocyte differentiation (130). However, one study carried out by

Dowell *et al.* (127) with 3T3-L1 adipocytes concluded that nelfinavir inhibits preadipocyte differentiation. This occurred at a point following C/EBPβ protein expression and mitotic clonal expansion and that the levels of C/EBPα and PPARγ protein, which are normally expressed after C/EBPβ, were markedly reduced in nelfinavir treated cells. The inconsistency between these results and ours can be on account of the different PI used and the higher concentration employed (20 uM).

Also, this study demonstrated the effect of HIV PIs on insulin binding and receptor processing in 3T3-L1 adipocytes at distinct stages of adipocyte differentiation. The data suggests that there is a decreased ability of 3T3-L1 cells to bind ^{125}I-Insulin in the presence of saquinavir, indinavir, and ritonavir (Fig 27). This occurred in a dose-dependent fashion at concentrations similar to those observed in plasma from patients administered therapeutic doses of PIs (127). Furthermore, binding of ^{125}I-Insulin decreased throughout adipocyte differentiation. These results clearly show that there can be a possible link between the decreased ability of insulin to bind to its receptor in the presence of PIs and insulin resistance seen in HIV patients taking PIs. In agreement with our studies, Caron *et al.* (135) showed that 3T3-F442A cells cultured with indinavir displayed an inhibition in insulin receptor β-subunit expression and insulin receptor binding activity. These results suggest several explanations on how PIs interfere with ^{125}I-Insulin binding to adipocytes *in vitro*. Foremost, PIs inhibit adipocyte differentiation, which would result in a decrease in the number of insulin receptors available for binding. This could be occurring at the molecular level causing a decrease in gene expression of the insulin receptor. Secondly, PIs could either be interfering directly or allosterically with insulin or the insulin receptor, disturbing insulin binding. Thirdly, PIs could be competing

with insulin for binding to the insulin receptor resulting in perturbation of the insulin response. And lastly, PIs could affect insulin receptor affinity. Competitive displacement experiments demonstrated that adipocytes exposed to 10 uM indinavir had no effect on the affinity of insulin for its receptor (Fig 28). Furthemore, insulin internalization and degradation processes were not affected by indinavir (Fig 30,31). Since insulin and PIs do not have similar structures, competitive binding between the two for the insulin receptor in highly unlikely. Therefore, allosteric interactions between PIs and insulin or PIs and the insulin receptor could be a cause for the reduction in insulin binding observed in our studies. Interestingly, inhibition of ^{125}I-Insulin binding to 3T3-L1 adipocytes is completely reversable upon the acute removal of the PIs. Removal of indinavir rapidly restored normal insulin binding to control levels (Fig 29). Therefore, if the inhibition can be acutely reversed then the effect of PIs on insulin binding does not occur at the molecular level (i.e. decreased transcription or translation of the insulin receptor) in 3T3-L1 adipocytes. Furthemore, clinical studies whereby patients had PIs removed from their regimens had a decrease or an overall improvement of the lipodystrophic symptoms, morphologically as well as clinically (136).

Patients treated with PIs frequently develop impaired glucose tolerance (IGT) or diabetes. The underlying cause seems to be a PI-induced insulin resistance (137). Alterations in the early steps of insulin signaling have been recognized as an important component of many insulin-resistant states. Decreased insulin binding, decreased receptor kinase activity, decreased IRS-1 protein, and decreased IRS-1-associated PI3-kinase have all been demonstrated in liver, muscle, and fat from ob/ob mice with type 2 diabetes (138). An IRS-1 related defect might be one of the causes of insulin resistance. Therefore, we

also investigated potential molecular mechanisms by which the protease inhibitor ritonavir might alter insulin signaling and in this way trigger insulin resistance. Insulin stimulation of cells that had not been exposed to ritonavir resulted in rapid increases of IRS-1 phosphorylation. We have shown that incubation of 3T3-L1 preadipocytes and adipocytes with ritonavir resulted in an increase in IRS-1 protein levels under basal conditions and reduced insulin effects on increasing IRS-1 tyrosine phosphorylation (Fig 32-37). It is not clear whether a ritonavir-induced reduction of insulin-stimulated IRS-1 phosphorylation in the initial phase of insulin signaling, as we observed, could itself lead to insulin resistance. It is, however, possible that intial burst in signaling by the early insulin signaling elements is important for the signaling to more longlasting downstream intermediates. Therefore, the ritonavir-induced impairment of the initial rise in insulin signaling could result in sustained reductions in later signals and downstream biological effects.

Chronic hyperinsulinemia induces serine/threonine phosphorylation of IRS-1 and reduces insulin signaling (139). It has been shown that increased serine phosphorylation of IRS-1 inhibits its ability to be tyrosine phosphorylated by the insulin receptor and to bind and activate PI3-kinase (140). Pederson *et al.* (141) have recently reported that serine/threonine phosphorylation of IRS-1, which occurs through a rapamycin-dependent pathway, precedes its degradation of the protein by hyperinsulinemia and that maintaining the tyrosine phosphorylation of IRS-1 may prevent its degradation. In our study, ritonavir decreased the tyrosine phosphorylation of IRS-1, suggesting that PIs could be involved in enhancing serine/threonine phosphorylation of IRS-1 and its subsequent degradation, resulting in a diminished insulin response when assessing glucose and lipid metabolism in vitro. Conversely, insulin resistance and compensatory hyperinsulinemia seen in HIV-1

patients taking PIs could trigger the enhanced degradation of IRS-1 leading to a diminished insulin response and an overall decrease in glucose and lipid metabolism. Murata *et al.* (142) observed a significant dose-dependent decrease in insulin-stimulated glucose uptake when 3T3-L1 adipocytes were exposed acutely (6 min) to indinavir (0-100uM). However, he reports that indinavir had no effects on insulin signaling events involving the tyrosine phosphorylation of IRS-1, the ability of PI3-kinase to phosphorylate Akt, and the translocation of intracellular GLUT 1 and GLUT 4 glucose transporters to the cell surface. He did, however, find that indinavir inhibited the intrinsic transport activity of the GLUT 4 transporter. The discrepancy involving the phosphorylation IRS-1 can be due to the use of different PIs, ritonavir versus indinavir and also that Murata exposed the cells only acutely to indinavir (i.e. 4 hours) whereby our adipocytes were cultured and differentiated in the presence of ritonavir (15 days). In addition, Murata *et al.* exposed their cells to 100 uM indinavir, which is above physiological levels. Nevertheless, the inhibitory effect of PIs on GLUT 4 is therefore likely to be one of the causes of insulin resistance following perturbation in IRS-1 phosphorylation observed in HIV patients receiving this class of drugs. Previous studies report that fat cells from subjects with manifest type 2 diabetes have low IRS-1 expression followed by a marked impairment in insulin signaling, including PI3-kinase activation and serine phosphorylation of PKB/Akt; maximally insulin-stimulated glucose transport is impaired; and GLUT 4 protein expression is also markedly reduced (106). In predisposed individuals, diabetes can result after pancreatic β cells fail to compensate for the insulin resistance. A recent clinical study employing a longitudinal design comparing fasting glucose and insulin levels before and after administration of PI therapy demonstrated that insulin resistance is apparent after a

relatively short period of time (an average of 3.4 months between measurements) before significant changes in body weight and fat distribution occur. The fact that insulin resistance appears to precede the manifestation of lipodystrophy is consistent with our results that PIs cause insulin resistance through its effects on insulin signaling events and on GLUT 4, rather than insulin resistance developing secondary to the lipodystrophy (142).

The next section does not involve results from our studies but gives an overview about the possible causes for the dyslipidaemic profile seen in HIV-1 patients taking PIs. Prospective studies have reported that a high accumulation of abdominal fat was a significant risk factor for diabetes (143) and cardiovascular disease (144). It was found that a high accumulation of upper body fat was associated with high fasting plasma triglyceride (145) levels, with reduced concentrations of plasma HDL-cholesterol (146) and with an increased proportion of dense, cholesterol ester-depleted LDL particles in the plasma (147). The criteria mentioned above are some of the manifestations that are present in lipodystrophic HIV-1 patients. Therefore, one would ask? Is dyslipidaemia mainly due to the insulin resistant state induced by HIV PIs, to the compensatory hyperinsulinaemia, or to the inhibition of adipocyte differentiation and lipid metabolism? Lenhard *et al.* (148) recently reported that ritonavir alone increased serum triglycerides (TG) in mice and that saquinavir and ritonavir but not indinavir increased TG synthesis in HepG2 cells. In addition, only ritonavir increased cholesterol synthesis in HepG2 cells. Furthermore, Ranganathan *et al.* (131) showed that saquinavir and not indinavir decreased the activity of the lipoprotein lipase (LPL) enzyme responsible for the catabolism of triglyceride-rich lipoproteins. However, LPL translation and its immunoreactive mass

were unaffected by saquinavir. Therefore, these results suggest that saquinavir might inhibit the post-translational processing of LPL, resulting in the synthesis of an enzyme with low activity. Studies conducted with visceral obese, insulin resistant patients showed that basal adipose tissue LPL activity is high but its response during a meal is blunted, which could contribute to the impaired tolerance to dietary fat. Furthermore, in the fasting state, skeletal muscle LPL activity is low. As the fasting skeletal muscle LPL activity is positively correlated to plasma cholesterol levels, it is suggested that its low activity may also contribute to the dyslipidademic profile of visceral obesity (149). Therefore, the above-mentioned can be applied to HIV-1 lipodystrophic patients. In vitro, saquinavir affects the overall activity of LPL and lipodystrophic patients exhibit the same dyslipidaemic profile as visceral obese, insulin resistant patients. Hence, HIV-1 insulin-resistant patients taking PIs have an impaired tolerance to dietary fat because of the blunted response of adipose tissue LPL resulting in high plasma triglycerides and low HDL-cholesterol levels. These and other observations indicate that select PIs affect multiple, distinct metabolic pathways, perhaps accounting for the different side effects observed for each PI in the clinic. This may be due to differences in affinity for cellular proteins (eg, proteases) cell permeability, tissue distribution, or metabolism of PI.

In conclusion, we report that PIs exerted deleterious effects on adipocyte differentiation, triacylglycerol synthesis, insulin binding and signaling in the 3T3-L1 cell line. Discrepancies between the different PIs and cell lines employed in several studies suggest that the clinical manifestations of lipodystrophy could be multifactorial, reflecting the contributions of drug treatment to multiple biochemical pathways. The relevance of our findings to *in vivo* adipose tissue homeostasis remains to be determined. Data from a

recently completed prospective study of HIV-infected patients suggest that PIs, promote metabolic abnormalities (hyperglycemia, hyperinsulinemia, and hyperlipidemia) before detectable changes in body composition (Dowell). These findings do not exclude the possibility that PIs may have direct, atrophic effects on subcutaneous adipose tissue subsequent to or detectable only after the development of metabolic abnormalities. The need to acquire a thorough understanding of the factors leading to HIV-related lipodystrophy is paramount because the detrimental effects of this syndrome threaten to erode strident gains in effective viral suppression and in lifespan extension of HIV-infected patients.

REFERENCES

1. Cullen, B.R. 1991. Regulation of human immunodeficiency virus replication. Annu.Rev.Microbiol. 45:219-250.

2. Kingsman, S.M. and A.J. Kingsman. 1996. The regulation of human immunodeficiency virus type-1 gene expression. Eur.J.Biochem. 240:491-507.

3. Levy, J.A. 1993. Pathogenesis of human immunodeficiency virus infection. Microbiol.Rev. 57:183-289.

4. Safrit, J.T. and R.A. Koup. 1995. The immunology of primary HIV infection: which immune responses control HIV replication? Curr.Opin.Immunol. 7:456-461.

5. Pantaleo, G. and A.S. Fauci. 1996. Immunopathogenesis of HIV infection. Annu.Rev.Microbiol. 50:825-854.

6. http://edcenter.med.cornell.edu.

7. Bour, S.R. Geleziunas, and M.A. Wainberg. 1995. The human immunodeficiency virus type-1 (HIV-1) CD4 receptor and its central role in promotiom of HIV-1 infection. Microbiol.Rev. 59:63-93.

8. Craven, R.C. and S.R. Hann. 1996. Dynamic interactions of the Gag polyprotein. Curr.Top.Microbiol.Immunol. 214:65-94.

9. Li, X.Y. Quan, and M.A. Wainberg. 1997. Controlling elements in replication of the human immunodeficiency virus type 1. Cell.Mol.Biol. (Noisy-le-grand) 43:443-454.

10. Romano, G., M. Kasten, and A. Giordano. 1999. Current understanding of AIDS pathogenesis. Anticancer Res. 19: 3157-3166.

11. http://www.tthhivclinic.com

12. Fouchier, R.A. and M.H. Malim. 1999. Nuclear import of human immunodeficiency virus type-1 preintegration complex. Adv.Virus. Res. 52:275-299.

13. Ptashne, M. 1988. How eukaryotic transcriptional activators work. Nature 335:683-689.

14. Freed, E.O. 1998. HIV-1 gag proteins: diverse functions in the virus life cycle. Virology 251:1-15.

15. Kohl, N.E., E.A. Emini, W.A. Schleif, L.J. Davis, J.C. Heimbach, R.A.F. Dixon, E.M. Scolnick and I.S. Sigal. 1988. Active human immunodeficiency virus protease is required for viral infectivity. Proc.Natl.Acad.Sci. USA 85:4686-4690.

16. Peng, C., B.K. Ho, T.W. Chang and N.T. Chang. 1989. Role of human immunodeficiency virus type 1-specific protease in core protein maturation and viral infectivity. J.Virol. 63:2550-2556.

17. Peng, C., K. Moelling, N.T. Chang and T.W. Chang. 1991. Identification and characterization of HIV-1 gag-pol fusion protein in transfected mammalian cells. J.Virol. 65:2751-2756.

18. Gottlinger, H.G., J.G. Sodroski and W.A. Haseltine. 1989. Role of capsid precursor processing and myristylation in morphogenesis and infectivity of human immunodeficiency virus type-1. Proc.Natl.Acad.Sci. USA 86:5781-5785.

19. Park, J. and C.D. Morrow. 1993. Mutations in the protease gene of human immunodeficiency virus type-1 affect release and stability of virus particles. Virology 194:843-850.

20. Pearl, L.H. and W.R. Taylor. 1987. A structural model for the retroviral proteases. Nature 329:351-354.

21. Orozlan, S. and R.B. Luftig. 1990. Retroviral proteinases. Curr.Top.Microbiol. Immunol. 157:153-185.

22. Loeb, D.D., R. Swanstrom, L. Everitt, M. Manchester, S.E. Stamper and C.A. Hutchison III. 1989b. Complete mutagenesis of the HIV-1 protease. Nature 340:397-400.

23. Giam, C.Z. and I. Boros. 1988. *In vivo* and *in vitro* autoprocessing of human immunodeficiency virus protease expressed in Escherichia coli. J.Biol.chem. 263:14617-14620.

24. Nutt, R.F., S.F. Brady, P.L. Darke, T.M. Ciccarone, E.M. Nutt, J.A. Rodkey, C.D. Bennet, L.H. Waxman and I.S. Sigal. 1988. Chemical synthesis and enzymatic activity of a 99-residue peptide with a sequence proposed for the human immunodeficiency virus protease. Proc.Natl.Acad.Sci. USA 85:7129-7133.

25. Katoh, I., Y. Ikawa and Y. Yoshinaka. 1989. Retrovirus protease characterized as a dimeric aspartic protease. J.Virol. 63:2226-2232.

26. Miller, M., M. Jaskolski, J.K.M. Rao, J. Leis and A Wlodawer. 1989a. Crystal structure of a retroviral protease proves relationship to aspartic protease family. Nature 337:576-579.

27. Miller, M., B.K. Sathyanarayana, M.V. Toth, G.R. Marshall, L. Clawson, L. Seik, J. Schneider, S.B.H. Kent and A. Wlodawer. 1989b. Structure of complex of synthetic HIC-1 protease with a substrate-based inhibitor at 2.3Å resolution. Science 246:1149-1152.

28. Navia, M.A., P.M.D. Fitzgerald, B.M. McKeever, C.T. Leu, J.C. Heimbach, W.K. Herber, I.S. Sigal, P.L. Darke and J.P. Springer. 1989. Three-dimensional structure of aspartyl protease from human immunodeficiency virus HIV-1. Nature 337:615-620.

29. Weber, I.T., M. Miller, M. Jaskolski, J. Leis, A.M. Skalka and A. Wlodawer. 1989. Molecular modelling of the HIV-1 protease and its substrate binding site. Science 243:928-931.

30. Wlodawer, A., M. Miller, M. Jaskolski, B.K. Sathyanarayana, E. Baldwin, I.T. Weber, L.M. Selk, L. Clawson, J. Schneider and S.B.H. Kent. 1989. Conserved folding in retroviral proteases: crystal structure of a synthetic HIC-1 protease. Science 245:616-621.

31. Rose, J.R., R. Salto and C.S. Craik. 1993. Regulation of autoproteolysis of the HIV-1 and HIV-2 proteases with engineered amino acid substitutions. J.Biol.Chem. 268:11939-11945.

32. Babe, L.M., J. Rose and C.S. Craik. 1992. Synthetic "interface" peptides alter dimeric assembly of the HIV-1 and 2 proteases. Protein Sci. 1:1244-1253.

33. http://www.acponline.org

34. http://hivinsite.ucsf.edu

35. Deeks, S.G., M. Smith, M. Holodnity, J. O. Kahn. 1997. HIV-1 protease inhibitors. JAMA 277:145-153.

36. Scevola, D., A. Di Matteo, F. Uberti, G. Minoia, F. Poletti, A. Faga. 2000. Reversal of cachexia in patients treated with potent antiretroviral therapy. The AIDS Reader 10 (6):365-375.

37. Carr, A., K. Samaras, A. Thorisdottir, G.R. Kaufmann, D.J. Chisholm, D.A. Cooper. 1999. The Lancet 353:2093-2098.

38. Wanke, C.A. 1999. Epidimiological and clinical aspects of the metabolic complications of HIV infection: The fat redistribution syndrome. AIDS 13:1287-1293.

39. Marlink, R.G. Winter 2001. Lipodystrophy from A to Z: An overview of lipodystrophy syndrome in patients with HIV infection. JIAPAC.

40. Kotler, D.P. 2000. Fat redistribution and metabolic abnormalities. Medscape HIV/AIDS: Annual Update 2000. http:// www.medscape.com

41. Carr, A., K. Samaras, D.J. Chisholm, D.A. Cooper. 1998. Pathogenesis of HIV-1 protease inhibitor-associated peripheral lipodystrophy, hyperlipidaemia, and insulin resistance. The Lancet 351:1881-1883.

42. Brinkman, K., J.A. Smeitink, J.A. Romiji, P. Reiss. 1999. Mitochondrial toxicity induced by nucleoside-analogue reverse-transcriptase inhibitors is a key factor in the pathogenesis of antiretroviral-therapy-related lipodystrophy. The Lancet 354:1112-1115.

43. Fajas, L., JC. Fruchart and J. Auwerx. 1998. Transcriptional control of adipogenesis. Curr.Opin.Cell Biol. 10:165-173.

44. Flier, JS. 1995. The adipocyte: storage depot or node on the energy information superhighway. Cell 80:15-18.

45. Rosenbaum, M., RL. Leibel, J. Hirsch. 1997. Obesity. N Engl J Med. 337:396-407.

46. Cowherd, R.M., R.E. Lyle, R.E. McGehee Jr. 1999. Molecular regulation of adipocyte differentiation. Cell Devel. Biol. 10:3-10.

47. Scott, RE. 1982. Coupling of preadipocyte growth arrest and differebtiation. A cell cycle model for the physiological control of cell proliferation. J Cell Biol. 94:400-405.

48. Comelius, P., O.A. MacDougald, MD. Lane. 1994. Regulation of adipocyte development. Annu.Rev. Nutr 14:99-129.

49. Tontonoz, P., BM. Spiegelman. 1995. Regulation of adipocyte gene expression and differentiation by peroxisome proliferator activated receptor-gamma. Curr.Opin Genet. Devel. 5:571-576.

50. Schoonjans, K., B. Staels, J. Auwerx. 1996. Role of the peroxisome proliferator activated receptor in mediating effects of fibrates and fatty acids on gene expression. J Lipid Res. 37:907-925.

51. Schoonjans, K., B. Staels, J. Auwerx. 1996. Peroxisome proliferator activated receptors and their effects on lipid metabolism and adipocyte differentiation. Biochim. Biophys. Acta 1302:93-109.

52. Tontonoz, P., BM. Spiegelmann. 1994. Stimulation of adipogenesis in fibroblasts by PPAR-gamma2, a lipid-activated transcription factor. Cell 79:1147-1156.

53. Tontonoz, P., R.A. Graves, A.I. Budavari, BM. Spiegelmann. 1994. MPPAR-gamma2: tissue-specific regulator of an adipocyte enhancer. Genes Devel. 8:1224-1234.

54. Cao, Z., RM Umek, SL McKnight. 1991. Regulated expression of three C/EBP isoforms during adipocyte conversion of 3T3-L1 cells. Genes Devel. 5:1538-1552.

55. MacDougald, OA, P. Cornelius, FT Lin, SS Chen, MD Lane. 1994. Glucorticoids reciprocally regulate expression of the CCAAT/Enhancer-binding protein alpha and delta genes in 3T3-L1 adipocytes and white adipose tissue. J Biol.Chem. 269:19041-19047.

56. Wang, N., MJ Finegold, A Bradley, C Ou, SV Abdelsayed, MD Wilde, LR Taylor, Dr Wilson, GJ Darlington. 1995. Impaired energy homeostasis in C/EBP-alpha knockout mice. Science 269:1108-1112.

57. Tontonoz, P., JB Kim, RA Graves, BM Spiegelman. 1993. ADD1: a novel helix-loop-helix transcription factor associated with adipocyte determination and differentiation. Mol. Cell Biol. 13:4753-4759.

58. Yokoyama, C., X Wang, MR Briggs, A Admon, J Wu, X Hua, JL Goldstein, MS Brown. 1993. SREBP-1, a basic helix-loop-helix-leucine zipper protein that controls transcription of the LDL receptor gene. Cell 75:187-197.

59. Kim, JB, BM Spiegelman. 1996. ADD1/SREBP1 promotes adipocyte differentiation and gene expression linked to fatty acid metabolism. Genes Dev 10:1096-1107.

60. Schwarz, EJ, MJ Reginato, D Shao, SL Krakow, MA Lazar. 1997. Retinoic acid blocks adipogenesis by inhibiting C/EBPb-mediated transcription. Mol. Cell Biol. 17:1552-1561.

61. Smas, CM, HS Sul. 1997. Cleavage of membrane-associated pref-1 generates a soluble inhibitor of adipocyte differentiation. Cell 73:725-734.

62. Prins, JB, S. O'Rahilly. 1997. Regulation of adipose cell number in man. Clinical Science 92:3-11.

63. Rodbell, M. 1964. Metabolism of isolated fat cells. I. Effects of hormones on glucose metabolism and lipolysis. J Biol.Chem. 239:375-380.

64. Baldo, A., AD Sniderman, S. St-Luce, et al. 1993. The adipsin-acylation stimulating protein system and regulation of intracellular triglyceride synthesis. J Clin. Invest. 92:1543-1547.

65. Petruschke, TH., H Hauner. 1993. Tumor necrosis factor-alpha prevents the differentiation of human adipocyte precursor cells and causes delipidation of newly developed fat cells. J Clin. Endocrinol. Metab. 76:742-747.

66. Denton, R., RW Brownsey, GJ Belsham. 1981. A partial view of the mechanism of insulin action. Diabetologia 21:347-362.

67. Reaven G. 1995. The fourth musketeer – from Alexandre Dumas to Claude Bernard. Diabetologia 38:3-13.

68. Inadera, H., S Ito, Y Ishikawa, et al. 1993. Visceral fat deposition is seen in patients with insulinoma. Diabetologia 36:91-92.

69. Taha, C., A. Klip. 1999. The insulin-signaling pathway. J. Membrane Biol. 169:1-12.

70. Ebina, Y., L. Ellis, K. Jarnagin, M. Edery, L. Graf, E. Clauser. 1985. The Human Insulin Receptor cDNA: the Structural Basis For Hormone- Activated Transmembrane Signalling. Cell 40:747.

71. Kasuga, M., Y. Fujita-Yamaguchi, D. Blithe, C.R. Kahn. 1983. Proc. Natl. Acad. Sci. USA 80:2137-2141.

72. White, M.F. 1997. The insulin signalling system and the IRS proteins. Diabetologia 40:S2-S17.

73. Bergeron, J., J. Cruz, M. Kahn, B. Posner. 1985. Uptake of Insulin and Other Ligands into Receptor-Rich Endocytic Components of Target Cells: The Endosomal Apparatus. Annu.Rev.Physiol. 47:383-403.

74. Goldfine, I. 1987. The insulin receptor: molecular biology and transmembrane signaling. Endocr.Rev. 8:235-255.

75. Kahn, C.R. 1976. Membrane receptors for hormones and neurotransmitters. J.Cell Biol. 70:261-286.

76. Geuze, H., J. Slot, G. Straus, H. Lodish, A. Schwartz. 1983. Intracellular Site of Asialoglycoprotein Receptor-ligand Uncoupling: Double-label Immunoelectron Microscopy during Receptor-mediated Endocytosis. Cell 32:277-287.

77. Baenziger, J., D. Fiete. 1986. Separation of two populations of endocytic vesicles involved in receptor-ligand sorting in rat hepatocytes. J.Biol.Chem. 261:7445-7454.

78. Marshall, S. 1985. Dual pathways for the intracellular processing of insulin. Relationship between retroendocytosis of intact hormone and the recycling of insulin receptors. J.Biol.Chem. 260:13524-13531.

79. Levy, J., J. Olefsky. 1986. Retroendocytosis of insulin in rat adipocytes. Endocrinology 119:572-579.

80. Marshall, S., A. Green, J. Olefsky. 1981. Evidence for recycling of insulin receptors in isolated rat adipocytes. J.Biol.Chem. 256:11464-11470.

81. Marshall, S. 1985. Kinetics of insulin receptor internalization and recycling in adipocytes. Shunting of receptors to a degradative pathway by inhibitors of recycling. J.Biol.Chem. 260:4136-4144.

82. White, M. 1998. The IRS-signalling system: A network of docking proteins that mediate insulin action. Mol.Cell Biochem. 182:3-11.

83. Kaburagi, Y., R. Honda-Yamamoto, K. Tobe, K. Ueki, M. Yachi, Y. Akanuma, R. Stephens, D. Kaplan, Y. Yazaki, T. Kadowaki. 1995. The role of the NPXY motif in the insulin receptor in tyrosine phosphorylation of insulin receptor substrate-1 and Shc. Endocrinology 136:3437-3443.

84. Inoue, G., B. Cheatham, R. Emkey, C.R. Kahn. 1998. Dynamics of insulin signaling in 3T3-L1 adipocytes. J.Biol.Chem. 273:11548-11555.

85. Hu, P., A. Mondino, E. Skolnik, J. Schlessinger. 1993. Cloning of a novel, ubiquitously expressed human phosphatidylinositol 3- kinase and identification of its binding site on p85. Mol.Cell Biol. 13:7677-7688.

86. Dhand, R., K. Hara, I. Hiles, B. Bax, I. Gout, G. Panayotou, M. Fry, K. Yonezawa, M. Kasuga, M. Waterfield.1994. PI 3-kinase: structural and functional analysis of intersubunit interactions. EMBO J. 13:511-521.

87. Shepherd, P., D. Withers, K. Siddle. 1998. Phosphoinositide-3-kinase: the key switch mechanism in insulin signaling. Biochem J 333:471-490.

88. Belacossa, A., J. Testa, S. Staal, P. Tsichlis. 1991. Science 254:244-247.

89. Kohn, A., K. Kavacina, R. Roth. 1995. Insulin stimulates the kinase activity of RAC-PK, a pleckstrin homology domain containing ser/thr kinase. EMBO J. 14:4288-4295.

90. Walker, K., M. Deak, A. Paterson, K. Hodson, P. Cohen, D. Alessi. 1998. Activation of protein kinase B b and q isoforms. Biochem J 331:299-308.

91. Alessi, D., P. Cohen. 1998. Mechanism of activation and function of protein kinase B. Curr.Opin.Gene and Devel. 8:55-62.

92. Alessi, D., M. Andjelkovic, B. Cauldwell, P. Cron, N. Morrice, P. Cohen, B. Hemmings. 1996. Mechanism of activation of protein kinase B by insulin and IGF-1. EMBO J. 15:6541-6551.

93. Andjelkovic, M., D. Alessi, R. Meier, A. Fernandez, N. Lamb, M. Frech, P. Cron, P. Cohen, J. Lucocq, B. Hemmings. 1997. Role of Translocation in the Activation and Function of Protein Kinase B. *J.Biol.Chem.* 272:31515-31324.

94. Martin, S., J. Tellam, C. Livingstone, J. Slot, G. Gould, D. James. 1996. The glucose transporter (Glut 4) and vesicle associated membrane protein-2 (VAMP-2) are segregated from recycling endosomes in insulin-sensitive cells. J.Cell.Biol. 134:625-635.

95. Martin, S., A. Shewan, C. Millar, G. Gould, D. James. 1998. Vesicle-associated membrane protein-2 plays a specific role in the insulin-dependent trafficking of the facilitated glucose transporter Glut 4 in 3T3-L1 adipocytes. J.Biol.Chem. 273:1444-1452.

96. Shepherd, P.R., B. Kahn. 1999. Glucose transporters and insulin action. New Engl J Med. 341:248-257.

97. Thomsom, M.J., M.G. Williams, S.C. Frost. 1997. Development of insulin resistance in 3T3-L1 adipocytes. J Biol Chem 272:7759-64.

98. De Herreros, A.G., M.J. Birnbaum. 1989. The acquisition of increased insulin-responsive hexose transport in 3T3- L1 adipocytes correlates with expression of a novel transporter gene. J Biol Chem. 264:19994-19999.

99. Piper, R.C., L.J. Hess, D.E. James. 1991. Am. J Physiol. 260:C570-C580.

100. Blok, J., E.M. Gibbs, G.E. Lienhard, J.W. Slot, H.J. Geuze. 1988. Insulin-induced translocation of glucose transporters from post-Golgi compartments to the plasma membrane of 3T3-L1 adipocytes. J Cell Biol. 106:69-76.

101. De Fronzo, R.A., E. Ferrannini. 1991. Insulin resistance. A multifaceted syndrome responsible for NIDDM, obesity, hypertension, dyslipidemia, and atherosclerotic cardiovascular disease. Diabetes Care. 14:173-194.

102. Reaven, G.M. 1995. Pathophysiology of insulin resistance in human disease. Physiol. Rev. 75:473-486.

103. Martin, B.C., J.E. Warram, A.S. Krolewski, R.N. Bergman, J.S. Soeldner, C.R. Kahn. 1992. Role of glucose and insulin resistance in development of type 2 diabetes mellitus: results of a 25-year follow-up study. Lancet 340:925-929.

104. Lillioja, S., D.M. Mott, M. Spraul, R. Ferraro, J.E. Foley, E. Ravussin, W.C. Knowler, P.H. Bennet, C. Bogardus. 1993. Insulin resistance and insulin secretory dysfunction as precursors of non-insulin-dependent diabetes mellitus. Prospective studies of Pima Indians. New Engl J Med. 329:1988-1992.

105. Carvalho, E., P.A. Jansson, I. Nagaev, A.M. Wenthzel, U. Smith. 2001. Insulin resistance with low IRS-1 expression is also associated with low Glut 4 expression and impaired insulin-stimulated glucose transport. FASEB J.

106. Carvalho, E., P.A. Jansson, M. Axelsen, J.W. Eriksson, X. Huang, L. Groop, C. Rondinone, L. Sjostrom, U. Smith. 1999. Low cellular IRS-1 gene and protein expression predicts insulin resistance and NIDDM. FASEB J. 13:2173-2178.

107. Venable, C.L., E.U. Frevert, Y.B. Kim, B.M. Fischert, S. Kamatkar, B.G. Neel, B. Kahn. 2000. Overexpression of protein-tyrosine phosphatase-1B in adipocytes inhibits insulin-stimulated phosphoinositide 3-kinase activity without altering glucose transport or Akt/PKB activation. J Biol Chem. 275: 18318-18326.

108. Moller, D., J. Flier. 1991. Insulin resistance: Mechanisms, syndromes, and implications. N Engl J Med 325:938-948.

109. Granberry, M. 1999. Insulin resistance syndrome: Options for treatment. Southern Medical Journal 92:2-14.

110. Defronzo, RA, E. Ferrannini. 1991. Insulin resistance: A multifaceted syndrome responsible for NIDDM, obesity, hypertension, dyslipidaemia, and athrosclerotic cardiovascular disease. Diabetes Care 14:173-194.

111. Reynisdottir, S, et al. 1997. Adipose tissue lipoprotein lipase and hormone sensitive lipase. Contrasting findings in familial combined hyperlipidaemia and insulin resistance syndrome. Arterioscler. Thromb. Vasc. Biol. 17:2287-2292.

112. http://web.indstate.edu

113. Carey, G.B. 1998. Mechanisms regulating adipocyte lipolysis. Skeletal Muscle Metabolism in Exercise and Diabetes. 157-168.

114. Holm, C., T. Osterlund, H. Laurell. J.A. Contreras. 2000. Molecular mechanisms regulating hormone-lipase and lipolysis. Annual Rev Nutr. 20:365-93.

115. Egan, JJ, AS Greenberg, MK Chang, SA Wek, MC Moos, et al. 1992. Mechanism of hormone-stimulated lipolysis in adipocytes: translocation of hormone-sensitive lipase to the lipid storage droplet. Proc.Natl.Acad.Sci. USA 89:8537-41.

116. Hirsch, AH, OM Rosen. 1984. Lipolytic stimulation modulates subcellular distribution of hormone-sensitive lipase in 3T3-L1 cells. J. Lipid. Res. 25:665-77.

117. Brasaemle, DL, DM Levin, DA Adler-Wailes, C londos. 2000. The lipolytic stimulation of 3T3-L1 adipocytes promotes the translocation of cytosolic hormone-sensitive lipase to the surface of lipid storage droplets.

118. Blanchette-Mackie, EJ, NK Dwyer, T Barber, RA Coxey, T Takida, et al. 1995. Perilipin is located on the surface layer of intracellular lipid droplets in adipocytes. J. Lipid Res. 36:1211-26.

119. Londos, C. 1996. Hormone-sensitive lipase and the control of lipolysis in adipocytes. In Diabetes Mellitus: A Fundamental and Clinical Text, ed. D. LeRoith, SI Taylor, JM Olefsky, pp223-27, Philadelphia, PA: Lippincott-Raven.

120. Souza, SC, LM de Vargas, MT Yamamoto, P Lien, MD Fransciosa, et al. 1998. Overexpression of perilipin A and B blocks the ability of TNF-α to increase lipolysis in 3T3-L1 adipocytes. J. Biol. Chem. 273:24665-69.

121. Degerman, E, P Belfrage, VC Manganiello. 1997. Structure, localization, and regulation of cGMP-inhibited phosphodiesterases (PDE3). J. Biol. Chem. 272:6823-26.

122. Elks, ML, VC Manganiello. 1985. Antilipolytic action of insulin: role of cAMP phosphodiesterase activation. Endocrinology 116:2119-21.

123. Ramirez-Zacarias, J.L., F. Castro-Munozledo, W. Kuri-Harcuch. 1992. Quantitation of adipose conversion and triglycerides by staining intracytoplasmic lipids with Oil red O. Histochemistry 97:493-497.

124. Glenn, K.c., K.S. Rose, G. Krivi. 1988. Somatotropin antagonism of insulin-stimulated glucose utilization in 3T3-L1 adipocytes. J Cell Biochem. 37:371-383.

125. Germinario, R.J., A.D. Sniderman, S. Manuel, S.P. Lefebvre, A. Baldo, K. Cianflone. 1993. Coordinate regulation if triacylglycerol synthesis and glucose transport by acylation-stimulating protein. Metabolism 42:574-580.

126. Levy, J.R., J.M. Olefsky. 1987. Intracellular insulin-receptor dissociation and segregation in a rat fibroblast cell line transfected with a human insulin receptor gene. J Biol Chem. 263:6101-6108.

127. Dowell, P, C. Flexner, PO Kwiterovich, MD Lane. 2000. Suppression of preadipocyte differentiation and promotion of adipocyte death by HIV protease inhibitors. J Biol Chem 275(52): 41325-41332.

128. Zhang, B., Macnaul K., Szalkowski D., Li Z., Berger J., Moller D.E. 1999. Inhibition of adipocyte differentiation by HIV protease inhibitors. J Clin Endo Metab 84(11): 4274-4278.

129. Gagnon, AM, Angel JB, Sorisky A. 1998. Protease inhibitors and adipocyte differentiation in cell culture. The Lancet 352:1032.

130. Wentworth, JM, Burris TP, Chatterjee VKK. 2000. HIV protease inhibitors block human preadipocyte differentiation, but not via the PPARγ/RXR heterodimer. J Endocrinology 164: R7-R10.

131. Ranganathan, S, Kern PA. 2002. The HIV protease inhibitor saquinavir impairs lipid metabolism and glucose transport in cultured adipocytes. J Endocrinology 172: 155-162.

132. Lenhard, JM, Furfine ES, Renu GJ, Ittoop O, Orband-Miller LA, Blanchard SG, Paulik MA, Weiel JE. 2000. HIV protease inhibitors block adipogenesis and increase lipolysis in vitro. Antiviral Research 47: 121-129.

133. Parker, RA, Wang S, Meyers D, Fenderson W, Mulvey R, Leet J, Peters A, Harrity T, Yang W-P, Flint OP. 2001. Differentiation of HIV protease inhibitors in models of lipid and glucose metabolism and gene expression in adipocytes and hepatocytes. 3rd International Workshop on Adverse Drug Reactions and Lipodystrophy in HIV Athens, Greece.

134. Stevens, GJ, Lankford AC, Chen M, Jessen B. Inhibition of adipocyte differentiation by HIV-1 protease inhibitors: Potential mechanisms based on changes in gene expression. . 3rd International Workshop on Adverse Drug Reactions and Lipodystrophy in HIV Athens, Greece. Poster # P3.

135. Caron, M, Auclair M, Vigouroux C, Glorian M, Forest C, Capeau J. 2001. The HIV protease inhibitor indinavir impairs sterol regulatory element-binding protein-1 intranuclear localization, inhibits preadipocyte differentiation, and induces insulin resistance. Diabetes 50: 1378-1388.

136. Martinez, E., I. Conget, L. Lozano, R. Casamitjana, J. Gatell. 1999. Reversion of metabolic abnormalities after switching from HIV-1 to nevirapine. AIDS 13(7): 805-810.

137. Schutt, M., M. Meier, M. Meyer, J. Klein, S.P. Aries, H.H. Klein. 2000. The HIV-1 protease inhibitor indinavir impairs insulin signaling in HepG2 hepatoma cells. Diabetologia 43:1145-1148.

138. Anai, M., M. Funaki, T. Ogihara, J. Terasaki, K. Inukai, H. Katagiri, Y. Fukushima, Y. Yazaki, M. Kikuchi, Y. Oka, T. Assano. 1998. Altered expression levels and impaired steps in the pathway to phosphotidylinositol 3-kinase activation via insulin receptor substrates 1 and 2 in Zucker fatty rats. Diabetes 47:13-23.

139. Paz, K., R. Hemi, D. LeRoith, A. Karasik, E. Elhanany, H. Kanety, Y. Zick. 1997. A molecular basis for insulin resistance: elevated serine/threonine phosphorylation of IRS-1 and IRS-2 inhibits their binding to the juxtamembrane region of the insulin receptor and impairs their ability to undergo insulin-induced tyrosine phosphorylation. J. Biol. Chem. 272: 29911-29918.

140. Li, J., K. DeFea, RA Roth. 1999. Modulation of insulin receptor substrate-1 tyrosine phosphorylation by an Akt/phosphatidylinositol 3-kinase pathway. J. Biol. Chem. 274: 9351-9356.

141. Pederson, T., D.L. Kramer, C.M. Rondinone. 2001. Serine/Threonine phosphorylation of IRS-1 triggers its degradation: Possible regulation by tyrosine phosphorylation. Diabetes 50:24-31.

142. Murata, H., P.W. Hruz, M. Mueckler. 2000. The mechanism of insulin resistance caused by HIV protease inhibitor therapy. J. Biol. Chem. 275: 20251-20254.

143. Ohlson, LO, B. Larsson, K. Svardsudd, et al. 1985. The infuence of body fat distribution on the incidence of diabetes mellitus- 13.5 years of follow-up of the participants in the study of men born in 1913. Diabetes 66: 2206-2210.

144. Lapidus, L., C Bengtsson, B Larsson et al. 1984. Distribution of adipose tissue and risk of cardiovascular disease and death : a 12 year follow-up of participants in the population study of women in Gothenburg, Sweden. British Medical Journal 289: 1261-1263.

145. Kissebah, AH, N Vydelingum, R Murray et al. 1982. Relation of body fat distribution to metabolic complications of obesity. J Clin Endo Metab 54: 254-260.

146. Despres, JP, C Allard, A Tremblay, et al. 1985. Evidence for a regional component of body fatness in the association with serum lipids in men and women. Metabolism 34:967-973.

147. Harris Peeples, L., JW Carpenter, RG Isreal, HA Barakat. 1989. Alterations in low-density lipoproteins in subjects with abdominal obesity. Metabolism 38: 1029-1036.

148. Lenhard, JM, Croom DK, JE Weiel, DA Winegar. 2000. HIV protease inhibitors stimulate hepatic triglyceride synthesis. Arterioscler Thromb Vasc Biol 20:2625-2629.

149. Eckel, RH. 1989. Lipoprotein lipase. A multifactorial enzyme relevant to common metabolic diseases. New Engl J Med 320: 1060-1068.